Inter- and intra-species sensitivity of aquatic arthropods to imidacloprid and flupyradifurone

Anna Huang

Propositions

1. Intraspecies differences in sensitivity to chemicals are important but neglected in risk assessment (This thesis).
2. Formation of toxic metabolites in organisms needs to be integrated into the risk assessment of chemicals (This thesis).
3. To understand experimental data, one needs to be a modeller.
4. A PhD program is an experiment to test a candidate's performance in coping with the unknown.
5. We should celebrate it, if an experiment fails.
6. Working with others is a prerequisite to understand one's own personality.
7. Diversity drives innovation in the workplace.

Propositions belonging to the thesis entitled:

"Inter- and intra-species sensitivity of aquatic arthropods to imidacloprid and flupyradifurone"

Anna Huang

Wageningen, 16 November 2022

Inter- and intra-species sensitivity of aquatic arthropods to imidacloprid and flupyradifurone

Anna Huang

Thesis Committee

Promotors
Prof. Dr Paul J. van den Brink
Personal chair, Aquatic Ecology and Water Quality Management
Wageningen University & Research

Dr Nico W. van den Brink
Associate professor of Toxicology
Wageningen University & Research

Co-promotor
Dr Ivo Roessink
Senior scientist, Environmental Risk Assessment
Wageningen University & Research

Other members
Prof. Dr Violette Geissen, Wageningen University & Research
Prof. Dr Kees van Gestel, VU University Amsterdam
Prof. Dr Martina Vijver, Leiden University
Dr Andre Gergs, Bayer AG, Germany

Inter- and intra-species sensitivity of aquatic arthropods to imidacloprid and flupyradifurone

Anna Huang

Table of Contents

1

CHAPTER 1.

General introduction.
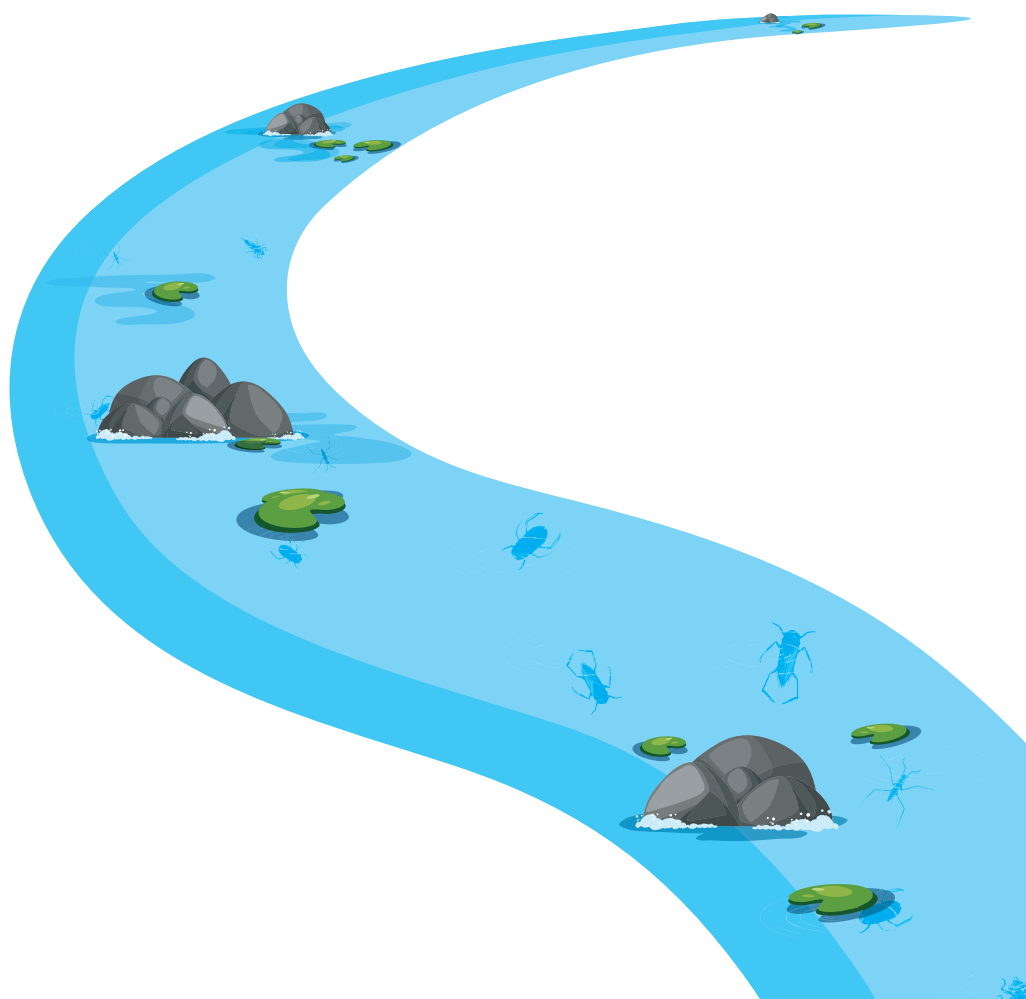
1.1 Commonly used insecticides: neonicotinoids

Worldwide food demand is increasing rapidly due to the exponential increase in the world population. The increasing use of pesticides in agricultural practices has significantly impacted crop growth efficiency, allowing a more than doubling in world food production during the last century (Hazell and Wood 2008, Carvalho 2017). Around one-third of today's agricultural products are cultivated with the use of pesticides, and estimations are that there would be a reduction of 78% in fruit production and 54% in vegetable production without the use of pesticides (Lamichhane 2017). The main pesticides used in agriculture are insecticides, herbicides, and fungicides. As the name suggests, insecticides are a type of pesticide that is used to specifically target and kill insects, and herbicides are used to kill undesirable plants or "weeds", while fungicides are pesticides that kill or prevent the growth of fungi and their spores (Abubakar et al. 2020).

In this thesis, we focus on insecticides, specifically on neonicotinoids (NNIs), which are the most used types of insecticides in the world (Bartlett et al. 2019b). Because of their structural similarity with a nicotine molecule, NNIs are able to act as an agonist of the nicotinic acetylcholine receptors (nAChRs). nAChRs are receptor polypeptides that respond to the neurotransmitter acetylcholine. nAChRs are found in the central and peripheral nervous system, muscles, and other tissues of many organisms. nAChRs are involved in rapid neurotransmission in insect and mammalian nervous systems and play significant roles in learning and memory (Taillebois et al. 2018). By acting as an agonist on the nAChRs, NNIs disrupt the central nervous system of insects (Motohiro Tomizawa 2000, Taillebois et al. 2018)

1.1.1. Neonicotinoids and their alternatives

NNIs have many advantages compared to their predecessors, mainly due to their extreme toxicity to most targeted insect species and low acute toxicity to mammals, including humans (Morrissey et al. 2015). Among the NNIs, imidacloprid (IMI) was the first NNI registered in the European Union (2000; EC/List no.: 604-069-3), followed by acetamiprid (2004; EC/List no.: 603-921-1), and thiacloprid (2004; EC/List no.: 601-147-9), clothianidin (CLO) (2006; EC/List no.: 433-460-1) and thiamethoxam (THM) (2007; EC/List no.: 428-650-4) (Commission 2004, 2005, 2006, 2008). Since then, the use of NNIs has grown exponentially, reaching 25% of global pesticide sales in 2014, with THM, IMI, and CLO accounting for almost 85% of the total neonicotinoid sales in crop protection in 2012 worldwide (Bass et al. 2015).

The intensive use of NNIs also brings many environmental problems. Because of their high solubility and relatively long half-life in soil and water, neonicotinoids are often transported from application fields to non-target field margins, adjacent floral communities, and wildlife habitats during crop planting and precipitation events (Hladik et al. 2018, Pietrzak et al. 2020). The associated chemical fate provides the potential for wild bee populations to be exposed to neonicotinoids via soil, plants (e.g., leaves, flowers), and pollen. Numerous studies have identified a range of neonicotinoid active ingredients in crops and non-target margin plant material, eventually causing declines in both managed and wild bee populations (Woodcock et al. 2016, Woodcock et al. 2017, Main et al. 2021, Siviter et al. 2021). In addition to the toxicity of the parent compound of NNIs, some metabolites of imidacloprid were found to be toxic to bees (Nauen et al. 2001).

Due to their risks to pollinators these three main neonicotinoids, IMI, THM, and CLO, were banned for outdoor use in Europe in 2018 (Commission 2018). This has led to the introduction of insecticidal alternatives on the global market.

One of the important alternatives to IMI is flupyradifurone (FPF), a new butenolide pesticide that launched globally (Giorio et al. 2017a). FPF was first commercially available in Honduras and Guatemala in 2014 (Nauen et al. 2015a) and has since then become available for use on a wide range of crops in Canada (PMRA 2015), the United States (EPA 2015), China (Zhong et al. 2021) and Europe (EFSA 2016). Compared with the class of neonicotinoid insecticides containing N-nitroguanidine-, N-cyano-amidine-, or nitromethylene pharmacophores, the butenolide insecticide flupyradifurone contains a different pharmacophore system as a new bioactive scaffold (Figure 1.1) (Jeschke et al. 2015a, Nauen et al. 2015b). Although FPF also targets at nAChRs, similar to neonicotinoids, it differs from most neonicotinoids due to its bioactive scaffold (Figure 1.1 b) (Jeschke et al. 2015a).

FPF is used for a wide range of crops as a foliar spray, soil drench, and seed treatment, targeting sucking pests such as aphids, hoppers, and whiteflies (Bayer 2012). Research shows that FPF seems comparatively safer for honeybees and bumblebees than IMI (Campbell et al. 2016). However, in the latest statement evaluated by EFSA, they found evidence that among solitary bee species – which was not addressed in the previous EU assessment – the species *Megachile rotundata* may be more sensitive to FPF (EFSA PPR Panel (Panel on Plant Protection Products and their Residues) et al. 2022).
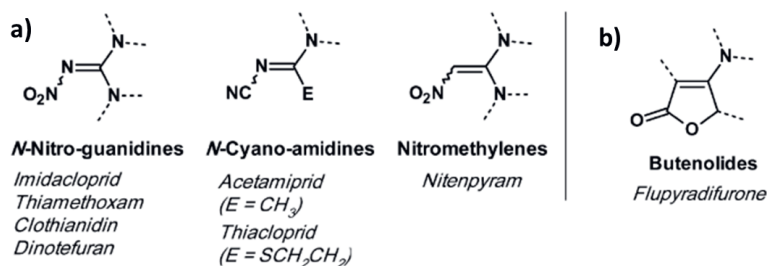
Figure 1.1: *Comparison of pharmacophore systems of nAChR agonists: (a) neonicotinoids, i.e. N-nitro-guanidines, N-cyano-amidines, nitromethylenes; (b) butenolides, adapted from (Jeschke et al. 2015a).*

1.1.2. Effects of imidacloprid and flupyradifurone in freshwater systems

Compared to the bees study, studies on the effects of NNIs in aquatic systems are limited. As highly water-soluble compounds, neonicotinoids have been frequently detected in waterways around the world, including surface water runoff (rivers, streams), groundwater, and wetlands (Morrissey et al. 2015, Hladik et al. 2018). Moreover, although IMI has been banned for outdoor use, it is still detected in the environment in Europe (Casillas et al. 2022). High concentrations, for example, are still observed in various water bodies near greenhouses in the Netherlands, where the use of IMI is still permitted (Thunnissen et al. 2020b, van Hagen 2020). Based on 2254 measurements, the RIVM (National Institute for Public Health and the Environment of the Netherlands) reported concentrations of up to 2.8 µg/L in surface waters (Lahr et al. 2019). In addition, some metabolites of IMI have been detected in environmental water samples through environmental degradation and biotransformation (Benton et al. 2015, Wan et al. 2020).

Because FPF has similar chemical properties to IMI, such as high water solubility, low volatility, and a high half-life value (Bayer 2012, Nauen et al. 2015a), it will be persistent in the environment, with a high potential for entering freshwater ecosystems via runoff, erosion, and leaching (Carleton 2014). Currently, only a few monitoring data for FPF in water systems are available, although more and more research encourages the inclusion of FPF in environmental monitoring programs (Kandie et al. 2020, Sanford and Prosser 2020). To our knowledge, the highest measured environmental concentration of FPF is 0.16 µg/L which has been recorded in a watershed of the Great Lakes basin in Canada, and the geometric mean concentration of FPF in 6 watersheds near cropland was 0.018 µg/L (Metcalfe et al. 2019). FPF

has also been detected in streams in Canada, with IMI being detected in 33% of the samples, while FPF was detected in 13% of samples, with the highest concentration of 0.11 µg/L (Sanford and Prosser 2020).

With ongoing concerns about NNIs in freshwater systems, several studies found that because of the accumulation and persistence of NNIs in waters (Shahid et al. 2018, Crayton et al. 2020), aquatic organisms' health and the aquatic ecological environment may be threatened (Morrissey et al. 2015). These highly neurotoxic insecticides may have the potential to significantly alter the community structure and functioning of invertebrate communities. For example, mesocosm experiments conducted by Merga et al. (2021) showed that the macroinvertebrate and zooplankton community structure changed significantly due to imidacloprid contamination in mesocosms repeatedly dosed with ≥ 0.1 and ≥ 0.01 µg/L, respectively (Merga et al. 2021).

1.2. Inter- and intra-species sensitivity differences in the ecological risk assessment

The concern of chemicals, such as NNIs, in the environment, can be addressed by ecological risk assessment (ERA) (Casillas et al. 2022). More specifically, ERA aims to quantify risk through an exposure and effect assessment (van Leeuwen and Vermeire 2007). The aim of the exposure assessment is to determine the concentration of a hazardous chemical in the environment which is called the predicted environmental concentration (PEC). When a chemical is released into the environment, many processes can influence the fate and behaviour of this chemical including transportation (e.g., run-off), (bio)degradation, adsorption, evaporation, leaching, and other forms of dissipation (van Leeuwen and Vermeire 2007). In the effect assessment, the predicted no-effect concentration (PNEC) is determined, which indicates the threshold concentration under which no significant adverse effects on the ecosystem are expected (van Leeuwen and Vermeire 2007).

The methods in chemical risk assessment, including the tests of neonicotinoids amongst other chemicals, are highly standardized. For this reason, there are numerous guidelines provided by the Organisation for Economic Co-operation and Development (OECD) and the International Organization for Standardization (ISO) to enable scientists all over the world to compare their results following standardized criteria (Moermond et al. 2016). The majority of these guidelines describe bioassays performed with a single test species and a single chemical in a simple setup that typically consists of a small glass container in which organisms are fed

specific food in a well-described medium and under strict temperature and light conditions (for example OECD, 2012(OECD 2012)). These experiments provide data that can be used to calculate PNECs using assessment factors. The data can also be used as an input for several models (such as 'species sensitivity distributions', SSD) upon which potential environmental risks can be estimated (De Zwart and Posthuma 2005).

However, this standardized testing method has advantages and disadvantages (Schaefer 2013). One of the advantages of standardized testing is facilitating the comparison of data and results and allowing replication of the test (Schaefer 2013, Martin et al. 2019). Contrary, one of the disadvantages is that we may neglect other species besides the standard test species or overlook the intraspecies sensitivity differences and environmental conditions outside the ranges prescribed in the protocols (Taylor and Scroggins 2013). Such neglection may lead to an underestimation of chemical risks and fail our goals of protecting the environment and human safety. Thus, assessing and understanding the intra- and inter-species differences in sensitivity is essential for an environmentally relevant ERA.

On the other hand, ecosystems can be populated by hundreds to thousands of species, and each species has the potential to show a different sensitivity toward each of the hundreds of thousands of different chemical compounds that can be present in our ecosystems (Van den Berg et al. 2019). Choosing which species is the representative species in ERA is also known as the myth of the "most sensitivity species" (Cairns 1986). It also resulted in the awareness of so-called inter-species sensitivity differences. In addition, intraspecies sensitivity is also an important factor in ERA. The variation in sensitivity of individuals within the same species may be influenced by the size, sex, and life stage of the individuals (McClellan-Green et al. 2007, Poteat and Buchwalter 2014) and environmental factors, such as temperature, salinity, geography and season (Hooper et al. 2013, Moe et al. 2013, Van den Brink et al. 2016, Bednarska et al. 2017, Sumon et al. 2018).

Besides the interspecies and intraspecies sensitivity difference, there is a discrepancy between acute and chronic toxicity of IMI to aquatic arthropods, also called time-accumulative toxicity. The effects of IMI on sensitive species, such as bees (Rondeau et al. 2014) and mayflies (Van den Brink et al. 2016, Macaulay et al. 2021), increased after long-term exposure, not reaching the incipient threshold value. The incipient value is the value that the LC_{50} will reach when the internal body concentration has reached an equilibrium with the external (constant) aqueous

concentration (Legierse et al. 1999). The concept of incipient value is essential in aquatic risk assessment for chemicals that exert an irreversible receptor interaction. The exact mechanism of IMI's increased toxicity with time is unknown, and whether this phenomenon exists in FPF also needs to be investigated.

1.3. Mechanistic effect modelling to increase understanding of inter- and intra-species variation

In addition to traditional laboratory toxicity testing, there is a growing trend to use mechanistic effect models to interpret results, predict effects, and ultimately understand the mechanisms of toxicity. Lately, EFSA concluded that toxicokinetics and toxicodynamics (TKTD) effect models are essential for the risk assessment of pesticides for aquatic organisms (EFSA PPR Panel (Panel on Plant Protection Products and their Residues) et al. 2018).

Traditionally, chemicals' toxicity on aquatic invertebrates is assessed by either an acute (2 or 4 days) or a chronic (21 or 28 days) toxicity test. However, these tests only provide us with the toxicity values for a certain endpoint and time point (e.g., mortality for 4 or 28 days). There are many shortcomings of this traditional descriptive dose-response model and the associated summary statistics like LC_{50}, ECx or NOEC values (Jager 2011). For example, the value of ECx depends on the experiment duration and environmental conditions, and it is only purely descriptive, without any mechanistic information (Jager 2011).

Instead, the TKTD effect models allow the interpretation and prediction of toxicity (EFSA PPR Panel (Panel on Plant Protection Products and their Residues) et al. 2018) and these models provide a modeling approach of intermediate complexity (Jager 2017b). TKTD models quantify the time-course of internal concentration, which is a result of uptake, elimination and biotransformation of the parent compound (TK), and the processes which lead to the toxic effects at the target site (TD) (Jager et al. 2011). As a first step, TK models translate an external concentration of a toxicant to an internal concentration over time. In their simplest form, TK models include the processes of uptake and elimination, but refined TK models may also include further processes that modify the concentration of the toxicant at the target site, such as biotransformation and internal distribution. As a second step, TD models quantitatively link the internal concentration to the effect at the level of the individual organism over time to the effect (e.g., mortality) (Jager et al. 2011). Among all TKTD models, the General Unified

Threshold model of Survival (GUTS) is mostly used for aquatic invertebrates (Jager et al. 2011) (Figure 1.2).

Nevertheless, GUTS only focuses on mortality and assumes that an organism does not grow or reproduce. This assumption is suitable for short-term testing (e.g., 4 days) but not for long-term experiments when an organism grows or even reproduces, and sublethal effects on these processes also need to be assessed. The need for the inclusion of sublethal effects calls for the integration of the dynamic energy budget model concept into TKTD models. The Dynamic energy budget (DEB) theory focuses on energy as a common currency (with units of, e.g., Joule). Mass and energy flow in an animal is linked. A certain mass of food represents a certain amount of energy, depending on its composition. The growth process represents an amount of energy obtained from food that is fixed in the new tissue and energy that is lost in the process of turning food into the new biological structure (overhead costs, which need to be accounted for in any biochemical transformation) (Jager 2017b). DEBtox models explore the effects of toxicants on growth and reproduction over time, even over the entire life cycle (EFSA PPR Panel (Panel on Plant Protection Products and their Residues) et al. 2018) (Figure 1.2).

Mechanistic modeling like the GUTS and DEB models has been used to understand species sensitivity, delayed effects, and temperature influence in a variety of chemicals and species (Gergs et al. 2015, Li et al. 2021, Na et al. 2021). This thesis uses these models to understand the differences in the sensitivity of species to our chemicals of interest. Specifically, the sensitivity differences in toxicokinetics and toxicodynamic processes are determined separately, and the potential drivers of interspecies and intraspecies sensitivity differences are explored.
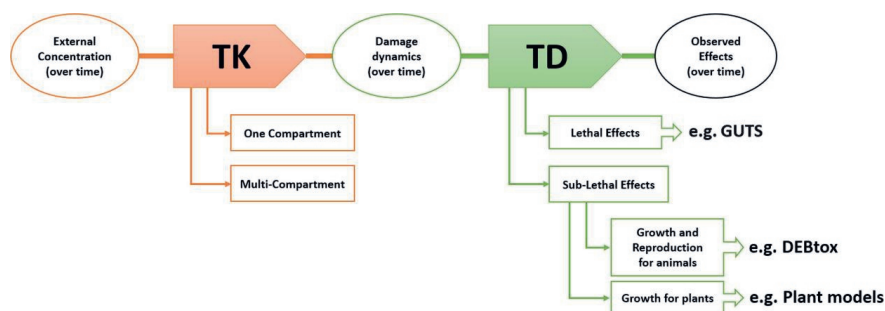
Figure 1.2: *Schematic presentation of the concepts behind toxicokinetic (TK)/toxicodynamic (TD) models; GUTS stands for the General Unified Threshold model of Survival, while DEBtox stands for toxicity models derived from the Dynamic Energy Budget (DEB) theory, adapted from(EFSA PPR Panel (Panel on Plant Protection Products and their Residues) et al. 2018)*

1.4. Research objectives and research questions

The main objective of this thesis is to use toxicokinetic and toxicodynamic models to understand the time-accumulative toxicity and inter- and intra-species sensitivity of imidacloprid and flupyradifurone in aquatic systems (Figure 1.3).

This understanding can help us develop a better risk assessment of neonicotinoids and their alternatives in aquatic systems. To accomplish this objective, we formulated six research questions:

1. How can the time-accumulative toxicity of IMI on certain aquatic arthropod species be explained?

2. What are the potential drivers of interspecies variation in the sensitivity of aquatic arthropods to IMI?

3. What are the potential drivers of intraspecies variation in sensitivity of aquatic arthropods to IMI?

4. What is the toxicity of FPF to aquatic arthropods?

5. Does FPF, like IMI, also show time-accumulative toxicity to some aquatic arthropods?

6. How does temperature modulate the toxicity of IMI and FPF to the arthropod *Gammarus pulex*?
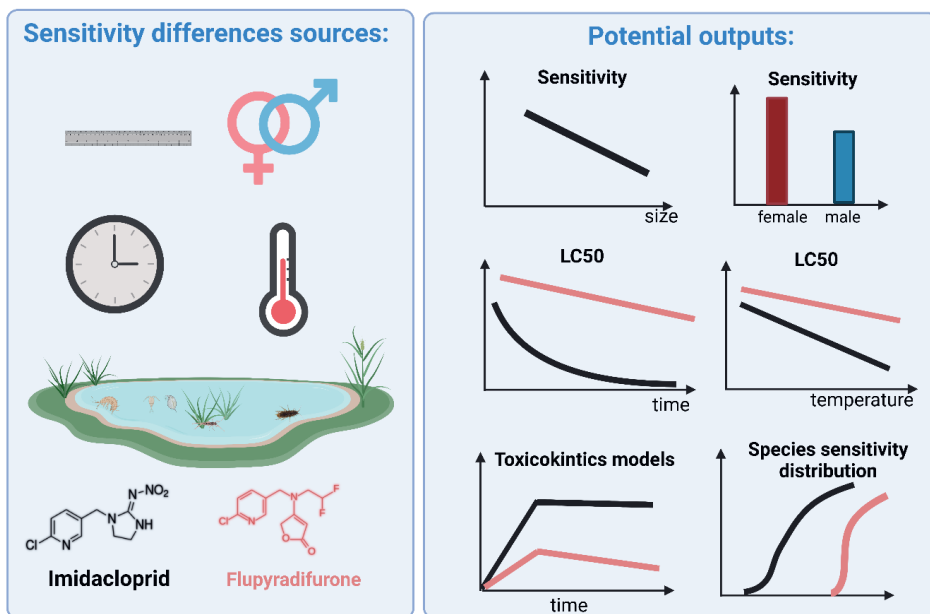
Figure 1.3*: Schematic overview of the intra- and interspecies sensitivity differences of aquatic arthropods will be investigated and the potential outputs in this thesis. This figure was created with BioRender (https://biorender.com/).*

1.5. Thesis outline

In order to answer the first and the second research questions, we explore the toxicity and toxicokinetics of IMI and a bioactive metabolite to two aquatic arthropod species in **Chapter 2.** Specifically, to assess the potential effects of the metabolization of IMI and the toxicokinetics and toxicity of the metabolite(s) on aquatic arthropods, we first study the acute toxicity of IMI and relevant metabolites to the mayfly species *Cloeon dipterum* (sensitive to IMI) and the amphipod species *Gammarus pulex* (less sensitive to IMI). Secondly, we conduct toxicokinetic experiments using the parent compound (IMI) and the toxic metabolite imidacloprid-olefin (IMI-ole).

To tackle the third research question, the size- and sex-related sensitivity differences of aquatic crustaceans to IMI are assessed in **Chapter 3**. We perform standard acute toxicity and toxicokinetic tests with *Gammarus pulex* and *Asellus aquaticus*. To investigate the intraspecies sensitivity differences, we use neonates, juveniles and male and female adults in separate

experiments, in which we expose the animals to imidacloprid and its bioactive metabolite, IMI-ole.

To answer the <u>fourth and fifth questions</u>, in **Chapter 4**, we assess the toxicity of FPF for several aquatic arthropod species and compare these results with those of IMI to evaluate whether FPF is a safer alternative for IMI in aquatic systems. Both acute and chronic toxicity tests are performed with FPF. An acute SSD is generated for FPF and compared with IMI, and the toxicokinetic differences between IMI and FPF are also compared. In this chapter, we address the question of whether there is a discrepancy between acute and chronic toxicity of FPF by using the GUTS models.

With the aim of answering the <u>sixth research question</u>, we explore the sensitivity differences of IMI and FPF to *Gammarus pulex* at different temperatures in **Chapter 5** and **Chapter 6**. In **Chapter 5**, we measure the toxicokinetics of IMI and FPF at different temperatures. In addition, we explore the lethal and sublethal effects of both IMI and FPF on *Gammarus pulex* at the three temperatures of 7, 11 and 15 °C over 28 days. In **Chapter 6**, DEB models are calibrated to understand the influence of temperature on the effect of IMI and FPF on the growth and survival of *Gammarus pulex*.

Finally, in **Chapter 7,** I discuss the findings of my thesis, especially the importance of biotransformation in explaining the interspecies and intraspecies sensitivity differences, emphasising the important need to consider the toxic metabolite as well as temperature in toxicity assessment. The final chapter also provides an outlook on the adverse-outcome-pathway (AOP), which links the TKTD models to a deeper biological perspective, to gain more understanding of the intra- and inter-species sensitivity differences in future studies.
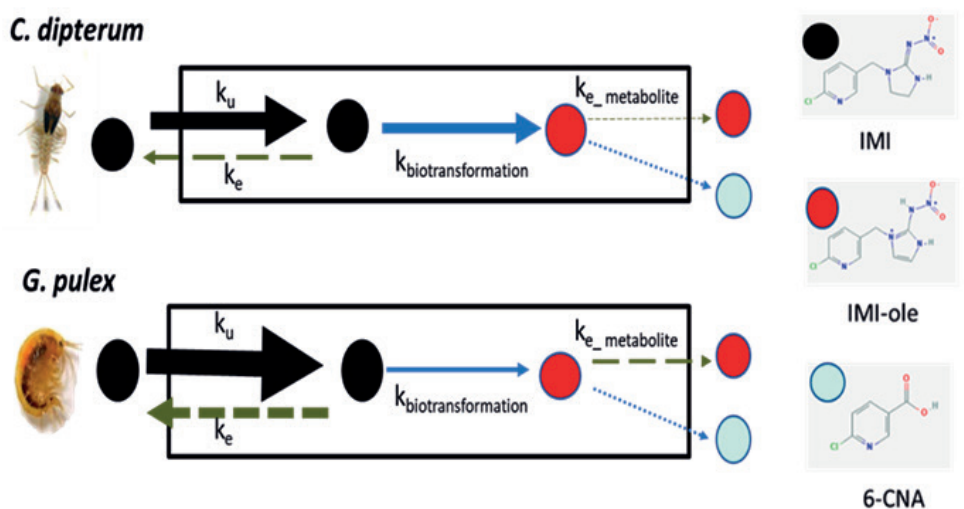
2

CHAPTER 2.

The toxicity and toxicokinetics of imidacloprid and a bioactive metabolite to two aquatic arthropod species.

Anna Huang, Nico W. Van den Brink, Laura Buijse, Ivo Roessink, Paul J. Van den Brink

Graphical abstract: A graphic diagram of the experimental design and the results

Abstract

Previous studies have explored effects of imidacloprid and its metabolites on terrestrial species, such as bees, and indicated the importance of some active metabolites. However, the biotransformation of IMI and the toxicity of its metabolites to aquatic arthropods are largely unknown, especially the mechanisms driving species sensitivity differences and time-accumulative toxicity effects. To assess the potential effects of the metabolisation of IMI and the toxicokinetics and toxicity of the metabolite(s) on aquatic arthropods, we first studied the acute toxicity of IMI and relevant metabolites to the mayfly species *Cloeon dipterum* (sensitive to IMI) and the amphipod species *Gammarus pulex* (less sensitive to IMI). Secondly, toxicokinetic experiments were conducted using both the parent compound and imidacloprid-olefin (IMI-ole), a metabolite assessed as toxic in the acute tests and defined as bioactive. Of the four tested metabolites, only IMI-ole was readily biotransformed from the parent IMI and showed similar toxicity to *C. dipterum* as IMI. However, *C. dipterum* was hardly able to eliminate IMI-ole from its body. For *G. pulex*, IMI-ole was also the only detected metabolite causing toxicity, but the biotransformation of IMI to IMI-ole was slower and lower in *G. pulex* compared to *C. dipterum*, and *G. pulex* eliminated IMI-ole quicker than *C. dipterum*. Our results on internal kinetics of IMI and IMI-ole, and on biotransformation of IMI indicated that the metabolite IMI-ole was toxic and was rather persistent inside the body tissue of both invertebrate species, especially for *C. dipterum*. In conclusion, as IMI and IMI-ole have similar toxicity and IMI was replaced rapidly by IMI-ole which in turn was poorly eliminated by *C. dipterum*, the overall toxicity is a function of dose and time. As a result, no long-term threshold of effects of IMI may exist for *C. dipterum* as the poor elimination results in an ongoing increase of toxicity over time for mayflies as also found experimentally in previous published papers.

2.1. Introduction

Neonicotinoids (NNIs) are a class of neuro-active insecticides acting in a similar manner as nicotine (Hladik et al. 2018), comprising different families i.e. the nitroguanidine insecticides (imidacloprid) and the cyanoguanidine insecticides (thiacloprid). They are used worldwide and spark increasing environmental concerns due to their potential risks to terrestrial and aquatic invertebrates (Morrissey et al. 2015, Hladik et al. 2018). Imidacloprid (IMI) is the most used NNI, and the toxicity of IMI has been extensively studied for terrestrial insects, like bees (Suchail. et al. 2001, Zaworra et al. 2019). As IMI gets into freshwater ecosystems readily and is relatively persistent, there are some aspects regarding IMI that need to be studied in order to fully understand its long-term toxicity to aquatic invertebrates (Starner and Goh 2012, Vijver and van den Brink 2014, Morrissey et al. 2015). The first one is the species sensitivity differences. For example, mayflies are among the most sensitive species to IMI with 96h-EC_{50} and 28d-EC_{50} values being 18 and 122 times lower than those of *G. pulex*, which is a macroinvertebrate with an average acute sensitivity to IMI (Ashauer et al. 2011b, Roessink et al. 2013). The second one is the time dependent increase of the effects of IMI for sensitive species, such as bees (Rondeau et al. 2014) and mayflies (Van den Brink et al. 2016) after a long term exposure. For example, the toxicity of IMI to *C. dipterum* increased from a 4d-EC_{50} value of 1.02 µg/L to a 28d-EC50 of 0.126 µg/L, while for the less sensitive *G. pulex* this shifted from a 4d-EC_{50} value of 18.3 µg/L to a 28d-EC_{50} of 15.4 µg/L (Roessink et al. 2013).

Studies have revealed that traits, such as organism size, respiration mode and lipid content (Rubach et al. 2010), as well as the formation of metabolites can be possible explanations for species specific toxicity (Kretschmann et al. 2011, McCarty et al. 2011, Fu et al. 2018). That metabolites of IMI, such as 5-hydroxyimidacloprid and olefin IMI, result in delayed and time-accumulative toxicity of imidacloprid has been propounded in some terrestrial studies (Suchail. et al. 2001, Tomalski et al. 2010). Furthermore, some studies have demonstrated that some metabolites of IMI display similar or even higher neurotoxicity than the parent compound in locust (Parkinson and Gray 2019) and bees (Nauen et al. 2001), but these studies exclusively focused on terrestrial species. In line with the previous recommendation (Starner and Goh 2012) of monitoring IMI metabolites, like imidacloprid-olefin (IMI-ole) and hydro imidacloprid in surface waters, a recent study detected IMI and its metabolites in source and tap water (Wan et al. 2020). Besides metabolites being present in the surface waters, organisms also can

take IMI up and biotransform it, as demonstrated in several species like rock oysters (Ewere et al. 2019), lizards (Wang. et al. 2019) and bees (Suchail. et al. 2001, Suchail et al. 2004a, Suchail et al. 2004b). In spite of the fact that metabolic pathways may be species-specific, one of the common pathways is that IMI is transformed to 5-OH-IMI, to IMI-ole and to 6-CNA (Nishiwaki et al. 2004, Fusetto et al. 2017, Li et al. 2019). To understand the effect pathway of IMI and its metabolites in aquatic invertebrates, we chose IMI and its metabolites imidacloprid-olefin, imidacloprid-urea, 6-chloronicotinic acid, and 5-hydroxy-imidacloprid in our study based on their commercial availability their potential toxicity (Nishiwaki et al. 2004, Suchail et al. 2004a, Tomalski et al. 2010, Ma et al. 2014, Fusetto et al. 2017, Li et al. 2019) and environmental occurrence (Benton et al. 2015, Wan et al. 2020).

To increase the understanding of the mechanism of toxicity and its increase with time, a toxicokinetic-toxicodynamic (TKTD) model, e.g. belonging to the General Unified Threshold model for Survival (GUTS) can be used (Ashauer et al. 2010). The TK part of the model describes the fate of a toxicant from the surrounding environment to the internal body and may consist of uptake, absorption, excretion, and biotransformation (Kretschmann et al. 2011), depending on the complexity of the model used. The TD part of the GUTS framework usually models survival, but, immobility without recovery can also be modelled by the GUTS model (Ashauer et al. 2011a, Jager et al. 2011). Immobility is a better endpoint for IMI since neonicotinoids are neurotoxic and expected to cause effects on behaviour (Morrissey et al. 2015). Currently, some studies are available which include bioaccumulation and metabolisation of IMI in bees (Nauen et al. 2001, Suchail et al. 2004a, Zaworra et al. 2019), plants (Mach et al. 2018), and lizards (Wang et al. 2018), while one study with internal concentration measurements is available for aquatic organisms (Ashauer et al. 2010). In that study, no metabolisation of the parent compound was observed in *G. pulex*. However, *G. pulex* may not be the most representative aquatic organism for IMI, as it is relatively insensitive compared to aquatic insect species (Roessink et al. 2013, Van den Brink et al. 2016).

To understand the mechanism of IMI toxicity to aquatic organisms and the roles of its metabolites, the current study was designed to address (1) whether the metabolites are similarly toxic as IMI to sensitive and less-sensitive species, using *C. dipterum* and *G. pulex* as representatives; (2) whether toxicokinetics (TK) of IMI and its toxic metabolites, can explain the difference in toxicity of IMI to two different species as well as the observed increase of

2

toxicity with time. To address this, two types of experiments were performed. First, the toxicity of IMI and different metabolites was assessed by an acute standard toxicity experiment. Secondly, kinetic and bioconcentration experiments were conducted and a one compartment TK model and biotransformation TK model approaches were used to address the necessity of including biotransformation in the assessment of the species specific overall risks of IMI. Besides, a full GUTS model was used to predict the long term effects of IMI and IMI-ole to both species.

2.2. Materials and methods

2.2.1 Chemicals and test organisms

Imidacloprid (IMI; CAS: 138261-41-3) and its commercial available metabolites imidacloprid-olefin (IMI-ole; CAS: 115086-54-9), 5-hydroxy-imidacloprid (5-OH-IMI; CAS: 155802-61-2), imidacloprid-urea (IMI-urea; CAS: 120868-66-8) and 6-chloronicotinic acid (6-CNA; CAS : 5326-23-8) were used in our experiments (Table S1). Imidacloprid-d4 (IMI-d4; CAS: 1015855-75-0) was used as an internal standard during the analytic measurements of any organism samples. The stock solutions of IMI (200 µg/mL) and IMI-d4 (200 µg/mL) were dissolved into 2% acetone (v : v) to ensure that the compounds were fully dissolved. The volume percentage of acetone in the experimental jars was less than 0.01% (v : v). IMI-ole, IMI-urea, 5-OH-IMI and 6-CNA were dissolved into MiliQ water.

Two species, the ephemeropteran *Cloeon dipterum* and the amphipod *Gammarus pulex*, were used in the experiments. *C. dipterum* was collected from an uncontaminated test system at the outdoor research site 'De Sinderhoeve' located in Renkum, the Netherlands (www.sinderhoeve.org). *G. pulex* was collected from an uncontaminated location, the Heelsumse Beek (a brook with the coordinates 51.973400, 5.748697). After collection, the organisms were kept in aerated tanks in the laboratory for at least 3 days to acclimate them to laboratory conditions. During the acclimation period, organisms were fed *ad libitum* with biofilm, organic matter and periphytic algae for *C. dipterum* and leached *Populus* leaves for *G. pulex* (Roessink et al. 2013). All jars containing the test organisms were placed in a water bath maintained at 18 ± 1 °C with a light regime of 12:12 hours light : dark. The light in our water bath did not contain ultraviolet light in order to prevent the photodegradation of IMI and its metabolites which was confirmed by the analytical measurement with LC/MS-MS. The groundwater obtained from the Sinderhoeve experimental station and also the freshwater

from the organisms collection locations have been evaluated by LC/MS-MS to confirm the lack of presence of all the tested analytes.

In addition to the number of organisms required for the toxicity experiments, approximately 50 extra organisms were collected at the beginning of each experiment to characterise the test population by measuring the length and lipid content of the individuals using methods described by Rubach and co-workers (Rubach et al. 2010).

2.2.2 Toxicity experiments

The acute toxicity of each compound (IMI, IMI-ole, IMI-urea, 6-CNA and 5-OH-IMI) was assessed by a 4-day standard acute toxicity test to assess, the EC_{50} and LC_{50} for *C. dipterum* and *G. pulex* (Roessink et al. 2013). In detail, separate tests were performed on each test compound and species combination. Per replicate system, 12 mayflies were placed in 1 L groundwater obtained from the Sinderhoeve experimental station. The volume was dosed with its respective compound to reach final exposure concentrations of 0, 1, 10, 30, 100 or 300 μg/L. The tests were performed between December 2018 and February 2019, using a winter generation of *C. dipterum*. For the tests with *G. pulex*, a replicate test system consisted of 10 individuals in 1 L groundwater, after which, the volume was dosed to reach concentrations of 0, 10, 30, 100, 300 or 1000 μg/L. These tests were performed in July 2019, using a summer generation of *G. pulex*. Experiments were performed with three replicates per treatment level, while five replicates were used for control and the solvent control. The test systems were not aerated during the experiments to minimise evaporation of chemicals, and the dissolved oxygen content was acceptable with a value of higher than 7 mg/L at the end of experiment (*SI.xlsx*). In the experiments with *G. pulex,* a piece of stainless steel mesh was added to provide shelter. Organisms were checked every day and the effect status (dead, immobile or mobile) of each individual organism was assessed according to (Roessink et al. 2013). Dead and immobilised organisms were both considered as immobile. Dead organisms and moults were removed daily. 1 mL of water was taken daily to verify the exposure concentration dynamics of the spiked chemical and to measure the concentration of the tested analytes (IMI, 5-OH-IMI, IMI-urea, IMI-ole, 6-CNA) using LC-MS/MS (see section 2.2.5). All jars were placed randomly in a water bath, temperature and light conditions were the same as the acclimation period. When control immobility exceeded 10%, the results of the whole experiment were considered to be indicative only (Roessink et al. 2013). Dissolved oxygen, pH,

electrical conductivity, and temperature were measured at the start and end of the test in the control group and the highest treatment only, and the results are provided in the support information (*SI.xlsx*).

2.2.3 Toxicokinetic experiments

In the toxicokinetic experiments, *C. dipterum* and *G. pulex* were both exposed to IMI and IMI-ole at a concentration lower than one-tenth of the 48h-EC$_{50}$ for immobilisation, as determined in the toxicity experiments, to ensure that no effects of the chemicals would occur on tested organisms. Exposure lasted for 2 days, after which organisms were transferred to new groundwater for a 3 days depuration period. In detail, for the tests with *C. dipterum*, 18 individuals were put in 1 L groundwater and exposed to 6.4 µg/L IMI or 5.4 µg/L IMI-ole. For the tests with *G. pulex*, 10 individuals were put in 1 L groundwater containing 12.5 µg/L IMI or 7.9 µg/L IMI-ole. After 2 days of uptake, the alive organisms were rinsed for 30 seconds using clean MillQ water, and transferred to 1 L clean groundwater to start the 3 days elimination phase. At around 0, 4, 9, 20, 25, 32, 48, 53, 74, 94, 104 and 120 hours, 1 mL water was collected from the jars and analysed by LC-MS/MS (for detailed timepoints, see the raw data in *SI.xlsx*). For the TK experiments with IMI and *C. dipterum* and *G. pulex* and IMI-ole and *C. dipterum*, three replicates were sampled at each timepoint while five replicates were used for the experiments with *G. pulex* and IMI-ole. Negative controls were added with five replicates containing organisms but no chemical or solvent, five replicates contained organisms and solvent but no chemical and three replicates contained the chemical but not the organisms. From the sampled jars all alive organisms were collected, washed by MillQ water for 30 seconds, and stored at -20°C for further chemical analysis. The concentration of IMI and IMI-ole, and the possible other analytes were measured in both the organisms and the water during the uptake and elimination phase. All remaining organisms were checked for status every day and the dead organisms and moults were removed daily.

2.2.4 Bioconcentration of IMI and the generation of its metabolites

To explore the contribution of the passive absorption of IMI to the body surface of the dead organisms, organisms collected in September 2019 were immediately frozen after collection (-20 °C, for 24 hours). After this, the organisms were thawed and added to groundwater containing 24 or 120 µg/L IMI in case of *C. dipterum* and to 240 or 1200 µg/L in case of *G. pulex*. The treatments and solvent control had three replicates. After 24 hours, all the organisms

were taken out and rinsed using clean MillQ water. The internal concentration through passive absorption will be compared to the internal concentrations measured in organisms which died on day 1 at the same concentration of exposure (see below).

In order to facilitate the detection of metabolites and also compare the bioconcentration ratio of IMI among different status (dead, immobile, mobile) of organisms after 4 days, we exposed the two species to a higher exposure concentration than in the TK experiment. These two higher concentrations intended to cause 50% and 100% immobilisation and 20% and 50% death based on previous acute toxicity results. The identification of organisms status was the same as in the acute toxicity experiments. After 4 days of exposure, the internal concentration of IMI and its metabolites was measured. In detail, 12 individuals of *C. dipterum* and 10 individuals of *G. pulex* collected in September 2019 were exposed in 1 L groundwater to 24 or 120 µg/L IMI in case of *C. dipterum* and to 240 or 1200 µg/L in case of *G. pulex*. Each treatment had six replicates while the control and solvent control contained five replicates. Dead organisms were removed every day and were stored in the freezer (-20 °C) for further analysis. After 4 days of exposure, the organisms were taken out from the jars and washed by clean water for 30 seconds. In order to evaluate to what extent the passive physical absorption can account for the estimated bioaccumulation, the internal concentration of the organisms which died during the first day will be compared with the passive absorption of the corpse organisms. For the other organisms, they were classified as dead, immobile or mobile and analysed for their internal concentration of IMI and the potential metabolites. When on a certain sampling date, only a few organisms died in one replicate, the dead organisms of different replicates within a treatment level were merged together to achieve enough material for the analysis of the internal concentration. Hence, the replication of the internal concentration results varied from 2 to 6 (for detailed information of replication, see the raw data in *SI.xlsx)*. The results were used to calculate the bioconcentration ratio (BCR) of IMI and the generation ratio of potential metabolites. The analytical verification of the concentrations can be found in section 2.2.5.

2.2.5 Chemical analysis

In the toxicokinetic experiment with IMI and IMI-ole (section 2.2.3) and the bioconcentration of IMI and the generation of its metabolites (section 2.2.4), the internal concentration of parent compounds and the potential metabolites (IMI-ole, 5-OH-IMI, IMI-urea, 6-CNA) were

measured at each timepoint in each test. For the analytical quantification of the concentrations, all samples were taken out of the freezer and the organisms were lyophilised for 1 day and weighted to get the dry weight of animals. 1 mL 1% acetic acid MeOH : Water (v : v = 5 : 1) extraction solution and 25 µL internal standard (imidacloprid-d4, 200 µg/L) were added. Then the samples were homogenised with a Minilys personal homogeniser (Bertin Instruments, France) using a Precellys ceramic lysing kit (1.4/2.8 mm; Bertin Instruments, France) for 3 times 60 sec at 3000 rpm using a 30s interval in between. After this, the sample was centrifuged at 10000 rpm at 10 minutes, and the supernatant was filtered over a PTFE syringe filter (pore size 0.45 µm), into a 2 mL injection vial. Filters were injected with 200 µL extraction solution again to regain the chemical may remain on the filter, this filtrate in turn, was centrifuged and filtered over a syringe filter (0.45 µm) as well. Afterwards, the two filtrates were combined and a final volume of 1.2 mL was collected, after which the sample was ready for analysis by LC-MS/MS. The water samples were analysed directly, without an extraction step.

All samples were analysed by reversed-phase liquid chromatography-tandem mass spectrometry (LC-MS/MS) (Kamel 2010, Roessink et al. 2013). The analyses were performed on an Agilent 1260 Infinity liquid chromatography coupled with a 6460 Triple quad mass spectrometer (Agilent Technologies, USA). Separations were carried out on an Agilent Eclipse Plus C18 column (4.6 × 150 mm, 5 µm) at 40℃. The injection volume of the samples was set at 30 µL. The mobile phase used was MeOH + 0.1% Formic acid (C) and Milli-Q water+ 0.1% Formic acid (D) with the following multistep gradient: 0-1.5 min: 90/10 (C/D, v:v); 1.5-2.5 min: 90/10 (C/D, v:v) to 50/50 (C/D, v:v); 8 min: 50/50 (C/D, v:v); 8-8.1 min: 50/50 (C/D, v:v) to 0/100 (C/D, v:v); 9 min: 0/100 (C/D, v:v); 9-9.1 min: 0/100 (C/D, v:v) to 90/10 (C/D, v:v); 9.1-12 min: 90/10 (C/D, v:v) at a flow rate of 0.7 mL/min. The mass spectrometer was operated using Agilent jet stream electrospray ionisation source (AJS-ESI) in positive mode. Nitrogen was used both as nebuliser and collision gas, the capillary voltage was 5000 V and the temperature of the ion source (TEM) was set at 300°C. The compounds were detected in multiple reaction monitoring (MRM) using two transitions per compound. The MS/MS transitions of all compounds are provided in Table S2.

Injected samples were quantified by peak area using the calibration curve constructed from calibration standards included in the same sample sequence. Agilent Masshunter software

(version 7.0) was used for instrument control and data acquisition. The extraction recovery of each tested analytes (IMI, IMI-ole, 5-OH-IMI, IMI-urea, 6-CNA) in the organisms, evaluated at two concentrations by spiking them into the clean organisms, were acceptable for both species based on recovery and repeatability (for further information of analysis methods and recovery results, see Text S2 and Table S3, S4, S5 in Support information).

2.2.6 TK and GUTS Modelling

2.2.6.1 First-order one compartment kinetic model

To determine the toxicokinetic rate constants of uptake and elimination for IMI and its metabolite IMI-ole, a first-order compartment kinetic model programmed in Matlab R2018b (http://www.debtox.info/byom.html) was used. The script was based on the method of byom_calanus_2016_onecomp in Acute Calanus package (*BYOM, version 1.1*), with a small modification that the lower limit of elimination rate was 0 instead of 0.1 in the original script.

The uptake and elimination rate of IMI and IMI-ole were estimated using a one-compartment, first-order kinetic model (Jager et al. 2011):

$$\frac{dC_{int}(t)}{dt} = k_{up} \cdot C_w(t) - k_{ep} \cdot C_{int}(t) \qquad \text{(Eq. 1)}$$

with t = time; C_{int} =internal concentration of exposed compound; C_w = concentration of exposed compound in water, k_{up} = the uptake rate constant of parent (exposed) compound and k_{ep} = the elimination rate constant of parent (exposed) compound.

The Bioconcentration factor (BCF) (L·kg^{-1}) was calculated by a kinetic method (BCF$_k$) :

$$BCF_k = \frac{k_{up}}{k_{ep}} \qquad \text{(Eq. 2)}$$

The elimination half-life ($t_{1/2}$) (day) was calculated from the elimination rate of IMI or IMI-ole:

$$t_{1/2} = \frac{ln2}{k_{ep}} \qquad \text{(Eq. 3)}$$

2.2.6.2 Biotransformation TK model (Bio-TK)

For a better understanding of the biotransformation of IMI in the two species, the biotransformation model as described by Kretschmann et al. (2011) (Kretschmann et al. 2011) was used, with one minor modification. The modification was that in our model we considered IMI-ole as the only metabolite of IMI, the remaining potential unknown metabolites were all

included in $b\_k_{e\_parent}$ (elimination rate) of IMI. The model script was based on the method of byom_bioconc_start (BYOM, version 5.2) with the modifications that we introduced the biotransformation parameter, $b\_k_{bio\_parent}$ (Eq. 4) and the elimination rate of metabolite $k_{e\_metabolite}$ (Eq. 5). To better distinguish the two model approaches, parameters in this biotransformation model have a prefix of b.

The uptake and elimination rate of IMI, as well as its biotransformation rate, was estimated using a one-compartment, first-order kinetic model:

$$\frac{dC_{int_{parent}}(t)}{dt} = b\_k_{u\_total} \cdot C_w(t) - b\_k_{e\_parent} \cdot C_{int_{parent}}(t) - b\_k_{bio\_parent} \cdot C_{int_{parent}}(t)$$

(Eq. 4)

with t = time; $C_{int_{parent}}$ = internal concentration of IMI, C_w = water concentration of IMI, $b\_k_{u\_total}$ = the uptake rate constant for IMI, $b\_k_{e\_parent}$ = the elimination rate constant of IMI and $b\_k_{bio\_parent}$ = the biotransformation rate constant of IMI to IMI-ole.

For the metabolite (IMI-ole) the TK model used was:

$$\frac{dC_{int_{metabolite}}(t)}{dt} = b\_k_{bio\_parent} \cdot C_{int_{parent}}(t) - b\_k_{e\_metabolite} \cdot C_{int_{metabolite}} \qquad \text{(Eq. 5)}$$

with t = time; $C_{int\_metabolite}$ = internal concentration of IMI-ole, $C_{int_{parent}}$ = internal concentration of IMI, $b\_k_{bio\_parent}$ = the biotransformation rate constant of IMI to IMI-ole and $b\_k_{e\_metabolite}$ = the elimination rate constant of IMI-ole.

The total elimination rate ($b\_k_{e_{total}}$) of IMI was:

$$b\_k_{e_{total}} = b\_k_{bio\_parent} + b\_k_{e\_parent} \qquad \text{(Eq. 6)}$$

The BCF kinetic of IMI (BCF$_k$) was calculated as:

$$b\_BCF_k = \frac{b\_k_{u\_total}}{b\_k_{e_{total}}} \qquad \text{(Eq. 7)}$$

Elimination half-life ($t_{\frac{1}{2}IMI}$) (day) was calculated from the elimination rate for IMI:

$$b\_t_{\frac{1}{2}IMI} = \frac{ln2}{b\_k_{e_{total}}} \qquad \text{(Eq. 8)}$$

2.2.6.3 Prediction of long term effects of each compound by the GUTS model

The GUTS model approach includes a reduced model and a full model depending on whether the measured internal concentration is included (Jager et al. 2011). Besides, GUTS uses individual tolerance (IT) and stochastic death (SD) concepts to describe the effect mechanism on the endpoint (Jager et al. 2011). IT assumes that organism die (or is immobilised) immediately on reaching a critical internal concentration, which is unique for each individual. SD assumes that all individuals are identical but mortality is a probabilistic process, which increases with increasing internal concentration of the substance (Van den Brink et al. 2013). Both are rational in explaining the effect mechanism, and this also illustrates the mechanism diversity of organisms exposed to different substances (Ashauer et al. 2016).

Both the reduced and the full GUTS models were used to describe the TKTD of IMI and IMI-ole in the two species. The models used were similar to the ones used by Jager and co-authors (Jager et al. 2017), with two minor modifications. First, we used the mobility fraction instead of the survival fraction, second, we set the lipid content percentage to zero, as none of the analytes in our tests are hydrophobic. For specific model scripts and optimisation used, see the Acute Calanus package (*BYOM, version 1.1*)(Jager et al. 2017). We calibrated both the reduced and full GUTS models including both the IT and SD mechanisms to our data sets, so 4 models in total were parameterised. Among the models for each data set, the Akaike information criterion (AIC) and goodness-of-fit measures were used to select the best-fitting model. This is not a formal significance test but has been broadly used to select alternative models (Anderson. 2002). A difference of AIC of more than 6 can be interpreted as that the poorest model is 0.05 times as probable as the best model to minimise information loss (Jager et al. 2017).

2.2.7 Statistics

Dose-response relationships were fitted using the nominal exposure concentration at the endpoints (mortality and immobilisation) with acute toxicity data using the following log-logistic equation, calculated using Genstat 19th edition (VSN International Ltd).

$$y(conc) = \frac{1-c}{1+e^{-b \times (\ln conc - a)}} \qquad \text{(Eq. 9)}$$

Where y is the fraction of dead or immobile test organisms, conc is the concentration (µg/L), a is ln(median effect concentration [EC_{50}]) or ln(median lethal concentration [LC_{50}]) (µg/L), b

is the slope (L/µg), and c is the fraction of control mortality or immobilisation(-) (Roessink et al. 2013).

As the steady state may not be reached within 4 days, especially in the higher exposure concentrations, the bioconcentration ratio (BCR) was used to describe the internal concentration of IMI (Eq. 10), and the generation ratio was used to describe the metabolite, IMI-ole (Eq. 11).

$$\text{Bioconcentration ratio of IMI} = \frac{\text{internal concentration of IMI}}{\text{exposure water concentration}} \qquad \text{(Eq. 10)}$$

$$\text{IMI-ole generation ratio} = \frac{\text{internal concentration of IMI-ole}}{\text{internal concentration of IMI-ole+internal concentration of IMI}} \quad \text{(Eq. 11)}$$

Significant differences between treatments were assessed using R (version 3.5.1). The assumptions of normality were assessed with a Shapiro-Wilk test, and the assumption of equal variance was assessed using a Spearman rank correlation between the residuals and dependent variable. If assumptions of normality and equal variance were passed, a one-way analysis of variance (ANOVA) with α=0.05 and a post-hoc Tukey's test was conducted. If assumptions failed, a Kruskal-Wallis test, with α=0.05, and a post-hoc Dunn's test was used.

2.3. Results and discussion

2.3.1 Sensitivity of IMI and its four metabolites to C. dipterum and G. pulex

All measured exposure concentrations at the start and the end of the test were within 10% variation (+,-) from nominal concentrations, thus the nominal concentrations of each analyte (IMI, IMI-ole, IMI-urea, 5-OH-IMI and 6-CNA) were used for all calculations. The control immobility of all tests was within 10%, therefore the results were considered reliable. Among the five analytes, only IMI and IMI-ole showed effects to the tested species within the test concentration range, therefore we defined that IMI-ole is the bioactive metabolite. Therefore, only the results of IMI and IMI-ole will be presented and discussed. All other analytes showed no toxicity at concentration levels $\leq$ 300 µg/L to *C. dipterum* and $\leq$ 1000 µg/L to *G. pulex.*

Based on the 96h-EC$_{50}$ values, IMI was a factor of 2.3 more toxic to *C. dipterum* than IMI-ole, while their 96h-LC$_{50}$ were close (Table 2.1). The 96h-EC$_{50}$ of IMI in our study was comparable to the 96h-EC$_{50}$ value of 18 µg/L, reported by Van den Brink and co-workers (Van den Brink et al. 2016) for a winter generation of *C. dipterum*. Although the toxicity of IMI-ole to *C. dipterum* was somewhat delayed at the start (day 1) compared to IMI it reached similar toxicity in terms

of lethality compared to IMI on day 4 (96h-LC_{50} for IMI was 90.6 µg/L and for IMI-ole 104 µg/L, Table 2.1). Our results agree with a study performed by Suchail et al. (2001), where an oral application IMI-ole exerted similar acute toxicity to honeybees as IMI, while two other imidacloprid metabolites (IMI-urea, 6-CNA) showed no or much lower toxicity.

Table 2.1: *The acute toxicity upon exposure of IMI and IMI-ole to C. dipterum and G. pulex provided in EC_{50} and LC_{50} values followed by the 95% confidence interval between brackets (an asterisk means that the CI could not be calculated) and the slope of the curve (parameter b) after the semicolon.*

Tested Species	Exposure Compound	Day	1	2	3	4
C. dipterum	IMI	EC_{50}	109 (102 - 116); 16.0	86.2 (73.9 - 101); 11.8	40.9 (32.9 – 60.0); 4.06	24.4 (*); 11.1
		LC_{50}	311 (259 - 374); 4.01	110 (102- 117); 14.9	105 (99.4- 111); 15.6	90.6 (73.9–111); 4.06
	IMI-ole	EC_{50}	318 (252 - 401); 3.29	100 (*); 16.0	88.5 (*); 14.0	57.1 (43.1 – 75.6); 4.15
		LC_{50}	> 300	> 300	380 (149 – 971); 4.26	104 (98.6 - 110); 14.8
G. pulex	IMI	EC_{50}	170 (*); 2.49	145 (*); 2.82	165 (122 - 222); 2.30	109 (101 - 117); 14.0
		LC_{50}	> 1000	> 1000	> 1000	731 (290 - 1844); 0.587
	IMI-ole	EC_{50}	681 (533 - 870); 3.13	382 (270 - 542); 1.57	594 (449 - 784); 2.70	456 (350 - 595); 3.17
		LC_{50}	> 1000	> 1000	> 1000	> 1000

Similar to *C. dipterum*, only IMI and IMI-ole showed a 96h-EC_{50} < 1000 µg/L for *G. pulex* (Table 2.1). IMI-ole was 4.2 times less toxic than IMI in terms of 96h-EC_{50} (Table 2.1). More specifically, the 96h-EC_{50} of IMI and IMI-ole to *G. pulex* were 109 and 456 µg/L, respectively, while the 96h-LC_{50} were 731 and > 1000 µg/L, respectively (Table 2.1). Our results for IMI to *G. pulex* are in line with those of Ashauer et al. (2011b) and Van den Brink et al. (2016), who reported 96h-EC_{50} values of 132 µg/L and 49 µg/L, respectively.

In addition, we measured all analytes (IMI, IMI-ole, 5-OH-IMI, IMI-urea, 6-CNA) in all water samples of all treatments. We only found 6-CNA in the water samples of the highest IMI-ole treatment and the percentage of 6-CNA to IMI-ole was about 2% - 3% for both species (Figure S1). Although no other aquatic study is available, our finding is indirectly supported by studies that found 6-CNA under IMI exposure in bees (Suchail et al. 2004a) and in plants and soil (Li et al. 2019). Since 6-CNA is highly water soluble and quite stable in the environment (Zabar et al. 2011), depuration from aquatic organisms is likely to be quick. This could explain why we could not detect it in the tested organisms but only in water. As honeybees are not surrounded by water, 6-CNA may be less effectively excreted by this species, explaining why the metabolite was still detected in the bees (Suchail et al. 2004a).

To the best of our knowledge, our study is the first one showing toxic effects of the metabolites of IMI on aquatic invertebrates. Our results show a similar toxicity of IMI and IMI-ole to mayflies as also has been recorded for bees (Suchail. et al. 2001, Zaworra et al. 2019). This may imply that the some toxicokinetic and toxicodynamic processes underlying the toxicity of IMI and IMI-ole might be similar between aquatic and terrestrial insect species. It is probably a result from the fact that both the parent and the metabolite possess the nitroguanidine group, which binds tightly to the receptors in insects (Motohiro Tomizawa 2000), IMI-ole showing a slightly greater affinity to nAChRs than IMI (Nauen et al. 2001, Casida 2011), In contrast, the oral toxicity of 5-OH-IMI to honey bees is close to that of IMI (Nauen et al. 2001, Suchail. et al. 2001), while no effects of 5-OH-IMI could be detected in our study on either aquatic macroinvertebrate species. This absence of in toxicity of 5-OH-IMI may firstly be explained by difference in exposure, in our study we used waterborne exposure of 5-OH-IMI while oral feeding was used in the bee study. Secondly, although 5-OH-IMI also shares the same nitroguanidine group as IMI and IMI-ole, the receptor affinity of 5-OH-IMI is 8 times lower than IMI and 53 times lower than IMI-ole for bees (Nauen et al. 2001), and it showed a 13-fold lower binding affinity to whitefly nicotinic acetylcholine receptors (Rauch and Nauen 2003).

Besides the receptor affinities, the difference in the toxicokinetics of imidacloprid and its metabolites in aquatic species could also explain the differences in toxicity, which will be discussed below.

2.3.2 TK of IMI and IMI-ole in both C. dipterum and G. pulex

2.3.2.1 One compartment TK model approach of IMI and IMI-ole in both species

In contrast to most studies that used a 1-day uptake period (Ashauer et al. 2010, Ashauer et al. 2012, Fu et al. 2018), we used a 2-days uptake period in our TK experiment. This is because the effects of IMI-ole in the acute toxicity study increased up to day 2 for both species (Table 2.1). The number of immobile organisms in all TK experiments was below 10%, confirming the initial assumption that the concentrations used were below acute toxicity levels. The water concentrations were stable during the uptake phase (*SI.xlsx*), and the average measured water concentration was used as the initial exposure concentration for each compound in each species. The change in fresh weight of the organisms overtime was not significant (Figure S2), showing that a five-day experiment without food did not result in weight loss, which was indicative of starvation.

Both *C. dipterum* and *G. pulex* were exposed to IMI or IMI-ole for 2 days to study their uptake, and subsequently to clean water for 3 days to study their elimination (Figure 2.1 and Figure 2.2). We determined an uptake rate constant of IMI in *G. pulex* of 5.21 ($L \cdot kg_{ww}^{-1} \cdot d^{-1}$), which was about 2.5 times higher compared to the k_u of 1.96 $L \cdot kg_{ww}^{-1} \cdot d^{-1}$ determined by Ashauer et al. (2010) (Ashauer et al. 2010). They reported an IMI elimination rate constant of 0.27 (d^{-1}), while we calculated one of 0.12 (d^{-1}). The differences between uptake parameters value might be due to differences in size and weight of the organisms used or the origin of the populations. Compared to the organisms of 32 mg used by Ashauer et al. (2010) (Ashauer et al. 2010), we used smaller organisms (7 mg) with larger surface-to-volume ration, potentially explaining a higher uptake rate. The difference in uptake rate constants of IMI between *C. dipterum* (2.96 $L \cdot kg_{ww}^{-1} \cdot d^{-1}$) and *G. pulex* (5.21 $L \cdot kg_{ww}^{-1} \cdot d^{-1}$) cannot be explained by length and weight (Figure S2 and Figure S3), as usually the smaller individuals accumulate more imidacloprid on a weight-specific basis than larger individuals.

After transfer of the contaminated organisms into clean water, internal IMI-concentrations decreased both in *C. dipterum* and *G. pulex*, showing that the chemical was being eliminated, metabolised or desorbed. The difference in elimination rates between the two species could attribute to the observed difference in sensitivity, as the sensitive *C. dipterum* (0.04 d^{-1}) eliminated slower than *G. pulex* (0.12 d^{-1}). As a result, the BCF$_k$ of IMI estimated by the one-compartment TK model for *C. dipterum* was 1.58 times higher than that of *G. pulex* (Table 2.2).

This might be partially explained by the fact that the elimination rate of IMI for *C. dipterum* was three times lower than for *G. pulex*, resulting in a three times longer persistence in the organisms (elimination half-life was 16.5 day for *C. dipterum* and 5.18 day for *G. pulex*).

Table 2.2: *The TK parameters of* IMI *and IMI-ole in C.* dipterum *and G.* pulex *as estimated by the simple TK model and the TK model that includes* biotransformation *(n.c represents not calculated).*

2

Species	Model type	Exposure chemical	Water concent- ration (µg/L)	Measured chemical	Parameter k_u (L·kgww^{-1}·d^{-1}) k_e (d^{-1}) b_k_{bio}_parent (d^{-1})	Value	95% CI	BCF$_k$ (L/kg)	$t_{1/2}$ (days)	R^2
C. dipterum	TK	IMI	6.36	IMI	k_{up}	2.96	2.62 - 3.33	70.11	16.44	0.92
					k_{ep}	0.04	0.00034 - 0.11			
		IMI-ole	5.44	IMI-ole	k_{up}	1.68	1.43- 1.94	8.00E+05	3.30E+05	0.81
					k_{ep}	2.10E-06	1.667e-08 - 0.1045			
	Bio-TK	IMI	6.36	IMI	b_k_{u_total}	3.18	2.973 - 3.381	36.14	7.88	0.92
					b_k_{e_total}	0.088	0.077-0.12			
					b_k_{e_parent}	1.49e-10	0 - 0.023			
					b_k_{bio_parent}	0.088	0.077 - 0.10			
				IMI-ole	$k_{e\_metabolite}$	0	0 - 0.0097	n.c	n.c	0.90
G. pulex	TK	IMI	12.54	IMI	k_{up}	5.21	4.87 - 5.54	44.41	5.91	0.98
					k_{ep}	0.12	0.11 - 0.16			
		IMI-ole	7.89	IMI-OLE	k_{up}	2.79	2.47 - 3.12	41.69	10.38	0.9
					k_{ep}	0.07	0.014 - 0.12			
	Bio-TK	IMI	12.54	IMI	b_k_{u_total}	5.13	4.66 - 5.77	39.59	5.15	0.98
					b_k_{e_total}	0.13	0.080-0.136			
					b_k_{e_parent}	0.076	0.034 - 0.13			
					b_k_{bio_parent}	0.053	0.046- 0.060			
				IMI-ole	$k_{e\_metabolite}$	0	0 - 0.057	n.c	n.c	0.98

The BCF of IMI-ole for *C. dipterum* was relatively high (8.00E+05 L·kg^{-1}) compared to IMI (70.11 L·kg^{-1}) as elimination rate of IMI-ole was very low (2.10E-06 d^{-1}), whereas the BCFk of IMI-ole was similar to IMI for *G. pulex*. The uptake difference of IMI and IMI-ole may be explained by their chemical properties as the lower Kow of IMI-ole compared to IMI (Table-S1), may result in a lower uptake rate. The elimination difference may result from the receptor affinities difference, since IMI-ole showed a slightly greater affinity to nAChRs than IMI (Nauen et al. 2001, Casida 2011). Moreover, when exposed to IMI only, the metabolite IMI-ole was also

detected in both taxa, indicating biotransformation of IMI into IMI-ole, which will be shown below.
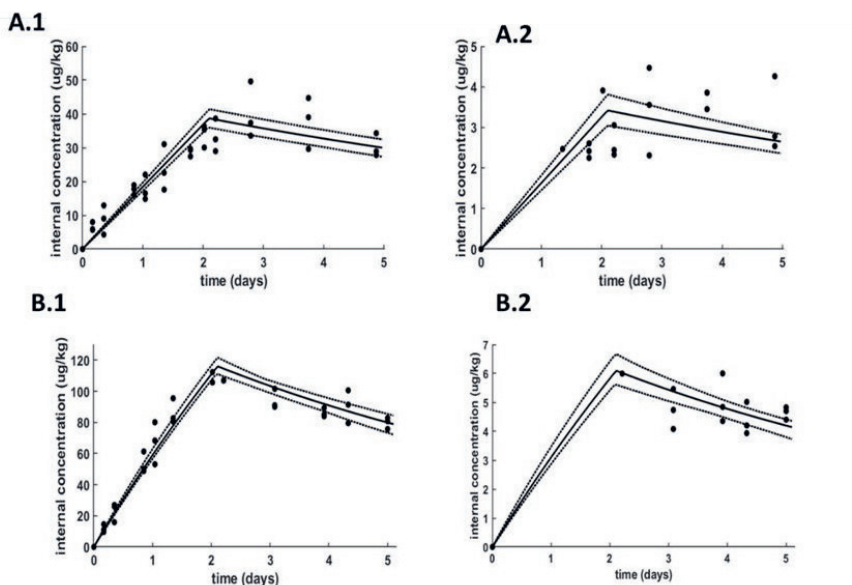
Figure 2.1: *The fit of the biotransformation TK model (bio-TK) for C. dipterum (A1: parent compound, IMI; A2: the metabolite, IMI-ole) and for G. pulex (B1: parent compound, IMI; B2: the metabolite, IMI-ole). The black lines represent the fit of the model generated by byom, the dotted line represented the confidence intervals of this fit while the dots represent the experimental results (n = 3 in A.1, A.2, B.1, B.2 with exception in Figure A.2, at day 1.35, day 2.02, n = 1; in Figure A.2, at day 2.02, n = 2, day 2.21, n = 1).*
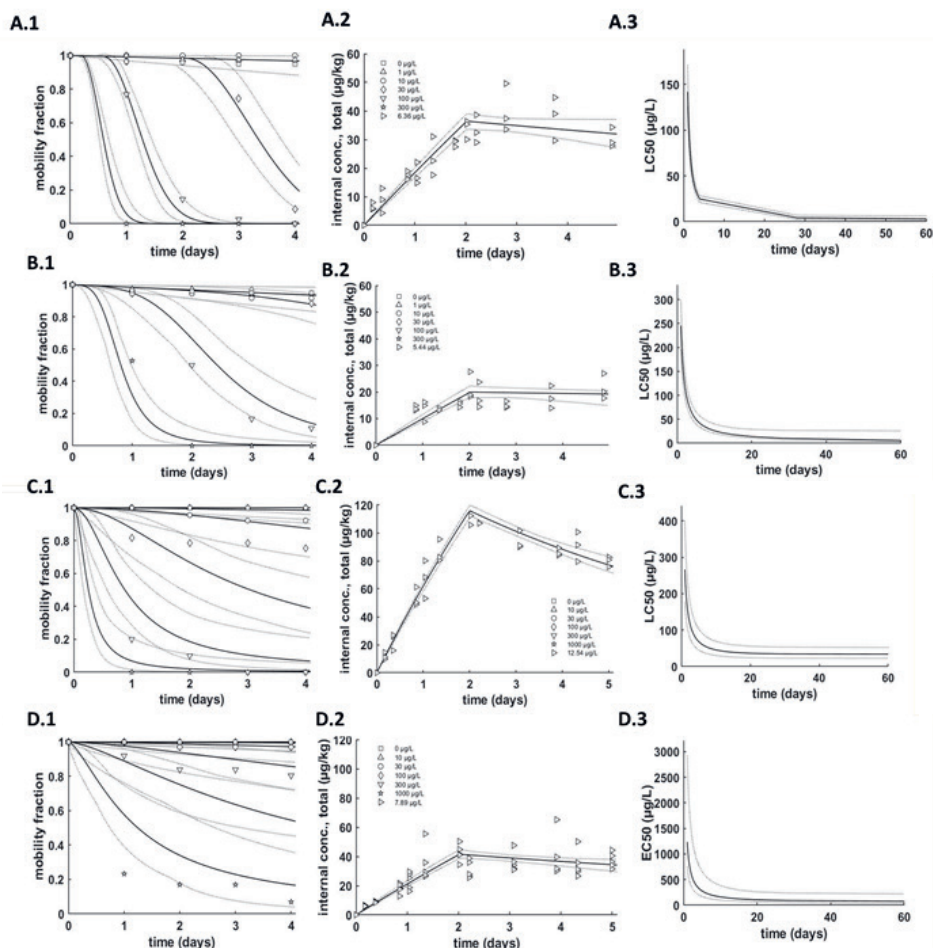
Figure 2.2: *The best-fitting GUTS model fitted on the data of IMI (A) and IMI -ole (B) for C. dipterum and of IMI (C) and IMI-ole (D) for G. pulex. The panels from left to right show (1) the mobility fraction (2) the internal concentration of IMI and (3) the predicted EC_{50} over time, respectively.*

2.3.2.2 Biotransformation TK model approach of IMI

Under IMI exposure, we detected both the parent compound and also the metabolite, IMI-ole (Figure 2.1 A2, B2). IMI-ole was the only metabolite detected among the four metabolites we tested. IMI-ole was even still being formed during the elimination phase in both organisms (Figure 2.1). The generation ratio of IMI-ole in *C. dipterum* was higher than in *G. pulex*, being 9.6% and 6.5%, respectively, at day 5 (see *SI.xlsx*).

Our result did not contradict the findings of Ashauer et al. (2010) (Ashauer et al. 2010), who did not find any metabolites in *G. pulex* after 1 day of IMI exposure, as in our tests the generation of metabolites in *G. pulex* was only detected after 2 days. The metabolisation may have started at day 1 but was only present in measurable amounts on day 2. In the two model approaches (biotransformation TK model approach and the regular TK model approach), the k_u (k_{up} in eq. 1 and $b\_k_{u\_total}$ in eq. 4), in theory, should be the same for both model approaches, but was slightly different due to the model calibration. In the biotransformation model, the $b\_k_{e\_total}$ of the parent compound was divided into two parameters, i.e. $b\_k_{bio\_parent}$ which is the biotransformation rate of IMI to IMI-ole and $b\_k_{e\_parent}$ which includes the elimination of IMI and the biotransformation rate of IMI to other potential metabolites than IMI-ole (eq. 4). For *G. pulex*, the elimination rate of IMI in both model approaches was close, while a difference factor of 2 was estimated for *C. dipterum*, although the confidence interval was overlapping. The BCFk values of IMI for each species were close for the two model approaches (Table 2.2).

The biotransformation model provided more details of the elimination pathway of IMI. In *C. dipterum* IMI was mainly depurated by biotransformation to IMI-ole (k_{bio} = 0.088 d^{-1}), which contributed 100% to the total elimination of IMI as the k_e of IMI or its transformation to other metabolites than IMI-ole was only 1.49E^{-10} d^{-1} (Table 2.2). In *G. pulex*, the k_{bio} of IMI was only 0.053 d^{-1} and biotransformation contributed only 41% to its depuration, as the k_e of IMI or its transformation to other metabolites than IMI was 0.076 d^{-1} (Table 2.2). Moreover, the estimated elimination rate of the metabolite, IMI-ole, by the biotransformation TK approach was 0 d^{-1} for both species. The very slow elimination of IMI-ole in *C. dipterum* was expected as it was also very slow when estimated by the one compartment TK model of IMI-ole exposure (Table 2.2, 2.10E^{-06} d^{-1}). When *G. pulex* is exposed to IMI-ole via the water phase, IMI-ole is eliminated quicker (k_{ep} = 0.07 d^{-1}; Table 2.2,) than when IMI-ole is formed as a metabolite ($k_{e\_metabolite}$ = 0 d^{-1}; Table 2.2), possibly because it is generated at the target sites and then bind tightly to them. To further confirm this internalising process, receptor binding assays need to be performed for aquatic invertebrates, as has been done for bees (Nauen et al. 2001).

The differences between the calculated BCF$_k$ of IMI for both species alone could not explain the EC$_{50}$ difference between them, as the results showed a 4.5 times difference with regard

to 96h-EC50 and a 1.6 times difference with regard to BCFs. Hence, the biotransformation product also likely contributed to the toxicity differences of IMI-exposures between these two taxa. The higher toxicity of IMI to *C. dipterum* may be due to the lack of elimination of the toxic metabolite IMI-ole from the test organism (Table 2.1 and Figure 2.2 B.2). *G. pulex* also biotransformed IMI to IMI-ole, but to a lower extent than *C. dipterum* which results in a lower overall exposure (Table 2.2). Likewise, Suchail et al. (2001) (Suchail. et al. 2001) suggested that for bees, imidacloprid seems to be a long-acting compound due to the generation of the metabolite IMI-ole.

Our results also indicate that a one compartment TK model was not informative enough to fully explain the difference in toxicity of IMI. This is because the metabolite IMI-ole was formed within the organisms and displayed similar toxicity as IMI, but had different elimination rates between the species. Hence, one needs to consider the toxicity and toxicokinetics of the biotransformation component as well, which is in agreement with other studies emphasising the importance of biotransformation in toxicity process (Kretschmann et al. 2011, Fu et al. 2018).

2.3.2.3 Prediction of long term effect of each compound by the GUTS model

We integrated the results of the toxicity and TK experiments performed with IMI and IMI-ole and for both species in the GUTS model to predict the long term effect of each compound as described by (Jager et al. 2017). For IMI we compared the prediction with experimental 28 days toxicity data gained from (Roessink et al. 2013, Van den Brink et al. 2016). Our results showed that the full GUTS model provided a closer prediction of the observed chronic toxicity of IMI than the reduced model (Table S7). Further, we found that the results using the IT mechanism fitted the chronic data better than the SD mechanism, based on the smaller AIC and the higher goodness-of-fit measures (Table S8). Except for the toxicity of IMI to *C. dipterum*, which fitted better to the SD mechanism. Our result of *C. dipterum* with IMI was consistent with (Focks et al. 2018), as they also found that the SD mechanism explained better the toxicity of IMI to a variety of aquatic organisms. The result of *G. pulex* was consistent with Nyman et al. (2013), which found that the IT assumption fitted better in terms of the effect of IMI to *G. pulex* (Nyman et al. 2013), indicating that immediate effect occurs when the internal concentration in an individual exceeds its threshold.

The prediction of the 28d-EC_{50} of IMI to *G. pulex* 34.7 (22.9 - 53.4) µg/L was close to the chronic experiment results (Roessink et al. 2013) of 15.4 (9.80 - 24.1) µg/L; whereas the prediction of 28d-EC_{50} of IMI to a winter population of *C. dipterum* (4.3 µg/L, 2.4-6.9 µg/L) was higher than the experimental results (0.68 µg/L, 0.45 - 1.0 µg/L) (Van den Brink et al. 2016). The possible reason could be they used smaller organism (0.38 ± 0.05 cm) than in our toxicity and TK experiments (0.50 ± 0.07 cm) or more likely due to the biotransformation process in *C. dipterum* and the generation of a toxic and hardly eliminated metabolite, IMI-ole, which was not included in our model prediction. The discrepancy also emphasised the importance of incorporating active metabolites in further studies.

The prediction of the 28d-EC_{50} of IMI-ole was 10.4 (7.59-26.9) µg/L for *C. dipterum* and 135 (54.0-237) µg/L for *G. pulex.* Recently, Wan, et al. (2020) detected IMI-ole in filtered source water at concentrations 0.14 ng/L (Wan et al. 2020). However, we do not know much about the aquatic environmental occurrence and concentrations of IMI-ole, while some related studies can support the existence of IMI-ole in surface water. For example, imidacloprid and its metabolites may move into the water column through leaf degradation, since IMI, IMI-ole, and 5-OH-IMI have been detected in hemlock foliage tissue (Coots et al. 2013, Benton et al. 2015). A recent study found that although no IMI-ole could be detected in the water samples from headwater streams adjacent to hemlock stands treated with imidacloprid, but they detected the bioaccumulation of IMI-ole (concentration of imidacloprid-olefin in the one sample was 28.9 ng/g) (Crayton et al. 2020). In a combination with our results and current literature, the environmental water concentration of IMI-ole is low and may be relevant for the overall effects of IMI because IMI-ole is only formed by biotransformation by organisms and its elimination may be slow.

2.3.3 *Bioconcentration of IMI and the generation of its metabolites*

The toxicity of IMI to *C. dipterum* in this experiment was higher than expected based on the acute toxicity test results (Table 2.1 and Figure 2.4). This was due to the use of smaller organisms in this experiment compared to previous acute toxicity tests (Figure 2.4 and Figure S3). For *G. pulex*, half of the organisms died on day 4 when exposed to 1200 µg/L, while all organisms were immobile (Figure 2.4). This was consistent with the results from the toxicity tests, and the sizes of *G. pulex* used in these two experiments were also similar (Figure 2.4 and Figure S3). As all *C. dipterum* died on day 4, we only could get the internal concentration

results in dead organisms (Figure 2.3 A, B), hence no comparison of the results for corpses, dead, immobile and mobile *C. dipterum* can be made. For *G. pulex*, the comparison amongst organisms of different status was usable (Figure 2.3 C, D, E, F).
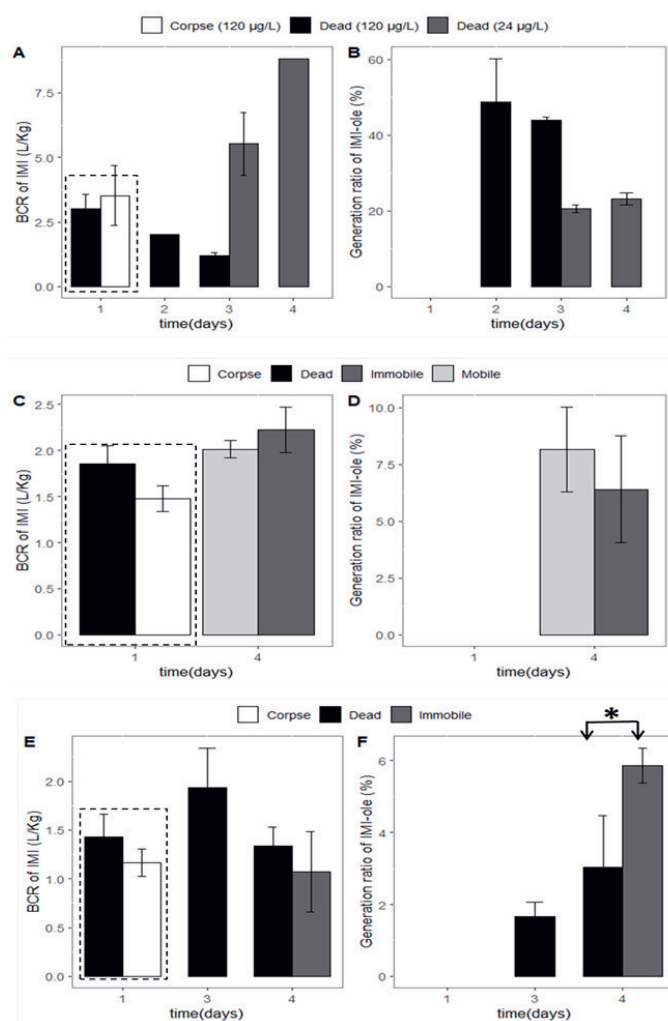
Figure 2.3: *The BCR (bioconcentration ratio) of IMI and generation ratio (in%) of IMI-olefin in C. dipterum are shown in panel A and B, respectively while those for G. pulex of the 240 µg/L treatment are shown in panel C, D and those for G. pulex of the 1200 µg/L treatment are shown in panel E and F, respectively. The dotted frame in A, C,E represents the comparison of passive absorption by deceased organisms (corpses) and the active and passive bioconcentration by organisms which died within day one. Corpse represented deceased organisms by freezing to evaluate the passive absorption of IMI, Dead represented organism who died during the experiment, immobile represented immobilised*

organisms during the experiment. * denotes a significant difference. Error bars represent standard error of the mean.

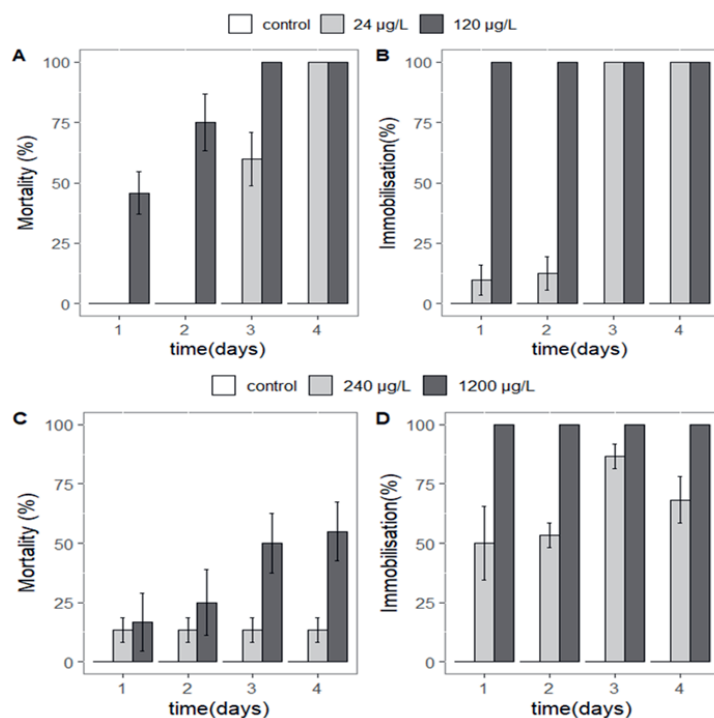**Figure 2.4**: *The mortality and immobilisation of C. dipterum (panel A and B), mortality and immobilisation of G. pulex (panel C and D) in the different concentration treatments (n = 6). Error bars represent standard error of the mean.*

2.3.3.1 The passive absorption and active bioconcentration comparison

This experiment aimed to estimate the contribution of passive absorption of IMI by the deceased organisms, in order to gain knowledge to what extend the physical absorption can account for the bioconcentration. The BCR of IMI for *C. dipterum* in the 120 μg/L treatments and *G. pulex* in 240 μg/L and 1200 μg/L treatments on the first day showed no difference between the passive absorption by deceased organisms (corpses) and the passive and active uptake by organisms which died within day 1 in the test (Figure 2.3 A, C, E dotted frame). But the BCR of IMI for the deceased *C. dipterum* was higher than for *G. pulex* (Figure 2.3 A, C, E dotted frame), which might be due to their length and weight (Figure S2 and Figure S3), as smaller individuals accumulate more imidacloprid on a weight-specific basis than larger individuals. Smaller organisms accumulated more in case of passive absorption (Figure 2.3 A,

2

C, E dotted frame part) and this relationship was also found by Rubach et al. (2010) for another insecticide, chlorpyrifos (Rubach et al. 2010). Although both the exact time of death and the dynamics of active bioconcentration within 1 day by the organisms were unknown, the comparison indicated that passive absorption should not be neglected. In other words, a considerable amount of IMI adsorbed to the animal's surface or exoskeleton passively. Miller et al. (2016), who analysed the exoskeleton of gammarids that moulted during the exposure period found that the percentage of the total body residue adsorbed to the exoskeleton was between 3 and 24% for five pharmaceuticals (Miller et al. 2016). In order to perform further research and compensate for the limitation of our method, some analysis methods, such as mass spectrometry imaging (Ewere et al. 2019) can provide more information on the distribution of compounds in or on the organisms.

2.3.3.2 The BCR of IMI and the generation ratio of its metabolites in organisms with different status

The BCR of IMI was higher in *C. dipterum* than in *G. pulex* (Figure 2.3 A, C, E). In addition, in both species, IMI-ole was the only metabolite detected in the body after day 1 for *C. dipterum* and after 2 days for *G. pulex*, while *C. dipterum* generated more IMI-ole than *G. pulex* (Figure 2.3 B, D, F), which agrees with the previous TK results (Figure 2.2). The BCR of IMI in the dead *C. dipterum* in the 120 μg/L treatment decreased over time (Figure 2.3 A, *p = 0.017*). This may be due to the generation of unknown metabolites because the ratio of IMI-ole did not change between day 2 and day 3 (Figure 2.3 B). The BCR of IMI in the dead *G. pulex* in the 1200 μg/L treatment did not change over time (Figure 2.3 E). The generation ratio of IMI-ole was significantly higher in immobile than in dead organisms *(*Figure 2.3 F, *p = 0.034,)* on day 4, as a result of the termination of the biotransformation of IMI when organisms died. As for the comparison among another status, there were no significant differences.

The high generation ratio of the toxic metabolite IMI-ole, especially for *C. dipeturm* (49%) was in line with another study which found IMI-ole concentrations to be 3.4 fold higher than that of IMI after a 46-day dietary exposure study with bees (Erban et al. 2019). Our findings are also consistent with other studies which found that IMI-ole was the major metabolite after exposing IMI to termites (Tomalski et al. 2010), lizards (Wang et al. 2018) and bees (Erban et al. 2019). In our study, compared to *G. pulex,* the more sensitive mayfly had a higher internal concentration of IMI and its toxic metabolite, IMI-ole. This result indicates that the generation

of the metabolite IMI-ole, which was persistent in the body (see section 2.3.2 TK results), contributes to the overall IMI toxicity.

We summarised four possible metabolic pathways based on published information on the biotransformation of IMI in organisms (Figure 2.5 A). These comprised 1) the pathway where IMI was transformed to 5-OH-IMI, then to IMI-ole (Tomalski et al. 2010), and might be further transformed to 6-CNA (Nishiwaki et al. 2004); 2) the pathway where IMI was transformed to IMI-urea, 3) the pathway where IMI was transformed immediately into 6-CNA (Fusetto et al. 2017); and 4) where IMI was transformed to IMI-ole (Fusetto et al. 2017) (Figure 2.5 A). Integrating all our toxicity, internal kinetic and biotransformation results, we conclude that among the four selected metabolites (IMI-ole, 5-OH-IMI, IMI-urea, 6-CNA), IMI-ole was generated within both organisms once they were exposed to IMI after 1 or 2 days; 6-CNA was detected in the water when both organisms were exposed to IMI-ole (Figure 2.5 B). Suchail et al. (2004) summarised that IMI generates 6-CNA through a putative metabolite, 6-chloropicolyl alcohol (Suchail et al. 2004a). We hypothesise that IMI was biotransformed to IMI-ole, after which IMI-ole may be biotransformed further to 6-CNA. To our knowledge, the formation of 6-CNA from IMI-ole has not been reported before for invertebrates.
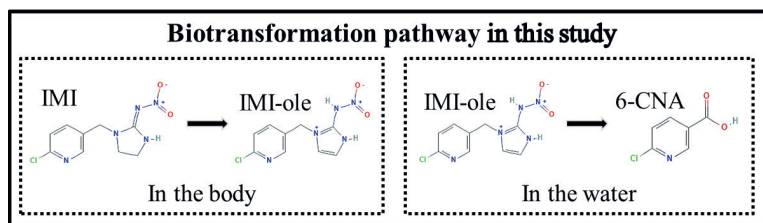
A
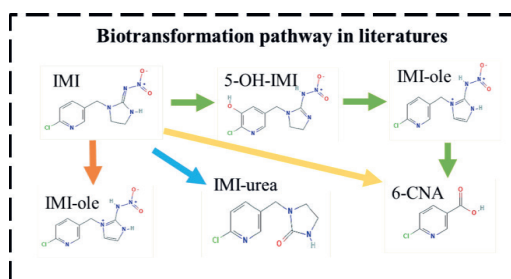
B

Figure 2.5: The biotransformation pathway of IMI deduced from the literature (A), different colours represent different pathways, and from the results of this study (B).

2

2.4. Conclusions

The biotransformation product IMI-ole showed similar toxicity to *C. dipterum* and somewhat lower toxicity to *G. pulex* compared to the parent compound IMI. Whilst IMI was biotransformed to IMI-ole in both species at considerable rates, it showed almost no elimination from *C. dipterum* and a slow one from *G. pulex*. During exposure to IMI, the bioactive metabolite IMI-ole could be detected after one-day of exposure and reach relatively high concentrations in *C. dipterum* compared to *G. pulex* contributing to the toxicity of IMI. Our results suggest that IMI-ole may gradually be generated, especially in *C. dipterum,* and not being eliminated by this species. Hence IMI-ole may be responsible for the chronic toxicity of IMI in *C. dipterum* with increasing exposure times. It also demonstrates that the sensitivity difference between invertebrates depends not only on the bioaccumulation of the parent compound, but also on its biotransformation and elimination.

Support Information

The support information of this chapter can be downloaded from:

https://www.sciencedirect.com/science/article/pii/S0166445X21000965

3

CHAPTER 3.

Size- and sex-related sensitivity differences of aquatic crustaceans to imidacloprid.

Anna Huang, Ivo Roessink, Nico W. Van den Brink, Paul J. Van den Brink
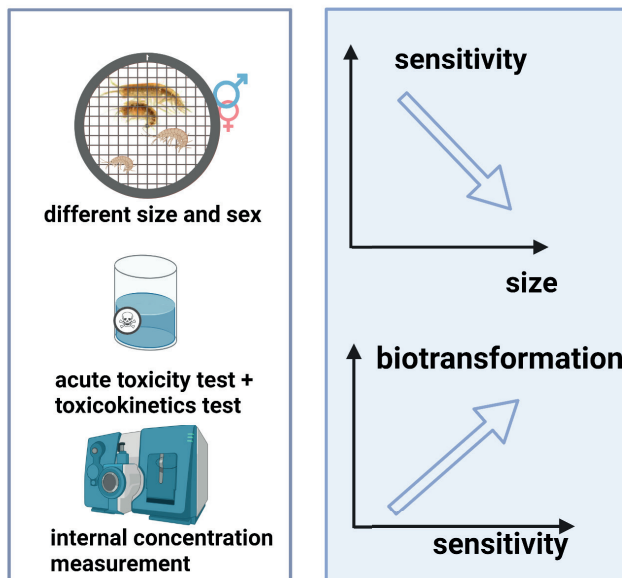
Graphical abstract: A graphic diagram of the experimental design and the results. Diagram created with BioRender (www.biorender.com).

Abstract

Field collected aquatic invertebrates are often used as test organisms in the refinement of the standard Tier 1 risk assessment of various pollutants. This approach can provide insights into the effects of pollutants on the natural environment. However, researchers often pragmatically select test organisms of a specific sex and/or size, which may not represent the sensitivity of the whole population. To investigate such intraspecies sensitivity differences, we performed standard acute toxicity and toxicokinetic tests with different size classes and sex of *Gammarus pulex* and *Asellus aquaticus*. Furthermore, toxicokinetics and toxicodynamics models were used to understand the mechanism of the intraspecies sensitivity differences. We used neonates, juveniles and male and female adults in separate dedicated experiments, in which we exposed the animals to imidacloprid and its bioactive metabolite, imidacloprid-olefin. For both species, we found that neonates were the most sensitive group. For *G. pulex*, the sensitivity decreased linearly with size, which can be explained by the size-related uptake rate constant in the toxicokinetic process and size-related threshold value in the toxicodynamic process. For *A. aquaticus*, female adults were least sensitive to imidacloprid, which could be explained by a low internal biotransformation of imidacloprid to imidacloprid-olefin. Besides, imidacloprid-olefin was more toxic than imidacloprid to *A. aquaticus*, with differences being 8.4 times for females and 2.7 times for males. In conclusion, we established size-related sensitivity differences for *G. pulex* and sex-related sensitivity for *A. aquaticus,* and intraspecies differences can be explained by both toxicokinetic and toxicodynamic processes. Our findings suggest that to protect populations in the field, we should consider the size and sex of focal organisms and that a pragmatic selection of test organisms of equal size and/or sex can underestimate the sensitivities of populations in the field.

3.1. Introduction

In ecological risk assessment (ERA), both standard and non-standard aquatic invertebrate species are used to increase environmental realism. However, non-standard aquatic invertebrate species are often not lab-cultured but collected from the field prior to actual testing, which introduces potential uncertainties. Extensive environmental and biological differences potentially exist between such field-collected organism populations, such as the time and location of collection (Van den Brink et al. 2016, Dalhoff et al. 2018, Sumon et al. 2018) and the size or sex of the collected organisms (McClellan-Green et al. 2007, Poteat and Buchwalter 2014). Moreover, the size- and sex-related variability are of great concern as they can significantly influence population demographics (Stark et al. 2004), which are often the protection goal for the ERA when it concerns invertebrates (Hommen et al. 2010). A few studies have explored the intraspecies sensitivity differences (Gergs et al. 2015, Jager et al. 2016, Gao et al. 2019, Gao et al. 2020). However, the study of sensitivity differences within populations of aquatic invertebrates is still limited, especially for the sex difference.

To understand the mechanism of the intraspecies sensitivity differences, effect models like toxicokinetics–toxicodynamics models (e.g., the General Unified Threshold Model of Survival) can be used (Van den Berg et al. 2019). Also, these models have been recommended to use in risk assessment for the risk assessment of pesticides for aquatic organisms (EFSA PPR Panel (Panel on Plant Protection Products and their Residues) et al. 2018). Toxicokinetics models describe the uptake and elimination process of chemicals in the organisms or tarted sites (Jager et al. 2011). The conventional toxicity approach estimates the EC_{50} or LC_{50} value of pollutants for the tested organism, which is based on the external water concentration (McCarty et al. 2011). Knowledge about the chemicals' TK (Rubach et al. 2012, Gergs et al. 2015) and the resulting internal concentration (Escher et al. 2011) are, however, essential to understand the intrinsic sensitivity differences between sub-groups of species (e.g. differing in sex and/or size). Furthermore, toxicodynamics can quantitatively link the internal (scaled) concentration to the effect at the level of the individual organism over time (e.g., mortality or immobility without recovery) (Ashauer et al. 2011a, Jager et al. 2011). Combing the TK and TD process together, there are two versions of TK-TD models, Full-GUTS and Reduced-GUTS, depending on whether the measured internal concentration was included. Full-GUTS apply the internal concentration directly to mortality. However, Reduced-GUTS assume that the

internal concentration leads to damage (which can be repaired at a certain rate), leading to mortality (Jager et al. 2011). The Reduce-GUTS outperforms Full-GUTS sometime when the concept of damage is more representative than the measured internal concentration (Jager et al. 2011).

Imidacloprid (IMI) is one of the most used neonicotinoids to protect crops from pest insects like aphids, leafhoppers, and whiteflies (Hladik et al. 2018). IMI has a high water solubility and a relatively long half-life in soil (Bonmatin et al. 2015). Therefore, it has the potential to accumulate in soils and to leach to surface water and groundwater (Morrissey et al. 2015, Hladik et al. 2018). Its toxicity to non-target aquatic species has been extensively evaluated (Morrissey et al. 2015, Thunnissen et al. 2020a). However, as we mentioned before, these tests often used one size of organisms without determining the sex of the individuals and may, therefore, misinterpret the toxic effect on the population level. Moreover, one of the metabolites of IMI, imidacloprid-Olefin (IMI-ole), was proven to be a bioactive metabolite (Huang et al. 2021). IMI-ole is one of the common metabolites of IMI, it contributes to the overall toxicity of IMI, and it causes the delayed effect of IMI for aquatic species and bees (Suchail. et al. 2001, Codling et al. 2016, Huang et al. 2021). In addition, IMI-ole can be further metabolized to 6-chloronicotinic acid (6-CNA), which is a much less toxic chemical to some aquatic species (Huang et al. 2021).

To address the knowledge gap in the sensitivity differences driven by size and sex, we studied the sensitivity of different size and sex groups of two aquatic crustaceans: *Gammarus pulex* and *Asellus aquaticus,* towards IMI. *G. pulex* and *A. aquaticus* are widely distributed invertebrates in Europe that play essential roles in maintaining the balance of freshwater ecosystems. Moreover, these two species have moderate susceptibility to IMI (Roessink et al. 2013). They are also among the most commonly tested wild-collected organisms that live in water throughout their life cycle and can be differentiated by sex (Bloor 2010).

In the present study, we hypothesized that, for both species, their sensitivity to IMI will decrease with size and will differ between sexes, and this sensitivity difference can be reflected by both TK and TD processes. We performed acute toxicity and simple toxicokinetic experiments with different size and sex groups (neonates of unknown sex, juveniles of unknown sex, adult females and adult males) for both crustacean species. The toxicokinetic and Reduced-GUTS models were calibrated to understand the mechanism of intraspecies

sensitivity difference. Furthermore, toxicity and TK experiments were also performed for the bioactive metabolite IMI-ole, in both female and male individuals of these two species to investigate the differences in sensitivity between sexes further.

3.2. Materials and methods

3.2.1 Chemicals and test organisms

Imidacloprid (IMI; CAS: 138261-41-3), imidacloprid-olefin (IMI-ole; CAS: 115086-54-9) and 6-chloronicotinic acid (6-CNA; CAS: 5326-23-8) were used in our experiments. Imidacloprid-d4 (IMI-d4; CAS: 1015855-75-0) was used as an internal standard during the analytic measurements of any organism sample. All stock solutions of IMI, IMI-ole, 6-CNA, IMI-d4 (200 µg/mL) were dissolved into Milli-Q water.

The tested organisms were collected from the non-agricultural sites where they dominated, and organisms from these sites have been used in a previous study (Roessink et al. 2013). *G. pulex* was collected from an uncontaminated location, the Heelsumse Beek (a brook with the coordinates 51.973400N, 5.748697E), while *A. aquaticus* was collected from an uncontaminated pond at the Wageningen University and Research campus (51.986859N, 5.668837E). To ensure the cleanliness of tested organisms, unexposed field water and organisms were measured by LC-MS/MS to verify the absence of chemicals of interest (IMI, IMI-ole, and 6-CNA); see Section 2.2.3 for measurement methods.

After collection in the field, all organisms were brought back to the lab and separated into four groups based on specific sizes and/or sexes. This resulted in groups of adult males, adult females, juveniles and neonates. Note that for the latter two groups, the sex of the organisms could not yet be determined. We used different selection processes for each group, considering their accessibility (Text S1, Table S1 for an overview). To be specific, for adults, we selected pre-copulation couples from the field with the males on top. Subsequently, we separated them and put them into different containers, and we visually selected similar size of males and females. We excluded pregnant females to rule out the potential influence of reproduction by only selecting females without black dorsolateral ovaries (Sutcliffe 1992). The average size of the males was larger than females (Table S2 for details). For juveniles, they were also from the field; we visually selected max 5 mm sized organisms as individuals are sexually mature when *G. pulex* and *A. aquaticus* are larger than 6 mm and 5 mm, respectively

(Welton and Clarke 1980, Murphy and Learner 1982). However, the neonates were from the lab. We obtained neonates from the gravid females previously collected because the field collection of neonates was not feasible. In detail, the gravid females not selected for any of the tests were collected into a new container, and they were checked every two days. Any offspring released was transferred to a different container and used as neonates in further testing. The age of neonates in our experiment was between 5 to 8 days, and their size was close to 1 to 2 mm for both species. All four groups of organisms were acclimated in separate containers in the lab for at least 3 days under test conditions with a 12 hour light : 12 hour dark cycle at 18°C in a water bath (Roessink et al. 2013). During the acclimation period, organisms of both species were fed ad libitum with leached *Populus* leaves. No observable mortality occurred during the acclimation period.

3.2.2 Acute toxicity and toxicokinetic experiments

3.2.2.1 Acute toxicity tests

The acute toxicity of IMI was assessed in a 4-day standard toxicity test to assess the EC_{50} and LC_{50} for *A. aquaticus* and *G. pulex,* which was similar to (Roessink et al. 2013). For each species and group combination, separate tests were performed. We exposed different groups at different concentration ranges of IMI because we expected their sensitivity to be different. Per replicate system, 10 adult *G. pulex* (females or males) or juveniles were placed in 1 L groundwater obtained from the Sinderhoeve experimental station (www.sinderhoeve.org). For the tests with *G. pulex*, the exposure concentrations for the tests with the adults and juveniles were 0, 10, 30, 100, 300 and 1000 µg/L and 0, 1, 10, 30, 100 or 300 µg/L, respectively. For the tests with *G. pulex* neonates, a replicate test system consisted of 16 individuals and was dosed to reach concentrations of 0, 0.1, 1, 10, 30, 100 µg/L. For the tests with *A. aquaticus*, 10 adults (males and females) or juveniles were placed in each replicate, and the exposure concentrations were 0, 10, 30, 100, 300 and 1000 µg/L. For the test with *A. aquaticus* neonates, 20 individuals were placed in each replicate with exposure concentrations of 0, 1, 10, 30, 100 or 300 µg/L.

The acute toxicity tests with IMI-ole were similar to IMI, but due to the limited availability of juveniles and neonates were only performed with the adult males and females of both species. Ten organisms of either of these four groups (female *G. pulex*, male *G. pulex*, female *A. aquaticus* and male *A. aquaticus*) were placed in 1 L groundwater, dosed to reach final

exposure concentrations of 0, 10, 30, 100, 300 and 1000 µg/L. Details on the setup of the acute toxicity are provided in Table S1.

The experiment setup was similar to a previous study (Roessink et al. 2013). In detail, experiments were performed with three replicates per treatment level, while 5 replicates were used for control. The test systems were not aerated during the experiments to minimize the volatilization of the chemicals, and no food was added. In all experiments, a piece of stainless steel mesh was added to each replicate to provide shelter. Organisms were checked every day, and the effect status (dead, immobile or non-affected) of each individual was assessed according to (Roessink et al. 2013). Dead and immobilized organisms were both considered as affected. Dead organisms and moults were removed daily. All jars were placed randomly in the water bath; temperature and light conditions were similar to the acclimatization period. Dissolved oxygen, pH, electrical conductivity, and temperature were measured at the start and end of the test in the control group and in the highest treatment. These water quality parameters remained stable during the 4 days experiment (*raw data, (Huang et al. 2022f)*). After 4 days experiment, the control mortality was less than 10% (*raw data, (Huang et al. 2022f))*.

After 4 days, 50% of the organisms in control and lowest treatment were collected for the toxicokinetic experiments (see section 3.2.2). The other organisms were collected, washed with clean flow water for 30 seconds, and stored at -20°C for further chemical analysis of the internal concentration. The concentration of IMI, IMI-ole and 6-CNA were measured in the organisms and water samples. Specifically, water samples were collected at the beginning and the end of the experiment in all jars to validate the dosing and to monitor the potential degradation of the chemicals (see section 3.2.3). The measured water concentration was close to the nominal concentration (within 80% to 100%) and remained the same concentration after 4 days experiment (*raw data, (Huang et al. 2022f))*.

3.2.2.2 Toxicokinetic experiments

To assess the uptake kinetics of IMI and IMI-ole, additional minimalized toxicokinetic experiments were performed, which included a 4 days uptake and 2 days elimination period as suggested in a previous study (Carter et al. 2014). The toxicokinetic experiment was not conducted for the neonates since the biomass of the neonates was not high enough to allow

an internal body residue measurement. A summary of the setup of simple toxicokinetic experiments is provided in Table S1.

At the end of the 4 days exposure in the acute toxicity experiments, half of the remaining organisms (see section 3.2.2.1) from the lowest exposure concentration treatment were cleaned with flow Milli-Q water and transferred to 1 L of clean groundwater, which started the 2 days elimination period. Specifically, for the tests performed with adults, 5 male or female individuals of both species from the 10 µg/L IMI treatment were transferred to clean water. For the tests performed with juvenile *G. pulex* and *A. aquaticus*, 5 organisms from the 1 and 10 µg/L treatment, respectively, were transferred to the clean water. For the IMI-ole toxicity test with both species, 5 male or female individuals were transferred from the 10 µg/L treatment to clean water. After 2 days of elimination, all alive organisms were collected, washed and stored at -20°C. The concentration of IMI, IMI-ole and 6-CNA were measured in the organisms (see section 3.2.3). All remaining organisms were checked for their status every day during the elimination period, and no organism died during the elimination period.

The water samples at the beginning and the end of the elimination phase were taken. Specifically, before adding the transferred organisms, the clean water was taken to ensure the absence of chemicals of interest; and after 2 days of elimination, water samples were retaken to detect the eliminated chemicals in the water phase.

3.2.2.3 Determination of size

We measured the length of 20 individuals from each group for each species, which were taken from the control treatment after the 4 days toxicity test. This was done to determine the average length for each group of both species, assuming that the length did not change after 4 days, which is supported by the slow growth rate of both species (Bloor 2010). The size measurement performed at the end of the experiment instead of the beginning was to avoid stress on tested organisms. *G. pulex* individuals were measured from the top of the cephalothorax to the base of the telson (Vellinger et al. 2012), and *A. aquaticus* body size was defined as the linear measurement from the front of the head to the tip of the pleotelson (Bertin and Cezilly 2003) by using image software analysis (ImageJ software, Version 1.52). Details on the size and the range in each group are provided in Table S2.

3.2.3 Chemical analysis

The internal concentration of the exposure chemical (IMI and IMI-ole) and the potential metabolites (IMI-ole and 6-CNA) were measured at the end of the toxicity tests (section 3.2.1) and toxicokinetic experiments (section 3.2.2) based on a method from a previous study (Huang et al. 2021) with some modifications. Prior to analytical quantification of the concentrations, all samples were stored at -20°C. Upon analysis, organisms were pooled and lyophilized for 1 day and weighted to the nearest mg to get the overall dry weight of all animals within each treatment. For extraction, 1 mL 1% acetic acid MeOH : Water (v : v = 5 : 1) and 25 µL internal standard (imidacloprid-d4, 200 µg/L) were added to the lumped individuals of the juveniles groups while 3 mL was used for the adult groups. The samples were homogenized with a Minilys personal homogenizer (Bertin Instruments, France) using a Precellys ceramic lysing kit (1.4/2.8 mm; Bertin Instruments, France) for 3 times 60 sec at 3000 rpm using a 30s interval. After this, the sample was centrifuged at 10000 rpm for 10 minutes, and the supernatant was filtered over a PTFE syringe filter (pore size 0.45 µm). Filters were washed with 200 µL extraction solution. The eluent was centrifuged as well and filtered over a syringe filter (0.45 µm). The two filtrates were combined and adjusted to get a final volume of 1.2 mL for juveniles and 3.2 mL for adults, after which the sample was ready for analysis by LC-MS/MS. The water samples were analyzed directly, without an extraction step.

All samples were analyzed by reversed-phase liquid chromatography-tandem mass spectrometry (LC-MS/MS), similar to the previous study (Huang et al. 2021). The only modification was that the injection volume of samples was 5 µL in this study. The chemicals were detected in the multiple reaction monitoring (MRM) using two transitions per compound (Table S3). Injected samples were quantified by peak area using a calibration curve constructed from the calibration standards included in the same sample sequence (Table S4 and S5). Agilent Masshunter software (version 7.0) was used for instrument control and data acquisition. The extraction recovery of each tested analyte (IMI, IMI-ole and 6-CNA) in the organisms were evaluated at two concentrations by spiking them into the clean organisms. The recovery was acceptable for both species based on recovery and repeatability results (Table S6, recovery rate between 80% - 120% and the standard deviation less than 20%). More information about chemical analysis see Text S2.

3.2.4 TK-TD models Calibration

In the present study, the TK and TD processes were modelled separately in GUTS. TK process was assessed by a one-compartment toxicokinetic model, while the TD process was assessed by Reduced-GUTS.

3.2.4.1 One-compartment Toxicokinetic Model

To determine the toxicokinetic rate constants for exposed chemical, a first-order one-compartment kinetic model programmed in Matlab R2021b was used (Jager et al. 2011) (https://www.debtox.info/byom.html.):

$$\frac{dC_{int}(t)}{dt} = k_u \cdot C_w(t) - k_e \cdot C_{int}(t) \qquad \textit{(Eq.1)}$$

With   t = time,

   C_{int} =internal concentration of exposed chemical,

   C_w = measured concentration of the exposed chemical in water,

   k_u = the uptake rate constant of the parent (exposed) chemical, and

   k_e = the elimination rate constant of the parent (exposed) chemical.

The bioconcentration factor (BCF) (L·kg^{-1}) was calculated using a kinetic method (BCF$_k$) :

$$BCF_k = \frac{k_u}{k_e} \qquad \textit{(Eq.2)}$$

The elimination half-life ($t_{1/2}$) (day) was calculated from the elimination rate of IMI or IMI-ole:

$$t_{1/2} = \frac{ln2}{k_e} \qquad \textit{(Eq.3)}$$

The biotransformation TK model, which includes the metabolite (IMI-ole) in the IMI exposure, is presented in the supporting information. This biotransformation model is limited because we have only one time point for metabolite formation.

3.2.4.2 Reduced-GUTS models calibration

The TD framework has been described earlier (Jager et al. 2011, Jager et al. 2017, Jager 2021). The Reduce-GUTS was performed in software (openGUTS) that incorporates this simplification and has been made publicly available recently and was used for the simulations (see https://openguts.info). We used only Reduced-GUTS for two reasons. The first reason was that Reduced-GUTS allowed us to consider neonates because Full-GUTS was not feasible for neonates because there was no TK test for neonates. Secondly, we already knew that the

metabolite (IMI-ole) also has a toxic effect; thus, the internal concentration of the parent chemical (IMI) alone was not representable for the damage. The actual damage was the sum-up of IMI and its metabolite, IMI-ole. However, the exact extent of the IMI-ole in the toxicity of IMI was not explored in the present study. Thus, the damage concept in Reduced-GUTS is more appropriate than the internal concentration in Full-GUTS. Moreover, two death mechanisms, individual tolerance (IT) and stochastic death (SD), were calibrated for each group. For model selection, smaller Akaike information criterion (AICs) and normalized Root Mean Square Error (NRMSE) values indicate better fitting (EFSA PPR Panel (Panel on Plant Protection Products and their Residues) et al. 2018).

3.2.5 Statistical significance tests

To assess the significance of the difference in EC_{50} and the toxicokinetic parameters among the groups, we compared the mean value with the 95% confidence interval. If the ranges did not overlap, then we conclude that the values were significantly different.

Linear regression between the average size of individuals and the mean value of toxicity (LC_{50}, EC_{50}), toxicokinetic parameters values (k_u, k_e) or toxicodynamics parameters values (hb, kd, mw, Fs, bw) was performed to investigate the relationship between sensitivity related parameters and size. The linear regression was presented only when the coefficient of determination (*adjusted R^2*) was *> 0.8*. We created linear regressions using the lm function of the base package stats using R (version 4.1.0).

In addition, significant differences in internal concentration among groups were assessed. The assumptions of normality were evaluated using a Shapiro-Wilk test, and the assumption of equal variance was evaluated using a Spearman rank correlation between the residuals and the dependent variable. If the assumptions of normality and equal variance were passed, a one-way analysis of variance (ANOVA) with *α=0.05* and a post-hoc *Tukey's test* was conducted. If assumptions failed, a *Kruskal-Wallis test*, with *α=0.05*, and a post-hoc *Dunn's test* was used. A two-tailed p-value (*p < 0.05*) was considered to be statistically significant. A *Bonferroni* correction approach was adopted in the multiple comparisons of the IMI exposure test.

3.3. Results

3.3.1 Internal concentration of the exposed chemicals

During quality control, no chemicals of interest were detected in the unexposed tested organisms and field water, proving that the measured internal concentration of exposed tested organisms was caused by experimental exposure.

3.3.1.1 Internal concentrations of IMI and its metabolite, IMI-ole

After 4 days of IMI exposure, we measured the internal concentration (in the whole organism) of IMI, and we detected its metabolite, IMI-ole, in the experiments with juvenile, female, and male groups of both species (Figure 3.1) (for neonates no analyses could be performed due to small sample sizes).

For *G. pulex*, the internal IMI concentrations in the juveniles were similar to those in males and females (Figure 3.1 A). However, the generation of IMI-ole was significantly higher in juveniles than in males and females in 30, 100 and the 300 µg/L treatments (Figure 3.1 B). The generation of the IMI-ole in females only occurred in the 1000 µg/L treatment, which was significantly higher than in males (Figure 3.1 B). The LOQ of IMI-ole was close in three groups (Figure 3.1 B dash lines and Table S6). In addition, for all three groups, the internal concentrations of IMI-ole in the 10 µg/L were not detected, and for male and female adults, no metabolites were detected in 30 µg/L, and the IMI-ole was not detected in the females group in the 100 and 300 µg/L; thus no results were shown.

For *A. aquaticus*, there was no difference between males and juveniles regarding the internal concentration of IMI (Figure 3.1 C). Males accumulated significantly more IMI than females (in 100 and 1000 µg/L, Figure 3.1 C). In addition, males produced significantly more IMI-ole in the two highest treatments (300 and 1000 µg/L) than juveniles or females (Figure 3.1 D). The LOQ of IMI-ole was close in three groups (Figure 3.1 D dash lines and Table S6). For all three groups, the internal concentrations of IMI-ole in the 10 and 30 µg/L were not detected, the IMI-ole was not detected in the females group in the 100 µg/L, thus no results were shown.
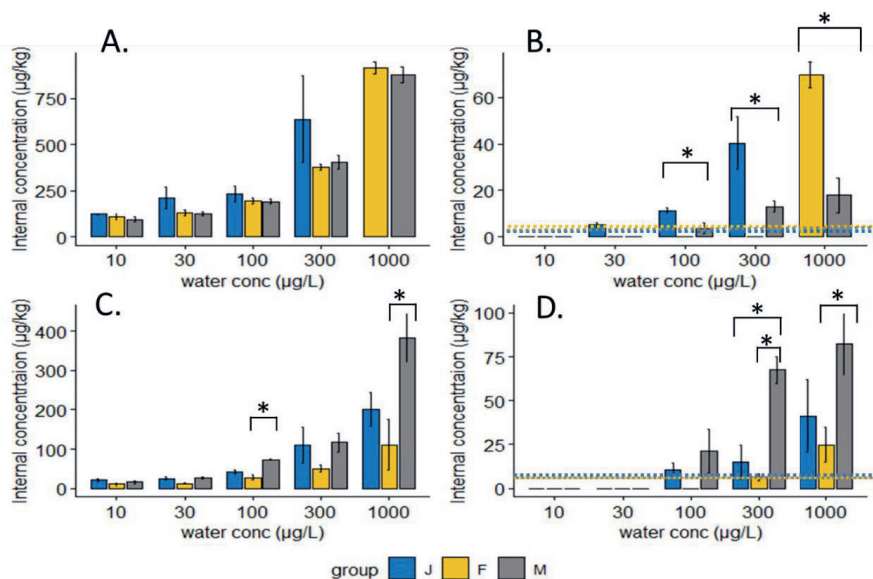
Figure 3.1: *The internal concentration of IMI (A) and IMI-ole (B) in G. pulex and IMI (C) and IMI-ole (D) in A. aquaticus as measured at the end of the 4 days toxicity test with IMI. Significant differences among groups (Tukey's test or Dunn's test with a Bonferroni correction) within the same concentration treatment are indicated. (p < 0.05) is represented by *. The dash lines represented the LOQ for each group (blue colour means juveniles, yellow colour means females, grey colour means males).*

3.3.1.2 The internal concentration of IMI-ole and its metabolite, 6-CNA

After 4 days of IMI-ole exposure, we measured the internal concentration (in the whole organism) of IMI-ole, and we detected its metabolite, 6-CNA, in the experiments with female and male groups of both species, but only in the two highest treatments (300 and 1000 µg/L). Furthermore, we detected 6-CNA in the water samples but only in the highest (1000 µg/L group) and for details, see Text S3 and Figure S1 in the support information.

For *G. pulex*, the internal concentration of IMI-ole was higher in females than in males (Figure 3.2 A). The generation of 6-CNA in the body was significantly higher in females in the 300 µg/L and 1000 µg/L treatment (Figure 3.2 B). The LOQ of 6-CNA in females were two times higher than that in males (Figure 3.2 B dash lines, Table S6). For *A. aquaticus*, males accumulated significantly more IMI-ole in the ≥30 µg/L treatment levels than females. Males produced more 6-CNA in the 300 µg/L treatment when the 6-CNA in females were not detected. In the 1000 µg/L treatment, the internal concentration of 6-CNA was similar in males and females

(Figure 3.2 D). Also, the LOQ of 6-CNA in females were two times higher than that in males (Figure 3.2 D dash lines, Table S6).
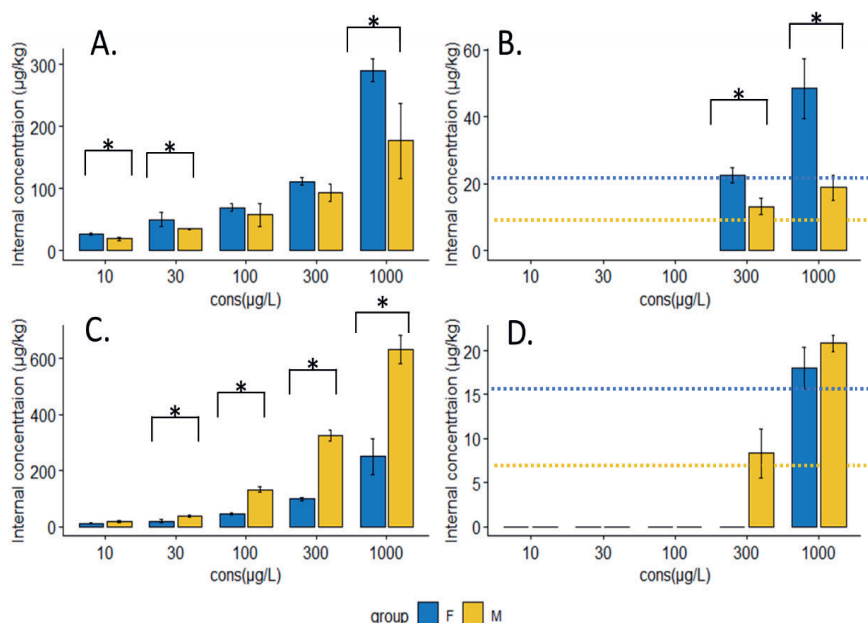
*Figure 3.2: The internal concentrations of IMI-ole (A) and 6-CNA (B) in G. pulex and IMI-ole (C) and 6-CNA (D) in A. aquaticus as measured at the end of the 4 days toxicity test with IMI-ole. Significant differences between sex groups (ANOVA or a Kruskal-Wallis test) within the same concentration treatment are indicated. (p < 0.05) is represented by *. The dash lines represented the LOQ for each group (blue colour means females, yellow colour means males).*

3.3.2 One-compartment toxicokinetics model of the exposed chemicals

For all tests, no mortality occurred in neither uptake nor elimination periods, and no eliminated chemicals were detected in the water during the elimination period (Figure S2 and S3). In addition, one-compartment TK models were calibrated for IMI or IMI-ole exposure because no metabolites were detected during this test (1 or 10 µg/L group) (Figure 3.1 and 3.2, Table S7). The metabolites (IMI-ole for IMI exposure, 6-CNA for IMI-ole exposure) were detected only in a higher exposure concentration and with only a timepoint (day4) (Figure 3.1 and Figure 3.2). Nevertheless, the biotransformation TK models of IMI were calibrated and applied for all treatment levels and discussed in the supporting information (Text S4, Table S8 and Figure S4).

3.3.2.1 One-compartment TK results of IMI

Generally, the uptake rate constant of IMI was higher in *G. pulex* than that in *A. aquaticus;* the elimination rate constant of IMI was lower in *G. pulex* than in *A. aquaticus* (Figure 3.3).

For *G. pulex*, compared to adult organisms, smaller juvenile *G. pulex* individuals had a higher uptake rate constant of IMI (Figure 3.3 A), while this difference was not observed for the elimination rate constant (Figure 3.3 B). The ranking of uptake rate constant from high to low was from juveniles, females to males, but the 95% confidence intervals for males and females did overlap (Table S7). The highest BCF_k of IMI in *G. pulex* was calculated for juveniles (92.2 L/kg), followed by males (34.6 L/kg) and females (24.8 L/kg) (Table S7).

For *A. aquaticus*, no size-related differences in the toxicokinetic experiments were detected, but sex differences existed (Figure 3.3 C and D). The uptake rate constant of IMI in juveniles was similar to males, but it was higher than that of females. The confidence intervals of the elimination rates constant of juveniles, females, and males overlapped. The BCF_k of IMI in *A. aquaticus* juveniles (2.03 L/kg), females (2.09 L/kg) and males (1.84 L/kg) were close (Table S7).
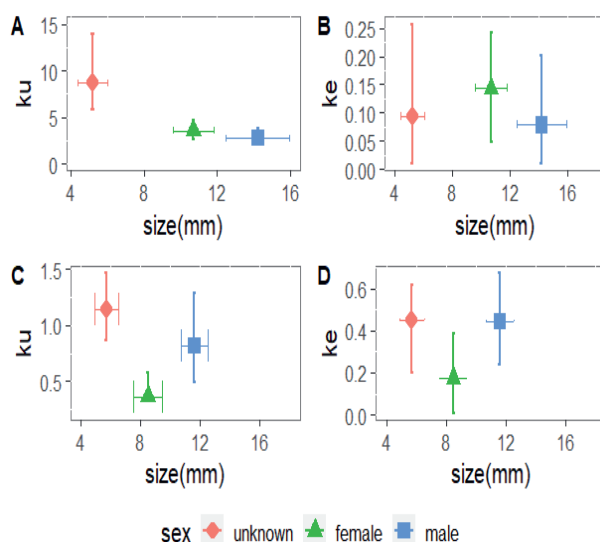

Figure 3.3: *Uptake rate constant (A) and elimination rate constant (B) of IMI in G. pulex; Uptake rate constant (C) and elimination rate constant (D) of IMI in A. aquaticus. The horizontal error bar is the size range, mean ± sd, n =20; the vertical error bar is the parameter range, mean ± 95% CIs.*

3.3.2.2 One-compartment TK results of IMI-ole

Similarly to IMI, the uptake rate constant of IMI-ole was higher in *G. pulex* than that in *A. aquaticus*, and the elimination rate constant of IMI-ole was lower in *G. pulex* than in *A. aquaticus* (Figure 3.4). For both species, the confidence intervals of the uptake and elimination rate constants of IMI-ole were overlapped for males and females (Figure 3.4).

Comparing the toxicokinetic results of IMI and IMI-ole, the confidence intervals of the uptake and elimination rate constants of IMI and IMI-ole overlapped regardless of sex. However, it should be noted that female *G. pulex* eliminated IMI-ole slower (0.03 d^{-1}) than IMI (0.14 d^{-1}), causing the higher BCF_k of IMI-ole (99.3 L/kg) than that of IMI (24.8 L/kg) (Table S7). Same as for *G. pulex*, the confidence intervals of the uptake and elimination rate constants for IMI and IMI-ole overlapped for the two sexes in *A. aquaticus*. However, it should be noted that for males, the elimination rate of IMI-ole (0.14 d^{-1}) was slower than that of IMI (0.44 d^{-1}) (Table S7), causing a higher $BCFk$ of IMI-ole (4.06 L/kg) than of IMI (1.84 L/kg) (Table S7).
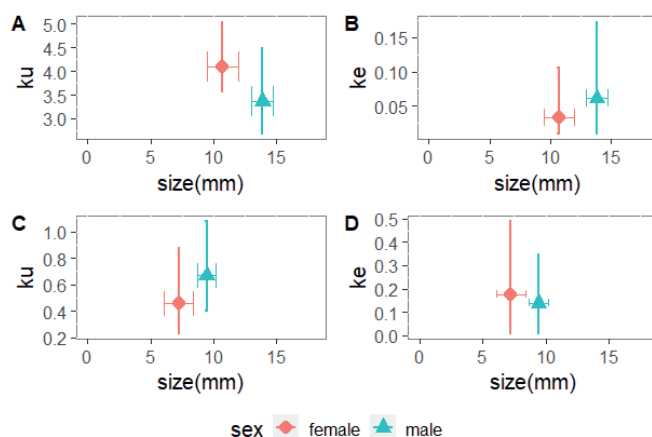
Figure 3.4: *Uptake rate* constant *(A) and elimination rate* constant *(B) of IMI-ole in G. pulex; Uptake rate* constant *(C) and elimination rate* constant *(D) of IMI-ole in A. aquaticus. The horizontal error bar is the size range, mean ± sd, n =20; the vertical error bar is the parameter range, mean ± 95% CIs.*

3.3.3 Toxicity and toxicodynamic of exposed chemicals

We have tested the toxicity of IMI for four groups: neonates, juveniles, adult females and adult males of both species. Also, we tested the toxicity of IMI-ole for two groups: adult females and adult males of both species. Furthermore, we calibrated reduced-GUTS to get the toxicodynamics process parameters for IMI. The overview of the model fitting is provided in

Table S9 and Table S10 for IMI and Table S11 and S12 for IMI-ole. Overall, for both IMI and IMI-ole, IT mechanism overperformed the SD mechanisms in most of the groups. Thus, we only showed the IT results here. The results of SD can be found in supporting information (Table S9-S12).

3.3.3.1 Mortality and immobility results of IMI and IMI-ole

Both lethal (LC_{50}) and affected (EC_{50}) results were provided for IMI (Figure 3.6). Overall, *G. pulex* was more sensitive to IMI than *A. aquaticus* (Figure 3.5). For *G. pulex*, on day 4, neonates were the most sensitive group of the two species, followed by juveniles and adults (Figure 3.5 A, B). Regarding EC_{50}, the toxicity of IMI to *G. pulex* decreased significantly with increasing size (Figure 3.5 B, black line). For *A. aquaticus*, similar to *G. pulex*, the sensitivity rank was neonates, juveniles, and adults (Figure 3.5 C, D). However, the sensitivity of smaller female *A. aquaticus* individuals was much lower than the larger males, especially in terms of EC_{50} (Figure 3.5 D).

For these two species, *A. aquatics* was more sensitive to IMI-ole than *G. pulex* (Figure 3.6). Compared to IMI, IMI-ole was less toxic to *G. pulex* (Figure 3.6 A, B) but more toxic to *A. aquatics* (Figure 3.6 C, D). In detail, for *G. pulex*, IMI-ole showed 4 days EC_{50} values of 349 (249.3 - 485.8) and 383.3 (274.1 - 542.1) µg/L for female and male individuals, respectively (Table S11). Compared to IMI, the toxicity of IMI-ole was 3.7 times lower in females and 3 times lower in males (Table S9 and S11). For *A. aquaticus,* comparing the toxicity results of IMI-ole with IMI, we found that IMI-ole was more toxic to *A. aquaticus* than IMI, with differences being 8.4 times for females and 2.7 times for males (Table S9 and S11).
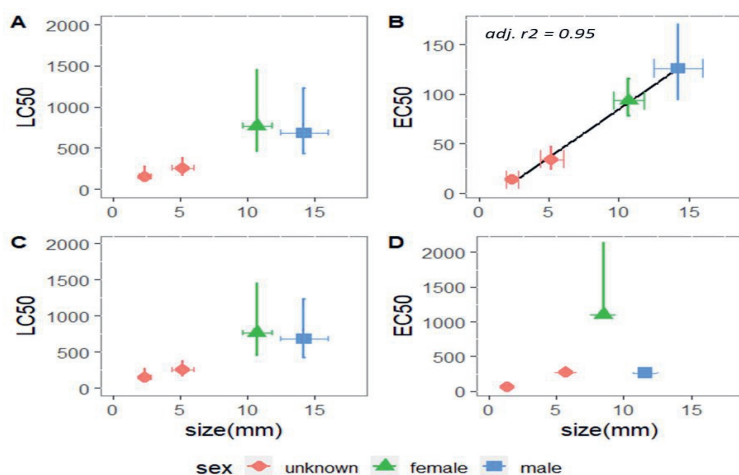
Figure 3.5: *Four-day LC$_{50}$ and EC$_{50}$ value of IMI for different group individuals of both species (horizontal error bar is the size range, mean ± sd, n =20; vertical error bar is the EC$_{50}$ range, mean ± 95% CIs). Panels A and B were for G. pulex; panels C and D were for A. aquaticus. The linear regression between size (mean value) and the IMI toxicity (mean value of EC$_{50}$) for G. pulex was significant and is represented by the black line.*
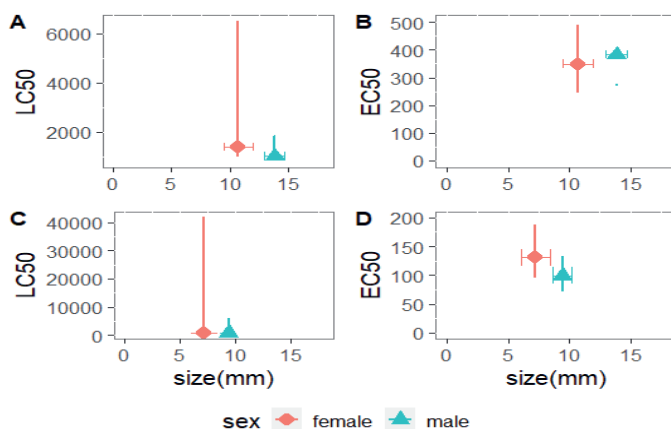
Figure 3.6: *Four-day LC$_{50}$ and EC$_{50}$ value of IMI-ole for different group individuals of both species (horizontal error bar is the size range, mean ± sd, n =20; vertical error bar is the EC$_{50}$ range, mean ± 95% CIs). Panels A and B were for G. pulex; panels C and D were for A. aquaticus.*

3.3.3.2 Toxicodynamics parameters of IMI in different groups

The affected result was more representative and a better indicator than lethal results, supported by the better fitting performance in affected results than lethal results (Table S9

and 10, Table S11 and S12). Thus we only showed the affected results below, and as we mentioned above, the IT mechanism outperformed the SD mechanism; hence, only IT parameters were presented.

The reduced-GUTS-IT parameters were illustrated for each size or sex group in Figure 3.7. For *G. pulex*, the background mortality (hb) for each group overlapped. The dominant rate constant (kd) tended to increase with size, while no significant linear regression was found. The threshold value (mw) showed a clear pattern that increased with size, and a significant linear regression with *adj. r2* of 0.99 was found. The Fs tended to decrease with size, while no significant linear regression was found. For *A. aquatics*, for all parameters, no significant linear regression has been found. In detail, no clear pattern for hb, kd and mw, while Fs tend to decrease with size (Figure 3.7 E, F, G, H).
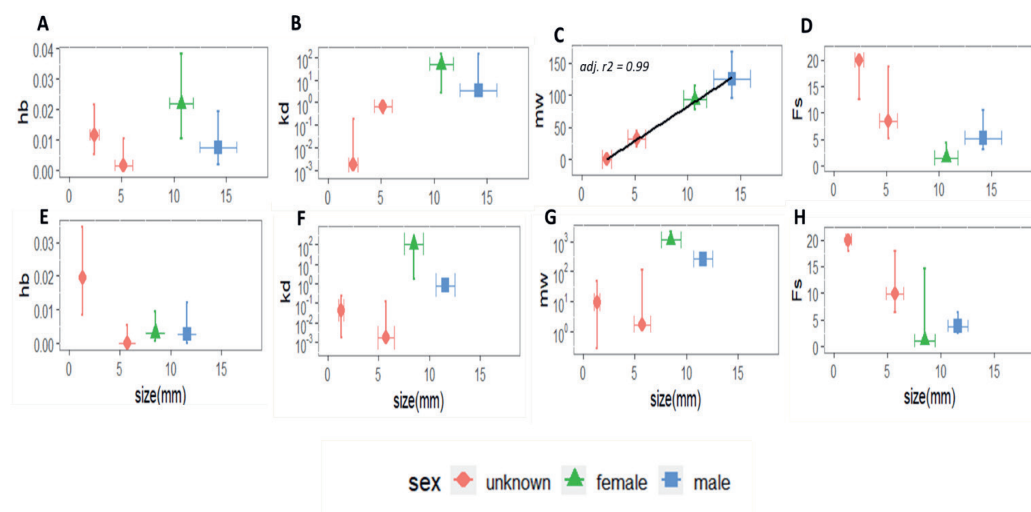
Figure 3.7: The reduced-GUTS-IT parameter in G. pulex (A, B, C, D) and A. aquatics (E, F, G, H). The horizontal error bar is the size range, mean ± sd, n =20; the vertical error bar is the parameter range, mean ± 95% CIs. The linear regression between size (mean value) and the mw (mean value of mw) for G. pulex was significant and is represented by the black line.

3.4. Discussion

Our hypothesis of size related sensitivity difference was well supported for *G. pulex*, while it was less evident for *A. aquatics*. We found that both the toxicokinetic and toxicodynamic processes of IMI could explain the intraspecies sensitivity difference.

3.4.1 Toxicokinetic and toxicodynamic models explain the intraspecies sensitivity difference of G. pulex

For *G. pulex*, we found size-related uptake rate constant, threshold values, and EC_{50} differences for IMI. The 96h EC_{50} based on external water concentration corresponded with the size for *G. pulex* (Figure 3.5 B). This finding was consistent with (Bottger et al. 2012), who found smaller gammarids (*Gammarus roeseli*) being more sensitive to imidacloprid than larger ones. However, current research usually uses juveniles or adults to assess the impact of pollutants, which might underestimate the impact on population levels when neonates are present (Di Lorenzo et al. 2019).

3.4.1.1 Toxicokinetics parameters difference among different size and sex groups of G. pulex

The present study found that the uptake rate constant tended to decrease with size, while the elimination rate constant remained the same (Figure 3.3 A and B). Some other studies also found that body size-dependent toxicokinetics could explain intraspecies variation in sensitivity (Rubach et al. 2010, Gergs et al. 2015, Gergs et al. 2016). In particular, we found that size-dependent differences in invertebrate sensitivity to IMI could be explained by differences in uptake rate constants (Figure 3.3 A) but independent of elimination rate constant. There is no relationship between elimination rate and size, probably due to chemical properties of IMI. Imidacloprid in this study is a highly water-soluble chemical with a logKow value of 0.57 and may easily be actively taken up by gills or passively absorbed into the exoskeleton of the organisms. It has been proved that the uptake process of IMI by *G. pulex* is partially a chemo/physical adsorption process, making it important given the differences in surface-volume ratios of different sizes. For example, previous studies found that the IMI adsorbed considerably on the surface of dead *Gammarus pulex* (Huang et al. 2021) and *Daphnia magna* (Li et al. 2021). In other words, uptake of IMI was related to external water concentrations and surface uptake. Furthermore, IMI could be biotransformed to IMI-ole (Figure 3.1); thus, elimination depends on internal concentrations and biotransformation capacity rather than size.

Besides the uptake rate differences, we also found biotransformation differences among different groups (juveniles, females and males). In the lower exposure concentrations (30, 100 and 300 µg/L), juveniles produced more IMI-ole, which may be linked to the faster uptake rate constant (Figure 3.1, Table S7) and a higher biotransformation capacity since the higher

energetic metabolism in younger *G. pulex* individuals compared to adult ones (Sutcliffe et al. 1981). Comparing the biotransformation between males and females, in the lower exposure (100 and 300 µg/L), generation of IMI-ole has not been detected in females when it was detected in males (Figure 3.1 B). However, in the highest exposure (1000 µg/L), the generation of IMI-ole was higher in females than males (Figure 3.1 B). Also, in the biotransformation model, the biotransformation rate of IMI was higher in females than in males (Table S8). This could be explained by the findings of previous studies, which found that P450 enzyme content, which contributes to the biotransformation of neonicotinoids (NNIs) (Casida 2011), is higher in females than males *G. pulex* (Dalhoff et al. 2018). Nevertheless, on the other hand, some other unknown intermediate metabolites, such as dihydroxy IMI, could be generated (Hoi et al. 2014, Fusetto et al. 2017), but the intact biotransformation pathway of IMI was not thoroughly studied in this study.

3.4.1.2 Toxicodynamics parameters difference among different size and sex groups of G. pulex

In the present study, immobility was a better indicator than mortality because the fitting performance was better (Table S9-S12). This result was consistent with a previous study, which used immobility as the endpoint in TKTD modelling (Huang et al. 2021). Immobility is a better endpoint for IMI since neonicotinoids are neurotoxic and expected to cause effects on behaviour (Morrissey et al. 2015).

We found differences in the toxicodynamics parameters between different size and sex groups. The dominant rate constant (k_d) tended to increase with size (Figure 3.7 B). Unlike uptake or elimination rate constant, which is only involved in chemical uptake and elimination, k_d is a "lumped" parameter, which is supposed to incorporate the most dominant processes of chemical elimination and damage recovery (EFSA PPR Panel (Panel on Plant Protection Products and their Residues) et al. 2018, Brock et al. 2021). The increasing pattern of k_d with size revealed that the damage recovery increased with size since there was not much difference in the elimination rate constant (Figure 3.3B). Our finding was consistent with a previous study, which found that the k_d was getting bigger with size in the case of *Mesocyclops leuckarti* exposed to triphenyltin (Gao et al. 2020).

On the other hand, the intrinsic sensitivity was also influenced by the size and sex. The threshold (m_w) defined in the toxicodynamic process increased with size (Figure 3.7 C) for *G. pulex*. This was also noticed in another study (Gao et al. 2020) in which the intraspecies

sensitivity of different species was investigated with respect to size and metal toxicity, and they found that body size of zebrafish obviously affects model parameters of threshold values (Gao et al. 2020). However, unlike their studies that integrated size into parametric models, we only calibrated the GUTS model for each group (neonates, juveniles, females and males). This was because we also investigated the sex difference in our study, not just size. In addition, the biotransformation of IMI and the toxic effects of its metabolite were not simply reflected by size.

3.4.2 Biotransformation contributes to the sex-related sensitivity difference of A. aquaticus

For *A. aquaticus*, we did not observe size-related sensitivity difference (Figure 3.5 C, D), and the most remarkable finding was that females were the most insensitive group to IMI when exposed to IMI, while they were the most sensitive group to IMI-ole when exposed to IMI-ole (Figure 3.5 D and 3.6 D). Uptake and biotransformation of IMI could explain the tolerance of females to IMI. Females took less IMI up (Figure 3.3 C), and more importantly, less IMI-ole was produced during 4 days of exposure compared to males (Figure 3.1 D). IMI-ole was a more toxic chemical compared to IMI in both males and females *A. aquaticus* (Figure 3.5 D and 3.6 D). In addition, the threshold value of females was higher than males, indicating that the intrinsic sensitivity of females was lower (Figure 3.7 G).

Our result of the tolerant female *A. aquaticus* was unexpected, as we assumed females were smaller and had a relatively higher biotransformation capability than males; hence, the female should be more sensitive. In the present study, based on the low biotransformation rate of females (Figure 3.1), we speculate that females have lower enzymatic activities for IMI biotransformation than males. However, the exact reason for this is unknown, as there are few studies on sex differences in aquatic crustaceans.

In addition, the low respiration rate and locomotion activity of the females may contribute to our result of tolerant female *A. aquaticus*, although we did not measure it in our study. A previous study found that male copepod individuals (*Calanus finmarchicus)* were more sensitive compared to female and juvenile individuals, which could have been caused by the fact that these copepod males have a 20% higher respiration rate than females (Jager et al. 2016). Similarly, we could speculate that the respiration rate of male *A. aquaticus* was higher than females, as we found that the uptake rate constant of IMI was slightly higher in males (Figure 3.3 C) than in females. Another explanation may be that the mobility of males was

higher than females. Personal observations during our experiment showed that males walked more often than females during the observation time of the experiment. Higher locomotion may lead to a higher sensitivity, as is indicated in a recent study (Andreazza et al. 2020), where *Diachasmimorpha longicaudata* males were significantly more susceptible to spinosad than females, which could be related to the differences in their movement since males walked longer distances and periods (Andreazza et al. 2020). However, the applicability of the positive relationship between locomotion and sensitivity needs more research.

3.4.3 General discussion

Besides differences in size and sex, the age and life stage of organisms (de Lima et al. 2021) may also affect sensitivity. However, this information was not explicitly collected in our research, and we cannot rule out their influence. For these two species, males grow faster than females, and the male is larger than the female. For instance, female adult *G. pulex* individuals are on average 7 mm while male individuals are 10 mm in a previous study (Horion et al. 2015). In addition, we visually chose females without eggs, but their reproductive stage was unknown. Pregnant females may be more sensitive to chemicals because they need to allocate energy to reproduction and have less energy to deal with chemical stress. To understand the influence of reproduction, the dynamic energy budget (DEB) theory should be applied. DEB is a mechanistic modelling approach to describe the effects of toxicant exposure (Jager 2020, Sherborne and Galic 2020) on the entire life history of the organism, such as growth and reproduction.

Despite the limitations of our study, our study found size-related differences in the sensitivities of *G. pulex,* which can be explained well by both TK and TD processes. The most sensitive group was the neonates for both species. The sensitive differences between neonates and juveniles are 2.6 times for *G. pulex* and 4.5 times for *A. aquaticus* (Table S9). The current research could underestimate the potential effect of IMI at the population level by excluding the potentially higher sensitivity of neonates.

Our study also found the sex-related difference, although we could not exclude the size influence since the females were naturally smaller than males (Horion et al. 2015). It was contrary in two species, and smaller female *G. pulex* was more sensitive to IMI than males; however, smaller female *A. aquaticus* was much less sensitive to IMI than males. It indicates that sex-related differences may vary in species. In the case of IMI, sex-related differences rely

on biotransformation because more biotransformation leads to higher sensitivity. Moreover, the generation of IMI-ole could cause a profound long-term effect, especially for females *G. pulex* and male *A. aquatics*, as the elimination of IMI-ole, an active metabolite, was eliminated slower than the parent chemical (Table S7). Our study highlighted the need to consider the size and sex differences in risk assessment to assess the impact of pollutants at the population level.

3.5. Conclusion

Our study compared the toxicity differences of IMI related to size and sex for two aquatic crustacean species. We have found that for both species, the neonates are the most sensitive group. For *G. pulex*, the sensitivity relies on the size. The size-related differences in the uptake rate constant in the toxicokinetics process and the threshold value in the toxicodynamics process could explain the sensitivity differences. However, for *A. aquaticus*, the males were more sensitive than females, which can be related to differences in the biotransformation rate and the threshold difference between males and females. For both species, the toxicokinetics and toxicodynamics models were proved to be proper tools to explore the mechanism of intraspecies sensitivity difference. Our study also raises the importance of providing the size and sex information in reporting the results of toxicity tests used in ecological risk assessment.

Support Information

The support information of this chapter can be downloaded from:

https://www.sciencedirect.com/science/article/pii/S0147651322007576#sec0160
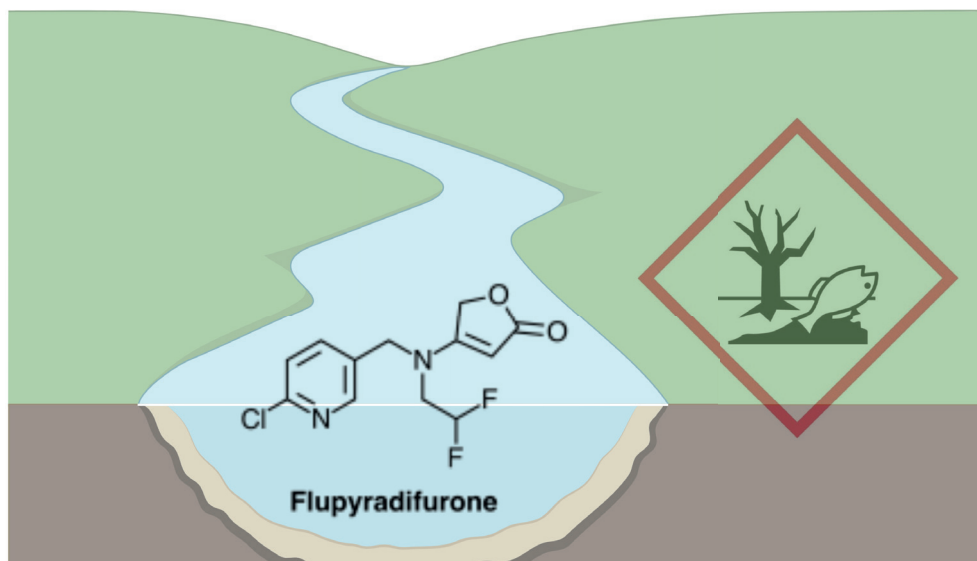
3

4

CHAPTER 4.

Comparing the acute and chronic toxicity of flupyradifurone and imidacloprid to non-target aquatic arthropod species.

Anna Huang, Annika Mangold-Döring, Andreas Focks, Chong Zhang, Paul J. Van den Brink

Graphical abstract: A graphic diagram of the experimental design and the results. Diagram created with BioRender (www.biorender.com).

Abstract

Flupyradifurone (FPF) is a new type of butenolide insecticide. It was launched on the market in 2015 and is considered an alternative to the widely used neonicotinoids, like imidacloprid (IMI), some of which are banned from outdoor use in the European Union. FPF is claimed to be safe for bees, but its safety for aquatic organisms is unknown. Its high water solubility, persistence in the environment, and potential large-scale use make it urgent to evaluate possible impacts on aquatic systems. The current study assessed the acute and chronic toxicity of FPF for aquatic arthropod species and compared these results with those of imidacloprid. Besides, toxicokinetics and toxicokinetic-toxicodynamic models were used to understand the mechanisms of the toxicity of FPF. The present study results showed that organisms take up FPF slower than IMI and eliminate it faster. In addition, the hazardous concentration 5th percentiles (HC_{05}) value of FPF derived from a species sensitivity distribution (SSD) based on acute toxicity was found to be 0.052 µmol/L (corresponding to 15 µg/L), which was 37 times higher than IMI (0.0014 µmol/L, corresponding to 0.36 µg/L). The chronic 28 days EC_{10} of FPF for *Cloeon dipterum* and *Gammarus pulex* were 7.5 µg/L and 2.9 µg/L, respectively. For *G. pulex*, after 28 days of exposure, the no observed effect concentration (NOEC) of FPF for food consumption was 0.3 µg/L. A toxicokinetic-toxicodynamic (TKTD) model parameterised on the acute toxicity data well predicted the observed chronic effects of FPF on *G. pulex*, indicating that toxicity mechanisms of FPF did not change with prolonged exposure time, which is not the case for IMI.

4.1. Introduction

Neonicotinoids are among the most used pesticides, and they are currently registered for hundreds of field crops in over 120 countries, accounting for one-third of the pesticide market share (Jeschke and Nauen 2008, Jeschke et al. 2011, Simon-Delso et al. 2015). However, the adverse effects of neonicotinoids on bees and non-target aquatic invertebrates have been raised with increasing concern (Morrissey et al. 2015, Jactel et al. 2019). In 2018, three neonicotinoids, imidacloprid (IMI) (European Commission 2018a), clothianidin (European Commission 2018b) and thiamethoxam (European Commission 2018c), were banned for outdoor use in Europe because of their risks to pollinators. One of the most important alternatives to neonicotinoids is flupyradifurone (FPF), a new butenolide pesticide (Giorio et al. 2017a). FPF was first commercially available in Honduras and Guatemala in 2014 (Nauen et al. 2015a) and has since become available for use on a wide range of crops in Canada (PMRA 2015), the United States (EPA 2015), China (Zhong et al. 2021) and Europe (EFSA 2016). It acts as an agonist on insect nicotinic acetylcholine receptor (nAChR), similar to neonicotinoids (Jeschke et al. 2015b), while it has a different pharmacophore system as a new bioactive scaffold (Nauen et al. 2015b). FPF is used for a wide range of crops as a foliar spray, soil drench, and seed treatment, targeting sucking pests such as aphids, hoppers, and whiteflies (Bayer 2012). According to a new economic assessment, FPF currently is one of the most commonly used imidacloprid substitutes in Californian agriculture (Goodhue et al. 2020). Research shows that FPF seems comparatively safer for honeybees and bumblebees than IMI (Campbell et al. 2016).

However, the knowledge of the safety of FPF to freshwater invertebrates is limited. Considering the chemical characteristics of FPF, i.e., high solubility in water, low volatility and high half-life values in water and/or soils (Bayer 2012, Nauen et al. 2015a), FPF will be persistent in the environment and has a high potential to enter freshwater ecosystems through runoff, erosion, and leaching (Carleton 2014). So far, there are not many studies on environmental concentrations of FPF, but one study found that the highest measured environmental concentration of FPF is 0.16 µg/L in a watershed of the Great Lakes basin (Metcalfe et al. 2019). To the best of our knowledge, toxicity data of FPF is alone available for three aquatic arthropod species: *Hexagenia* spp. (Bartlett et al. 2018), *Chironomus dilutus* (Maloney et al. 2020) and *Hyalella azteca* (Bartlett et al. 2019a). Notably, data for Daphnia

were excluded because FPF is, like IMI, not toxic to cladocerans (Lewis et al. 2016). These available studies focused on lethal endpoints, such as mortality and immobility, conventionally assessed in 2 or 4 days acute and 28 days chronic tests. Acute and chronic toxicity tests have been performed with aquatic invertebrates extensively for neonicotinoids, especially for IMI (Roessink et al. 2013, Morrissey et al. 2015). Besides lethality-related endpoints like mortality and immobilisation, insecticides may also affect sublethal endpoints, such as feeding rate (Nyman et al. 2013), growth, reproduction, and emergence (De França et al. 2017). In the case of IMI, the sublethal effect concentration was found to be several orders of magnitude lower than the lethal concentration, and importantly, the sublethal effect on individuals may result in a profound impact on populations (Rico et al. 2018, Van de Perre et al. 2021). Therefore, more studies on the effects of FPF on freshwater invertebrates focussing on the lethal and sublethal endpoints, are needed.

To understand the mechanism of the toxicity of pesticides, toxicokinetic-toxicodynamic (TKTD) models can be used (Ashauer and Escher 2010). Specifically, models from the General Unified Threshold model for Survival (GUTS) can help to understand the mechanisms and characteristics of lethal effects. Recently, an EFSA (European Food Safety Authority) working group concluded that the GUTS models are fit for purpose of being used for the risk assessment of pesticides for aquatic organisms (EFSA PPR Panel (Panel on Plant Protection Products and their Residues) et al. 2018). GUTS modelling was also successfully used to predict survival over time of aquatic invertebrates exposed to time-variable exposure patterns of IMI (Focks et al. 2018).

To assess the toxicity of FPF for aquatic arthropods, we selected three species, the ephemeropteran *Cloeon dipterum*, the amphipod *Gammarus pulex,* and the isopod *Asellus aquaticus*. They are widely distributed invertebrates in Europe and play an important role in freshwater ecosystems (Hynes 1970). Besides, because of their high abundance, high reproduction rate, and comparably short life cycle, they are suitable organisms for laboratory toxicity tests (Williams et al. 1984, McCahon and Pascoe 1988, Johnson et al. 1993). Also, the insect species *C. dipterum* is one of the most sensitive species to IMI, while *G. pulex* and *A. aquaticus* are macrocrustaceans and are intermediately sensitive to IMI (Roessink et al. 2013). Using these three species, we aimed to compare the toxicity of IMI and FPF for species belonging to different taxonomic groups.

The objectives of this study were to evaluate the effects of FPF on lethal and sublethal endpoints resulting from acute and chronic exposure and to use GUTS modelling to test for consistency between acute and chronic toxicity of FPF. For these objectives, we performed a 4-day acute toxicity test with three species, *C. dipterum*, *G. pulex,* and *A. aquaticus*, and consecutive toxicokinetic experiments with the same species. From that, uptake and elimination rates of FPF were derived and compared to literature values available for IMI. Previous acute toxicity tests performed with arthropods obtained from the literature were integrated with our results to generate an acute species sensitivity distribution (SSD) for FPF and IMI. Effects on mortality, immobility, size, emergence, food consumption and internal concentrations were assessed in the chronic test of FPF with *C. dipterum* and *G. pulex*.

4.2. Materials and methods

4.2.1 Chemicals and test organisms

Flupyradifurone (CAS: 951659-40-8) and the commercially available metabolite, 6-chloronicotinic acid (6-CNA; CAS: 5326-23-8), were used in the experiments. The stock solutions of FPF (10 and 1 µg/mL) were dissolved into MiliQ water. Imidacloprid-d4 (IMI-d4; CAS: 1015855-75-0) was used as an internal standard during the analytical measurements of all organism samples. The stock solutions of IMI-d4 (200 µg/mL) were dissolved into 2% acetone (v: v) to ensure that the compound was fully dissolved. The FPF stock solution was stored at 4 °C in the dark when it was not used. A fresh stock solution was prepared for each test.

Three species, *C. dipterum*, *G. pulex* and *A. aquaticus*, were used in the experiments. *C. dipterum* was collected from an uncontaminated test system at the outdoor research site 'De Sinderhoeve' located in Renkum, the Netherlands (www.sinderhoeve.org). *G. pulex* was collected from an uncontaminated location, the Heelsumse Beek (a brook with the coordinates 51.973400N, 5.748697E), while *A. aquaticus* was collected from the campus of Wageningen University and Research (a pond with the coordinates 51.986859N, 5.668837E). After collection, the organisms were kept in aerated tanks in the laboratory for at least 3 days to acclimate them to laboratory conditions. During the acclimation period, organisms were fed with fish food for *C. dipterum* and leached *Populus* leaves for *G. pulex* and *A. aquaticus* (Roessink et al. 2013). All containers containing the test organisms were placed in a water bath

maintained at 18 ± 1 °C with a light: dark regime of 12:12 hours. The light in our setup did not contain ultraviolet light to prevent photodegradation of FPF.

In order to confirm the absence of all tested analytes in the collected water and organisms samples, we analysed the water and organisms samples by LC/MS-MS before the exposure. For the details of chemical analysis, see section 4.2.5.

4.2.2 Acute toxicity experiments

The acute toxicity of FPF was assessed by a 4-day standard acute toxicity test to estimate the 96 h EC_{50} and LC_{50} for *C. dipterum*, *A. aquaticus* and *G. pulex* (Roessink et al. 2013). In detail, separate tests were performed for each species. For *C. dipterum,* each replicate consisted of 16 mayflies placed in a glass jar containing 1 L groundwater obtained from the Sinderhoeve experimental station. This volume was dosed with FPF to reach exposure concentrations of 0, 1, 3, 10, 30, 100 and 300 µg/L. For the tests with *G. pulex* and *A. aquatics*, each replicate consisted of 16 individuals (*G. pulex)* or 10 individuals (*A. aquaticus)* in 1 L groundwater, after which the volume was dosed to reach concentrations of 0, 3, 10, 30, 100, 300 and 1000 µg/L. These experimental concentrations were achieved by adding an appropriate portion of the stock solution to the test system, and the selection of the concentration was based on the results of previous IMI and FPF toxicity studies with aquatic arthropods (Roessink et al. 2013, Maloney et al. 2020). These tests were performed in May 2020, using a summer generation of all species. Experiments were performed with three replicates per treatment level, while five replicates were used for controls. The test systems were not aerated during the experiments to minimize water evaporation. In the experiments with *G. pulex* and *A. aquaticus,* a piece of stainless steel mesh was added to serve as a substrate for organisms and reduce cannibalistic behaviour. Organisms were checked every day, and the status (dead, immobile or mobile) of each individual was assessed according to Roessink et al. (2013) (Roessink et al. 2013). Dead organisms and moults were removed daily.

Daily, 1 mL of water was taken to verify the exposure concentration of FPF by using LC-MS/MS (see section 4.2.5). All jars were placed randomly in a water bath; temperature and light conditions were the same as during the acclimation period. Dissolved oxygen, pH, electrical conductivity and temperature were measured at the start and end of the test in the control group and in the highest treatment only. The dissolved oxygen content was acceptable at the

end of the experiment, with a minimum value of 8.7 mg/L. These results are provided in the raw dataset (Huang et al. 2022b).

4.2.3 Toxicokinetic tests

At the end of the acute toxicity test (day 4), less than 10% of the individuals were affected in the 10 µg/L treatment for all three species. With the remaining organisms of these treatments, a toxicokinetic test was conducted. In detail, after 4 days of exposure, for the acute tests with *C. dipterum* and *G. pulex*, 8 individuals were randomly selected from each replicate separately, rinsed for 30 seconds with clean MiliQ water, and transferred to 1 L clean groundwater to assess the elimination of FPF after 2 days. The remaining 8 individuals were cleaned and stored at -20°C for further chemical analysis and were used to determine the uptake after 4 days. The test with *A. aquaticus* used 5 individuals for the uptake and 5 individuals for the elimination phase. At the end of the elimination phase, all alive organisms were collected from the three replicates, washed with MillQ water for 30 seconds, and stored at -20°C for further chemical analysis.

The concentration of FPF was measured in both organisms and water samples during the uptake, and elimination phase for each replicate separately. For quality control of the experimental setup, three replicates containing organisms but no chemicals (from the previous control groups) were also kept during the elimination phase to evaluate the status of the organisms.

4.2.4 Chronic experiment

As *A. aquaticus* was the least sensitive species in the acute experiments, the chronic tests were only performed with *C. dipterum* and *G. pulex* in September and November 2020. The experimental conditions and spiking procedure of FPF were the same as in the acute tests. The volume was dosed to reach final exposure concentrations of 0, 0.1, 0.3, 1, 3, 10, 30 µg/L for *C. dipterum* and 0, 0.3, 1, 3, 10, 30 µg/L for *G. pulex.* These experimental concentrations were achieved by adding an appropriate portion of the stock solution to the test system, and the selection of the concentration was based on our previous FPF acute test results. Gentle aeration was provided, and the animals were fed with appropriate species-specific food, weekly for *C. dipterum* and biweekly for *G. pulex*. 1 mL of fish flask slurry, consisting of 6 g ground fish flask added to 40 mL MillQ water and homogenised by stirring with the magnet

mixer, was added to each replicate for *C. dipterum*, and two pieces of discs of leached *Populus* leaves (3.2 cm radius) for *G. pulex*. The jars were completely refreshed with a new test medium and food every week for *C. dipterum* and every two weeks for *G. pulex,* and the living test animals were transferred with care to the new test system. Immobility and mortality were monitored every 2 to 3 days during the experiment, and the physicochemical water parameters were measured weekly. For *C. dipterum,* the emergence of individuals occurred mostly in the fourth week of the experiment. Emerged *C. dipterum* was counted as missing in the statistical analysis because, after emergence, it is no longer possible to determine whether the individual would have been affected or not.

The food consumption of *G. pulex* was measured every two weeks in this study. The pre-treated (leached into the water before use) (McGrath et al. 2007) *Populus* leaves were cut into circles with the same surface area (3.2 cm radius) using a cork borer and dried at 60 °C for at least 48 h. Two pieces of leaf discs were provided for every replicate. The dry weight of the leaves of each replicate was recorded before putting them into the jar. The dry leaves were added to each replicate for 3 days before adding the organisms and the chemical to allow the leaves to soak in the clean water. The leaves in the test jars were changed every two weeks together with the refreshment of the system. The weight of the remaining leaves was recorded after drying at 60°C in the oven for at least 48 h. Apart from the jars with *G. pulex*, a blank food treatment without organisms was added. Two jars with only stainless-steel mesh and conditioned Populus leaves were installed to estimate the microbial degradation of the leaves. The food consumption of each replicate was calculated as the difference between the initial leaves weight and the remaining leaves' weight after the loss was corrected for microbial degradation.

At the beginning and during the system renewal process, *C. dipterum* was taken out to measure their length using a binocular with a camera (Olympus, U-TV0.5XC-3, Japan). At the beginning and the end of the experiment, a short video (less than 10 seconds) of all *G. pulex* individuals present in a replicate was taken. The video screenshots were extracted from the videos with Elmedia Video Player (7.17, Elmedia Software). The body length of *C. dipterum* was measured from the anterior margin of the mesothorax to the posterior end of the abdominal segment. The body length of *G. pulex* was measured from the anterior margin of the caput to the posterior end of the pleon (not including telson), along with the curved shape

of the pereon (Figure S1). Each organism was observed under the microscope with a reference object for scale. The program ImageJ (1.53, National Institute of Health, USA) was used for image analysis and length measurements (SI Text S1).

After 28 days of exposure, all remaining organisms were washed with MillQ water for 30 seconds and stored at -20°C for further chemical analysis. The concentration of FPF was measured in both the organisms and the water.

4.2.5 Chemical analysis

In the toxicokinetic experiment (section 4.2.3) and at the end of the chronic experiment (section 4.2.4), the internal concentration of FPF was measured at each time point in each test. The remaining organisms from the same jar were pooled for the measurement, which resulted in 3 replicates for each concentration level. The methods were similar to those in (Huang et al. 2021). In detail, for the analytical quantification of the concentrations, all samples were taken out of the freezer, and the organisms were lyophilised for 1 day and weighted to obtain the dry weight of the animals. 1 mL 1% acetic acid MeOH : Water (v : v = 5 : 1) extraction solution and 25 µL internal standard (imidacloprid-d4, 200 µg/L) were added. Then the samples were homogenized with a Minilys personal homogeniser (Bertin Instruments, France) using a Precellys ceramic lysing kit (1.4/2.8 mm; Bertin Instruments, France) for 3 times 60 sec at 3000 rpm using a 30 sec interval in between. After this, the sample was centrifuged at 10000 rpm for 10 minutes, and the supernatant was filtered over a PTFE syringe filter (pore size 0.45 µm) into a 2 mL injection vial. Filters were injected with 200 µL extraction solution again to regain the chemical which may remain in the filter. This filtrate, in turn, was centrifuged and filtered over a syringe filter (0.45 µm) as well. Afterwards, the two filtrates were combined, and a final volume of 1.2 mL was collected, after which the sample was ready for analysis by LC-MS/MS. The water samples were analysed directly, without an extraction step.

All samples were analysed by reversed-phase liquid chromatography-tandem mass spectrometry (LC-MS/MS) using the protocol of imidacloprid, with small modifications (Huang et al. 2021). The injection volume of the samples was set at 10 µL. The mobile phase used was MeOH + 0.1% Formic acid (C) and Milli-Q water+ 0.1% Formic acid (D) with the following multistep gradient: 0-1.5 min: 90/10 (C/D, v:v); 1.5-2.5 min: 90/10 (C/D, v:v) to 50/50 (C/D, v:v); 8 min: 50/50 (C/D, v:v); 8-8.1 min: 50/50 (C/D, v:v) to 0/100 (C/D, v:v); 9 min: 0/100 (C/D,

v:v); 9-9.1 min: 0/100 (C/D, v:v) to 90/10 (C/D, v:v); 9.1-12 min: 90/10 (C/D, v:v) at a flow rate of 0.7 mL/min. The mass spectrometer was operated using an Agilent jet stream electrospray ionization source (AJS-ESI) in positive mode. Nitrogen was used both as nebulizer and collision gas, the capillary voltage was 5000 V, and the temperature of the ion source (TEM) was set at 300°C. The compounds were detected in the multiple reaction monitoring (MRM) using two transitions per compound.

The MS/MS transitions of all compounds are provided in Table S1. Injected samples were quantified by peak area using the calibration curve constructed from the calibration standards included in the same sample sequence (Table S2 and Table S3). Agilent Masshunter software (version 8.0) was used for instrument control and data acquisition. The extraction recoveries of FPF in the organisms, evaluated at two concentrations (a low and a high concentration) by spiking them into the clean organisms, were acceptable for all three species tested based on recovery and repeatability (Table S4). The limit of quantification (LOQ) was calculated based on the measurement of the analyst responses in the sample matrix corresponding to a signal-to-noise ratio (S/N) of 10:1. Determination of the S/N was performed by comparing measured signals from samples with known low concentrations of analyte with those of blank samples and by establishing the minimum concentration at which the analyte can be reliably quantified (Table S2 - S4). More information on the measurement is presented in Text S2.

4.2.6 Data analysis

4.2.6.1 Species Sensitivity Distribution (SSD)

We used the Ecotox database (www.epa.gov/ecotox) to collect acute toxicity data for IMI and FPF of aquatic arthropods. A direct comparison between the IMI and the FPF toxicity was made based on the mortality or immobility toxicity values of the same six benthic arthropod invertebrate species (Table 4.1 and references therein). For this comparison, the toxicity values for IMI and the FPF were obtained from the same study or the same research group.

Species sensitive distributions (SSD) were generated based on all currently available data. All the criteria (test duration, etc.) for data selection were based on a previous study (Maltby et al. 2005). To be specific, the taxa of interest were aquatic Arthropoda. The selected endpoints were the median effect concentration (EC_{50}) regarding immobility of animals or the median lethal concentration (LC_{50}) when the EC_{50} value was not available. Effect concentration (ECx)

is a better indicator of toxicity than the lethal concentration (LC_{50}) for IMI since most organisms in short-term acute toxicity tests are only immobilized but not dead, but they will die after prolonged exposure (Roessink et al. 2013, Raby et al. 2018). Only test results with a duration between 1 to 7 d were included. A genus-specific geometric mean was used when no specific species names were provided. For species with multiple entries in the database, we first distinguished them by the duration of experiment and then by study group. Specifically, If they were from the same study, but on different days, we only selected the last day's value; if they were from different studies, we used the geometric mean of all values. The SSDs based on these EC_{50} or LC_{50} values were fitted using a log-normal distribution using maximum likelihood (Xu et al. 2015, EPA 2016). To be noted, the values for Daphnia were excluded as both chemicals are not toxic to cladocerans (Morrissey et al. 2015, Li et al. 2021). In summary, we had data for 6 species (including 3 species from our study) to generate the acute SSD of FPF and 39 species for IMI. Furthermore, to compare the difference between the Crustacea and Insecta, subphyllum-specific SSDs were calculated for IMI (see SI Text S3).

4

Table 4.1: *Comparison of effect concentrations (in two units, μg/L and μmol/L) causing 50% mortality (LC_{50}) or immobility (EC_{50}) of imidacloprid (IMI) and flupyradifurone (FPF)*

Species	Class	Life stage	Size/weight/ age	endpoint category	IMI (μmol/L)	IMI (μg/L)	FPF (μmol/L)	FPF (μg/L)	Temp-erature (°C)	Reference
Cloeon dipterum	Insect	juveniles	5 mm big	EC_{50}	3.9E-03	1[b]	0.1[a]	42	18	(Roessink et al. 2013) and present study;
Gammarus pulex	Crustacean	juveniles	5 mm big	EC_{50}	0.1	18[b]	0.3[a]	94	18	
Asellus aquaticus	Crustacean	juveniles	5 mm big	EC_{50}	0.5	119[b]	0.5[a]	137	18	
Hyalella azteca	Crustacean	juveniles	2 - 10 days old	LC_{50}	0.9	230	0.1	26	25	(Bartlett et al. 2019a)
Chironomus dilutus	Insect	larvae	6 -7 days old	LC_{50}	2.7E-02	7	0.1	17	23	(Maloney et al. 2020)
Hexagenia spp.	Insect	larvae	5 - 8 mg weight	EC_{50}	3.9E-02	10	0.3	81	n.d	(Maloney et al. 2020)

Note: a= Data from the present study, b= Data from the same group

n.d = not mentioned

4.2.6.2 Lethal concentrations and effect concentrations

Lethal concentrations (LCx) and effect concentrations (ECx), were determined for each observation time point by fitting the number of dead and affected organisms, respectively, to a 4-parameter log-logistic model (LL.4) with the drc package (Ritz and Streibig 2005) in the open-source software R version 4.1.0 (Ritz et al. 2015).

$$f(x) = c + \frac{d-c}{1+exp\ (b(log(x)-\log(e)))} \qquad \text{(Eq. 1)}$$

With *f(x)* is the fraction of affected or dead organisms, *b* is the slope around LC_{50} or EC_{50} (which is *e*), *c* denotes the control mortality, *x* is the water concentration, and *d* is the upper limit.

Mortality and immobility data fit the LL.4 model with the upper limit of 1 and are based on a binomial distribution.

4.2.6.3 Food consumption

Dry mass (DM, mg) of leaves consumed by *G. pulex* per jar (L_e) after two weeks was calculated as:

$$L_e = L_i - L_f - Lc. \qquad \text{(Eq. 2)}$$

Where L_i and L_f *are* the initial and final dry mass (mg) of leaves, and Lc is the average dry mass loss of the blank food treatment accounting for microbiological degradation.

To gain food consumption per organism, we divided the total amount of food consumed per jar by the numeric mean of the remaining organisms at each observation time (Eq. 3). The food consumption rate per organism (F_{total}) after two weeks was calculated as:

$$F_{total} = \frac{L_e}{average\ (n1+n2+\cdots+nt)} \qquad \text{(Eq. 3)}$$

Where n is the numeric mean of remaining organisms at each observation time, day 1, 4, 7, 9, 11 and 14 for the first two weeks and day 14, 16, 18, 21, 23, 25 and 28 for the last two weeks.

4.2.6.4 Calibration of TKTD models and predictions of survival

The GUTS TKTD framework has been described earlier (Jager et al. 2011, Jager et al. 2017, Jager 2021). The GUTS models were calibrated using MATLAB (2021b), using the BYOM modelling platform (www.debtox.info/byom.html). We used both the reduced and the full

cases for the two death mechanisms (SD, IT). We started by fitting the reduced model (GUTS-RED) to the acute survival data (section 4.2.2) alone. The use of GUTS-RED allows fitting a TKTD model in the absence of information on body residues.

Also, the full model (GUTS-FULL) was used for fitting survival and body-residue data together; more precisely acute survival data (section 4.2.2) and the internal concentration measurements of toxicokinetic (section 4.2.3) were used. In addition, we compared the toxicity predictions based on the calibrated GUTS-RED and GUTS-FULL models with our FPF chronic test results to evaluate the possibility of extrapolating acute toxicity values to chronic toxicity values using a TKTD model. For *G. pulex*, 28-day chronic data were used. As *C. dipterum* emerged after 21 days, only the chronic survival data within 17 days was used for the prediction. The Normalised Root Mean Square Error (NRMSE) was used in our study to evaluate model performance (EFSA PPR Panel (Panel on Plant Protection Products and their Residues) et al. 2018). A further description of the GUTS framework is provided in the supporting information Text S4.

4.2.6.5 Statistical analysis

Significant differences between treatments and controls were assessed by using R (version 4.1.0). The assumptions of normality were evaluated with a Shapiro-Wilk test, and the assumption of equal variance was assessed using a Spearman rank correlation between the residuals and the dependent variable. If the assumptions of normality and equal variance were passed, a one-way analysis of variance (ANOVA) with $\alpha=0.05$ and a post-hoc Tukey's test was conducted. If assumptions failed, a Kruskal-Wallis test, with $\alpha=0.05$, and a post-hoc Dunn's test were used.

4.3. Results and discussion

In both acute and chronic experiments, the water concentration of FPF was stable and within 20% deviation from the nominal concentration (Huang et al. 2022b). Thus, the nominal concentrations have been used to describe the treatment levels in the following results and discussions. However, in order to be more accurate and to be able to capture subtle differences, the average measured water concentration was used in the TK and GUTS modeling.

4.3.1 The accumulation, uptake and elimination of FPF

4.3.1.1 The accumulation of FPF after 28 days of exposure

After a chronic 28-day experiment, we measured the internal concentration of FPF in the remaining living organisms (Table 4.2). The bioconcentration factor (BCF) was calculated as we expected that the bioconcentration process would reach a steady state after 28 days of exposure because of the quick elimination time (t_{95}) of FPF (Table 4.3). The concept of t_{95} is the time that it would take the organism to eliminate 95% of the accumulated toxicant when returned to clean water, which is equivalent to the time to reach the steady state (Ashauer et al. 2010, Rubach et al. 2010). Because FPF is highly water-soluble, we estimated that the contribution of food uptake to the accumulation of FPF was low (Nauen et al. 2015a); thus, no accumulation via food intake was considered in the present study.

Overall, *C. dipterum* accumulated less FPF than *G. pulex* under the same exposure concentration (Table 4.2). For *C. dipterum,* the BCF values were similar for the different treatments (Table 4.2). However, for *G. pulex,* the BCF values decreased with increasing concentration levels. Although we did not evaluate passive absorption in this study, the adsorption of FPF on the surface of the Gammarus exoskeleton could explain this. A previous study demonstrated that a certain amount of IMI accumulated on the surface of pre-killed Gammarus (Huang et al. 2021). In addition, Dalhoff et al. (2020) distinguished the sorbed fraction and the internalised fraction of cypermethrin for several aquatic species, including *G. pulex*, and they found a significant fraction of the total measured body concentration to be adsorbed to the surface of the organisms (Dalhoff et al. 2020).

Generally, FPF is not likely to bioconcentrate or bioaccumulate in aquatic organisms due to its low log K_{OW} value of 0.08 (Carleton 2014). Our low BCF value results, which were less than 3 L/kg for *C. dipterum* and 50 L/kg for *G. pulex,* were consistent with this statement (Table 4.2).

The metabolite of interest (6-CNA) was measured but not detected in this study. Based on previous studies, 6-chloronicotinic acid (6-CNA) could be one of the biotransformation metabolites of FPF, and it was observed in soil and rats (Bayer 2012). However, it was not found in our study. To the best of our knowledge, no biotransformation of FPF has been found in bee studies (Nauen et al. 2015a).

Table 4.2: *The bioconcentration factor (BCF) and internal concentration of flupyradifurone in two species after 28 days of exposure.*

Species	exposure concentration (µg/L)	BCF (L/kg)	internal concentration (µg/kg) (mean value ± sd, n=3)	
C. dipterum	1	0.71	0.71	± 0.44
	3	2.26	6.79	± 1.46
	10	1.47	14.7	± 7.11
G. pulex	0.3	49.5	14.9	± 2.32
	1	35.4	35.4	± 6.71
	3	19.2	57.5	± 2.07
	10	7.56	75.6	± 6.75

4.3.1.2 Toxicokinetics of FPF and comparison with that of IMI

The 10 µg/L treatment of the acute toxicity test of each species was subsequently used for the TK experiment. During the 2 days elimination period, no mortality occurred, and no eliminated FPF was detected in the water at the end of the elimination period.

The first-order one-compartment toxicokinetic model was fitted for three species. The order of the uptake rate from high to low was *G. pulex*, *C. dipterum* and *A. aquaticus* (Table 4.3). *G. pulex* eliminated FPF as fast as *C. dipterum*, while *A. aquatics* eliminated the slowest (Table 4.3).

Comparing the toxicokinetics of IMI and FPF, the uptake rate of FPF was lower than the value of IMI for all three species, while the elimination rate of FPF was faster in *C. dipterum* and *G. pulex* and slower in *A. aquaticus* than IMI (Huang et al. 2021) (Table 4.3).

In addition, calculated uptake and elimination rates can be used to calculate BCF values as well. In order to differentiate between BCF values based on measured concentrations and BCF values based on rate constants calibrated by TK modeling, we call the latter one bioconcentration factor kinetic (BCF_k), which is calculated directly by dividing the uptake rate by the elimination rate (Huang et al. 2021, Li et al. 2021). Comparing the BCF values based on

body residue and water concentrations measured at the end of the chronic test (28 days) in the 10 ug/L treatment (Table 4.2) with the BCF_k (Table 4.3), the two values were very similar. In other words, our results indicate that at 10ug/L, the accumulation of FPF has reached a steady state after 28 days because the BCF was close to $BCFk$.

To our knowledge, no other toxicokinetic studies have been performed with FPF and aquatic arthropods. However, previous pharmacokinetic studies of FPF (Haas et al. 2021) and IMI (Zaworra et al. 2019) with bees revealed that, compared to IMI, FPF uptake was slower through the honey bee cuticle over 24 h and eliminated faster. Their studies were similar to our findings for *C. dipterum* and *G. pulex,* but not for *A. aquaticus*. The only difference between *A. aquaticus* and the other two species was the elimination rate of FPF, which was slower than IMI. This indicated that *A. aquaticus* might bind FPF stronger than IMI.

Moreover, FPF and IMI are chemically different; FPF contains the butenolide group, while IMI contains the N-Nitro-guanidine group as the nAChR agonist (Jeschke et al. 2015a). The kinetic differences between IMI and FPF could be caused by differences in their receptor binding affinity. A previous bee study found that the binding affinity of FPF to honey bee nAChR preparations was 6-times lower than IMI (Haas et al. 2021). In addition, Jeschke et al. (2015) found that FPF reversibly binds and activates endogenous insect nAChRs (Jeschke et al. 2015a). In contrast, the receptor binding of IMI, especially its toxic biotransformation product IMI-olefin, has been reported to appear irreversible in invertebrates (Tennekes 2011, Huang et al. 2021).

Table 4.3: *Parameters of the first-order one-compartment toxicokinetic model for FPF and IMI in the three tested species.*

Species	compound	Parameter	value	95% CI	Elimination time t_{95} [a] (d)	BCF_k (L/kg)	R^2	references
		k_u(L·kg$_{ww}^{-1}$·d^{-1}) k_e(d^{-1})						
C. dipterum	FPF	k_u	0.59	0.44 - 0.77	10.70	2.12	0.98	Present study
		k_e	0.28	0.17 - 0.39				
	IMI	k_u	2.96	2.62 - 3.33	74.89	70.11	0.92	(Huang et al. 2021)
		k_e	0.040	$3.4 \cdot 10^{-4}$ - 0.11				
G. pulex	FPF	k_u	1.62	1.47 - 1.79	14.27	7.76	0.99	Present study
		k_e	0.21	0.17 - 0.25				
	IMI	k_u	5.21	4.87 - 5.54	24.96	44.41	0.98	(Huang et al. 2021)
		k_e	0.12	0.11 - 0.16				
A. aquaticus	FPF	k_u	0.39	0.32 - 0.51	59.91	7.65	0.99	Present study
		k_e	0.05	0.01 - 0.14				
	IMI	k_u	1.10	0.87 - 1.50	6.66	2.52	0.99	(Huang et al. 2022g)
		k_e	0.45	0.33 - 0.57				

a: $t_{95} = -ln(1 - 0.95)/ke$.

4.3.2 Acute toxicity of FPF

4.3.2.1 The lethal and sublethal acute effect of FPF

The species sensitivities based on 96h EC_{50} values were ranked from high to low as follows, *C. dipterum* (42.4 µg/L), *G. pulex* (94.2 µg/L) and *A. aquaticus* (137 µg/L) (Table S7). Based on these values, *C. dipterum* was 2 times more sensitive than *G. pulex* and 3 times more sensitive than *A. aquaticus.* However, *C. dipterum* (117 µg/L) was equally sensitive to *G. pulex* (112 µg/L) when based on 96h LC_{50} values. For *A. aquaticus,* the LC_{50} was higher than our highest treatment concentration (1000 µg/L), making it at least 10 times less sensitive than the other species (Table S7).

Among the three species evaluated in this study, the acute sensitivity of the three species to FPF was ranked similarly to IMI, i.e., more toxic to mayflies than to crustaceans (Roessink et al. 2013). However, the difference between the acute LC_{50} and EC_{50} values of FPF was different from those observed for IMI (Huang et al. 2021). In Huang et al. (2021), the difference between EC_{50} and LC_{50} values of IMI for *C. dipterum* increased over time, resulting in a 4-time difference on day 4. In their study with *G. pulex*, the difference between LC_{50} and EC_{50} values decreased over time but still exhibited a 7-time difference on day 4 (Huang et al. 2021). For FPF, these differences between LC_{50} and EC_{50} were much smaller after 4 days (Table S7). For *C. dipterum*,

the LC$_{50}$ value was always 2 to 3 times higher than the EC$_{50}$ value within the 4 days experimental period, while for *G. pulex,* the LC$_{50}$ value was 2 to 3 times higher than the EC$_{50}$ value in the first 3 days and on day 4 a difference of a factor of 1.2 was observed (Table S7). The closeness of LC and EC values may be related to the rapid elimination of FPF, or the lack of active metabolites, resulting in no delay in the effect of FPF. See Section 4.3.3.1 for more discussion.

4.3.2.2 Acute SSD

Among the selected species (Table 4.1), the toxic effect of FPF and IMI were similar among crustaceans (*G. pulex*, *A. aquaticus* and *H. azteca*). Compared to IMI, FPF was less toxic to insects (Table 4.1). We made the species sensitivity distribution (SSD) based on the acute toxicity of 6 species for FPF and 39 species for IMI (Figure 4.1). The HC$_{05}$ of FPF was 0.052 (0.025 - 0.14) µmol/L, while the value of IMI was 0.0014 (3.27e-04 - 0.06) µmol/L, corresponding to 15 and 0.36 µg/L, respectively.

FPF was 37 times less acutely toxic to aquatic arthropods than IMI (Figure 4.1). To our knowledge, the highest measured environmental concentration of FPF is 0.16 µg/L which was recorded in a watershed of the Great Lakes basin, and the geometric mean in 6 watersheds near cropland was 0.018 µg/L (Metcalfe et al. 2019). It was also detected in streams, with IMI being detected in 33% of the samples, while FPF was detected in 13% of samples, with the highest concentration of 0.11 µg/L (Sanford and Prosser 2020). Based on our SSD result and current environmental monitoring results, we could conclude that FPF is safe to date for acute exposure to aquatic arthropods. However, more toxicity assessments of FPF should be performed to incorporate more aquatic arthropods into the SSD, as it currently only consists of 6 data points, which is too limited as a minimum number of 13 taxa is recommended (Carr and Belanger 2019). In addition, as more research encourages the inclusion of FPF in environmental monitoring programs, we will have a better understanding of its environmental concentrations in the future (Kandie et al. 2020, Sanford and Prosser 2020).
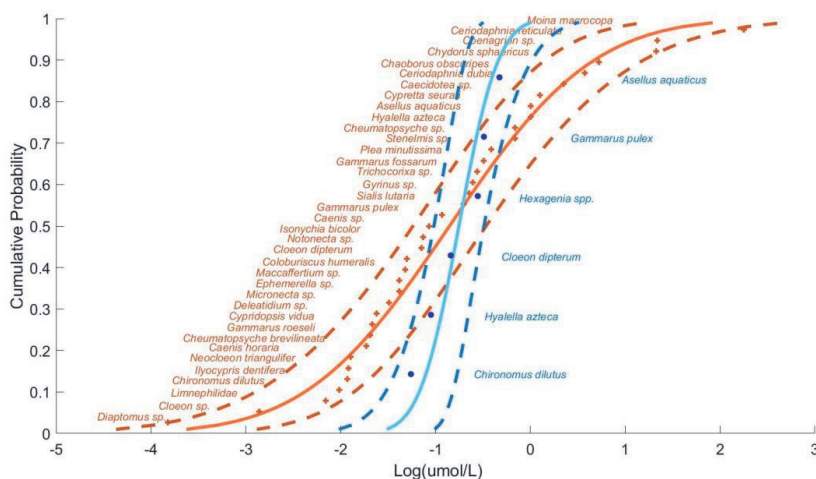
Figure 4.1: *Species sensitivity distributions for acute toxicity based on the results of laboratory single species tests performed with 39 different aquatic invertebrate species for imidacloprid (red) and 6 species for flupyradifurone (blue). The dots are the experimental data, the solid lines are the fitted curve, and the dash lines denote the corresponding 95% confidence interval.*

4.3.3 Chronic toxicity of FPF

4.3.3.1 The lethal and sublethal chronic effect of FPF on C. dipterum and G. pulex

During the 28 days experiment, some emergence of *C. dipterum* was observed. The first emergence occurred on day 14 in the control group, the second emergence occurred on day 17 in the control group, and the rest emergence happened in the last week (day 21-28). The percentage of the emerged individuals was not different among treatments (Figure S11). A further description and discussion on the emergence are provided in the supporting information Text S5.

The effective concentrations for mortality and immobility calculated for the different sampling dates of FPF for *C. dipterum* were close, and the value remained stable over time (Table S8). This study found that the 28d EC_{10} and EC_{50} values were 7.5 µg/L and 9.1 µg/L, respectively (Table S8). In a previous study, the 28d EC_{10} and EC_{50} of IMI for *C. dipterum* were 0.03 µg/L and 0.1 µg/L, respectively, with the toxicity decreasing from a 96h EC_{50} of 1.0 µg/L to a 28d EC_{50} of 0.1 µg/L (Roessink et al. 2013). Hence, compared to IMI, the chronic toxicity of FPF was much lower than that of IMI and did not increase over time as observed for IMI.

For *G. pulex*, control mortality was 23% at the end of the experiment and 12% on day 21. A discussion of the control mortality is provided in the supporting information (Text S6). The effective concentrations of FPF for mortality and immobility of *G. pulex* were close, and these values decreased over time (Table S8). The 28d EC_{10} and EC_{50} values were 2.9 µg/L and 10.6 µg/L, respectively (Table S8). The chronic toxicity of FPF to *G. pulex* was similar to that of IMI as the 28d EC_{10} and EC_{50} of IMI to *G. pulex* were 3.0 (1.2 – 7.6) µg/L and 15.4 (9.80 – 24.1) µg/L, respectively (Roessink et al. 2013), while the molar mass of FPF is only 13% higher than that of IMI.

The large discrepancy between EC and LC values is a remarkable feature of the toxicity of IMI (Roessink et al. 2013). IMI resulted in immobilisation, but the organisms remain alive for quite some time, also known as delayed effects due to cumulative toxicity (Maloney et al. 2017, Li et al. 2021). This delay in mortality of IMI was attributed to the production of a bioactive metabolite over time (Huang et al. 2021). In the present study, this difference between EC and LC values was not significant for FPF, at least for the two tested species, *G. pulex* and *C. dipterum*. This might be explained by the lack of production of the active metabolite, as we detected none in the internal concentration measurements (section 4.3.1).

4.3.3.2 The food consumption inhibition of FPF on G. pulex

We observed the inhibition of FPF on the food consumption for *G. pulex*, especially after two weeks (Figure 4.2). During the first two weeks, none of the treatments significantly inhibited the food consumption compared to the control group (Figure 4.2 A). During the latter two weeks, the 1 and 3 µg/L treatments significantly inhibited ($P < 0.05$) the food consumption compared with the control group (Figure 4.2 B). This 28d NOEC of 0.3 µg/L based on food consumption inhibition is a factor of 10 lower than the 28d EC_{10} based on immobilisation (2.9 µg/L) (Table S8; Figure 4.2).

Again, since data on the effects of FPF on the food consumption of aquatic species was not available, we compared our results with a honey bee study (Tosi et al. 2021). In their study, Tosi and co-workers provided the first evidence that FPF reduces the food consumption of bees after chronic exposures of 20 days. Furthermore, they found that the inhibition of food consumption caused by FPF became more pronounced over time, even at lower doses (Tosi et al. 2021). We had the same observation in our study that food consumption inhibition only

became significant after 2-4 weeks of exposure (Figure 4.2). This can be explained by the low uptake rate and fast elimination of FPF (data shown in Section 4.3.1.2), so it takes longer to exert the effects at low concentrations.

We found two studies (Nyman et al. 2013, Agatz et al. 2014) that studied the effects of IMI on the food consumption of *G. pulex*. They found that the feeding rate of *G. pulex* was significantly reduced after continuous exposure to 30 µg/L IMI for 4 days (Agatz et al. 2014) and 15 µg/L IMI for 14 days (Nyman et al. 2013). However, in their study, the feeding rate was calculated by either the number of disappeared leaves (Nyman et al. 2013) or the fresh weight of *G. pulex* (Agatz et al. 2014), whereas our study used the decrease in dry weight of leaves per individual as a measure. These differences in approaches make the results difficult to compare in order to assess whether the food consumption inhibition effect of FPF is higher than that of IMI.

Nevertheless, our findings suggest that an inhibitory effect of FPF on *G. pulex* food consumption (NOEC was 0.3 µg/L) may occur at the same order of magnitude as the currently measured maximum environmental concentration of FPF (0.16 µg/L) (Metcalfe et al. 2019). Our findings indicate that FPF could disturb the ecosystem process of leaf litter breakdown via changes in the shredding activity of *G. pulex*.
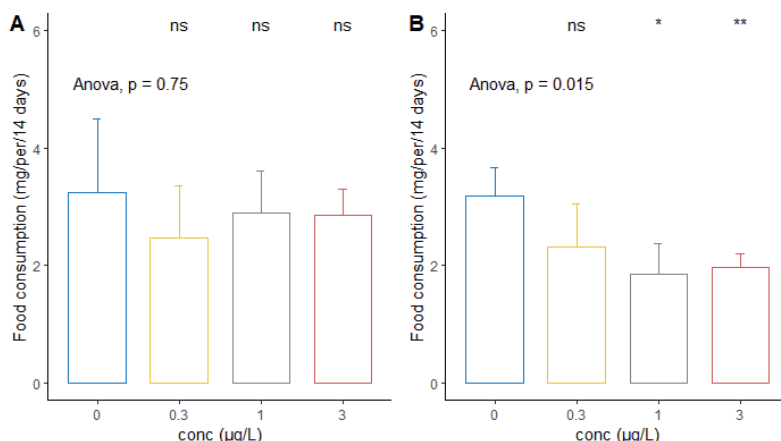

Figure 4.2: Food consumption per G. pulex individual for the first two weeks (A) and the latter two weeks (B) in the different treatments (mean ± sd, n = 5 in control, and n = 3 in the treatments).

4.3.4 The calibration and the prediction of the TKTD for FPF

After calibration on acute data, we used the resulting GUTS-FULL and GUTS-RED models to predict the observed chronic survival for each species. The SD model fitted the acute data better than the IT model both for GUTS-FULL and GUTS-RED, indicated by lower AIC and log-likelihood values (Table S6).

Model predictions of both the GUTS-FULL and GUTS-RED models matched the observed chronic effects not so well for *C. dipterum*, despite NRMSE values being relatively low at 20% for the GUTS-FULL-SD and 19% for the GUTS-RED-SD. On visual examination, predictions of the full and the reduced model underestimated the onset of chronic toxicity to a certain extent (Figure 4.3 B, Figure S5B). For *G. pulex*, the chronic toxicity predictions matched better with the observations with NRMSE values of 17% for GUTS-FULL-SD and 15% for GUTS-RED-SD (Figure 4.4 B, Figure S6B). Surprisingly, the GUTS-RED predicted the chronic toxicity better than the GUTS-FULL model for *G. pulex*, predominantly visible in the better fit for the 10 µg/L treatment (Figure S6, B5). The fact that the GUTS-RED predicted the chronic toxicity better than the GUTS-FULL model for *G. pulex* is surprising at first look; however, it could give an indication that measured internal concentrations were not an ideal predictor of the concentrations at target sites. Here, the additional information included in measured and modelled internal concentrations did not increase the predictive capacity, which is also seen in the lower NRMSE values for the reduced models (Table S6).

In general, GUTS modeling could predict the mortality of *G. pulex* under chronic exposure reasonably well based on acute effect data, while for *C. dipterum* the prediction was possible only with limited accuracy. The IT models underestimated the observed effects under chronic exposure for both tested species (Figure S7-S10).

To the best of our knowledge, only one other study has explored the calibration and validation of the GUTS model for the toxicity of FPF to aquatic invertebrates (Gergs et al. 2021). They performed the calibration and validation of the GUTS-RED for three compounds, imidacloprid, thiacloprid, and flupyradifurone with *Chironomus riparius*, and they found that the validation of FPF was better than that of the other two compounds. This finding indicates that the chronic effect of FPF on *C. riparius* could be predicted based on the mechanisms exerted in the acute study (Gergs et al. 2021). Our calibration and prediction result of *G. pulex* was in line with their study.

In addition, a similar calibration and prediction study has been performed for IMI with *C. dipterum* and *G. pulex* (Huang et al. 2021). In their study, a GUTS-FULL model was calibrated by using 4 days acute toxicity test data plus a toxicokinetic test, and they compared the experimental 28 days EC_{50} values (Roessink et al. 2013) with predictions based on the GUTS-FULL model. They found that the predicted chronic toxicity value was higher than the experimental results, which could be explained by the fact that the slower eliminated active biotransformation metabolite, IMI-ole, was not included in the model prediction. Our results of FPF indicate that before performing GUTS modeling to extrapolate acute toxicity data to chronic toxicity, it should be investigated whether a bioactive metabolite is present.

It should be noted again that the emergence of *C. dipterum* was not included in the GUTS model. A more detailed model, such as a dynamic energy budget model (DEB), which includes the life cycle and energy allocation of organisms, could be used to further investigate FPF effects on sublethal endpoints like growth, reproduction, and emergence (Sherborne and Galic 2020).
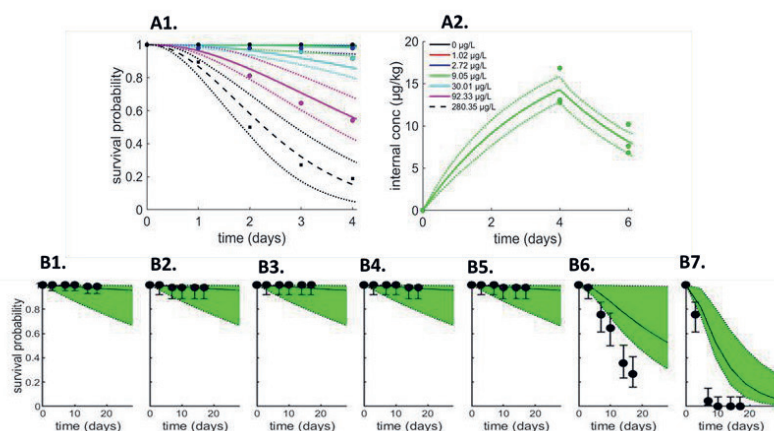
Figure 4.3: The calibration (A) and prediction (B) of GUTS-FULL-SD for flupyradifurone (FPF) toxicity to C. dipterum. From left to right, panel A shows the survival fraction in the acute study (A1) and the toxicokinetics of FPF (A2). The dots, dashed lines, and dotted lines represent measured values, fitted values and confidence intervals, respectively. From left to right, panels B show the prediction of chronic survival data in the 0, 0.1, 0.3, 1, 3, 10 and 30 μg/L treatments, respectively. The dots represent the survival data from chronic test; bars represent Wilson score confidence intervals. The line and the green area represent the prediction and the 95 % confidence interval from the GUTS-FULL prediction, respectively.
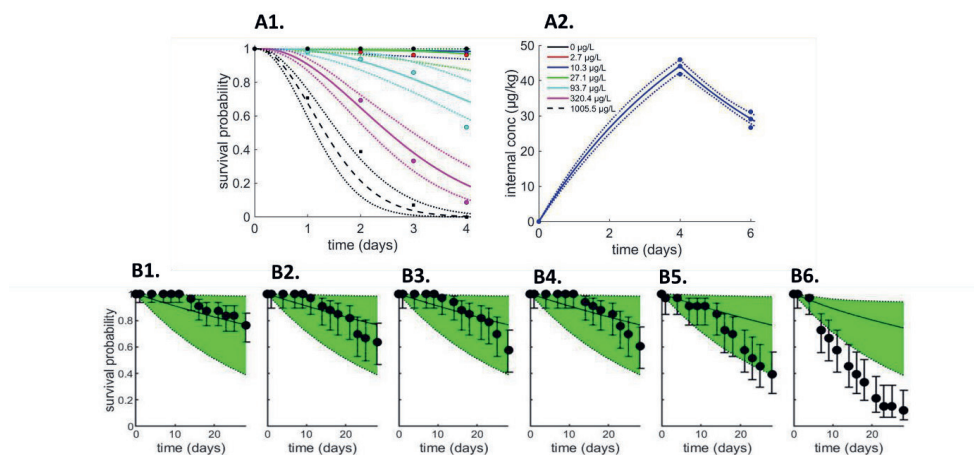
Figure 4.4*: The calibration (A) and prediction (B) of the GUTS-FULL-SD model of FPF toxicity to G. pulex. From left to right, panel A shows the survival fraction in the acute study (A1) and the toxicokinetics of FPF (A2). The dots, dashed lines, and dotted lines represent measured values, fitted values and confidence intervals, respectively. From left to right, panels B show the* prediction *of chronic survival data in the 0, 0.3, 1, 3, 10 and 30 µg/L treatments, respectively. The dots represent the survival data from chronic tests; bars represent Wilson score confidence intervals. The line and the green area represent the prediction and the confidence interval from the full-GUTS prediction, respectively.*

4.4. Conclusions

We assessed the acute and chronic toxicity of FPF to aquatic arthropod species and compared it with the toxicity of IMI. We found that, compared to IMI, *C. dipterum* and *G. pulex* show a slower uptake and faster elimination rates for FPF. FPF was less acutely toxic than IMI based on the HC_{05} values. The chronic 28d EC_{50} and EC_{10} values of FPF were higher or similar to those of IMI. However, FPF inhibited the food consumption of *G. pulex* at a concentration of the same order of magnitude as the current environmental realistic concentration (NOEC = 0.3 µg/L). More environmental monitoring studies of FPF should be performed to know the environmental concentration of FPF better. Overall, chronic effects of FPF on aquatic arthropod species seem to be predicted better than those of IMI, at least for the tested species.

4

Support Information

The support information of this chapter can be downloaded from:

https://www.sciencedirect.com/science/article/pii/S014765132200817X#sec0140
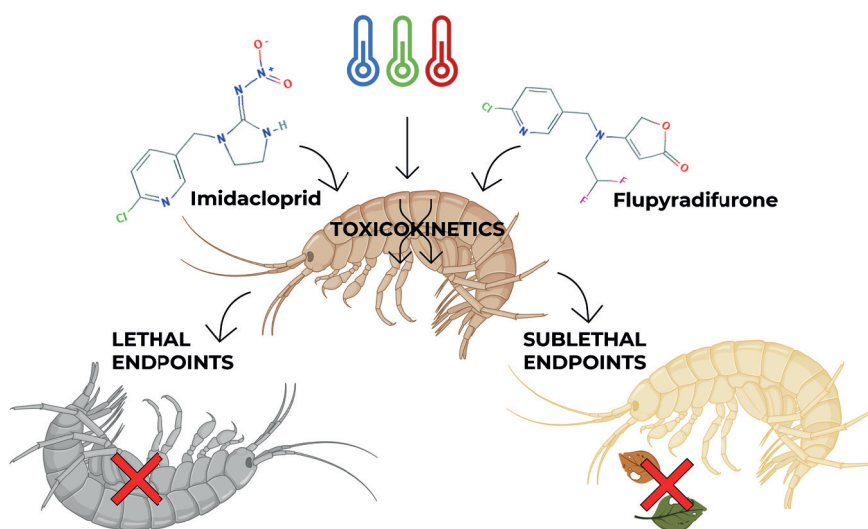
5

CHAPTER 5.

The effect of temperature on toxicokinetics and the chronic toxicity of insecticides toward Gammarus pulex.

Anna Huang and Annika Mangold-Döring, Huitong Guan, Marie-Claire Boerwinkel, Dick Belgers, Andreas Focks, Paul J. Van den Brink

Graphical abstract: A graphic diagram of the experimental design and the results. Diagram created with BioRender (www.biorender.com).

Abstract

A comprehensive understanding of chemical toxicity and temperature interaction is essential to improve ecological risk assessment under climate change. However, there is only limited knowledge about the effect of temperature on the toxicity of chemicals. To fill this knowledge gap and to improve our mechanistic understanding of the influence of temperature, the current study explored toxicokinetics and the chronic toxicity effects of two insecticides, imidacloprid (IMI) and flupyradifurone (FPF), on *Gammarus pulex* at different temperatures (7 – 24 °C). In the toxicokinetics tests, organisms were exposed to IMI or FPF for 2 days and then transferred to clean water for 3 days of elimination at 7, 18, or 24 °C. In the chronic tests, organisms were exposed to the individual insecticides for 28 days at 7, 11, or 15 °C. Our research found that temperature impacted the toxicokinetics and the chronic toxicity of both IMI and FPF, while the extent of such impact differed for each insecticide. For IMI, the uptake rate and biotransformation rate increased with temperature, and mortality and food consumption inhibition was enhanced by temperature. While for FPF, the elimination rate increased with temperature at a higher rate than the increasing uptake rate, resulting in a smaller pronounced effect of temperature on mortality compared to IMI. In addition, the adverse effects of the insecticides on sublethal endpoints (food consumption and dry weight) were exacerbated by elevated temperatures. Our results highlight the importance of including temperature in the ecological risk assessment of insecticides in light of global climate change.

5.1. Introduction

There is growing awareness that climate change may affect the toxicity of many chemicals to aquatic organisms (Noyes and Lema 2015, Polazzo et al. 2022). Thus, the influence of temperature needs to be incorporated into the ecological risk assessment (ERA) of chemicals (Noyes and Lema 2015, Van den Brink et al. 2018). In protocolised toxicity studies, researchers are required to use a set temperature in both acute and chronic tests (e.g., between 18 and 22 °C for Daphnia (OECD 2004, 2012), which can underestimate or overestimate the effects of chemicals for realistic temperature scenarios. Therefore, studying a range of temperatures, including low and high temperatures, is critical to understanding the interactive effect of temperature on chemicals (Hooper et al. 2013, Moe et al. 2013).

The key to understanding chemical toxicity is comprehending its toxicokinetics inside the organism. Toxicokinetic (TK) processes are the chemical uptake into the organism, its biotransformation inside the organism, and finally, the elimination of the chemical out of the organism. The temperature can influence these kinetic processes by speeding up the underlying physiological mechanisms (i.e., increased respiration due to higher oxygen demand at higher temperatures) (Pörtner 2010). However, only limited knowledge exists on the influence of temperature on TK processes of imidacloprid (IMI) (Camp and Buchwalter 2016), while this has not been studied to our knowledge for flupyradifurone (FPF).

In addition, current ecotoxicity studies are mainly conducted over a short period (4 to 7 days) and focus on lethal effects (Schuijt et al. 2021). For example, it was previously shown that the acute lethal effects of IMI on several aquatic arthropods were higher at higher temperatures (Camp and Buchwalter 2016). However, the life-history traits of organisms, such as feeding rate, growth, and reproduction, may be influenced by temperature as well and also govern the population dynamics (Vellinger et al. 2012, Macaulay et al. 2019, Tran et al. 2020). Hence, the impact of temperature on the long-term effects of chemicals on lethal and non-lethal endpoints needs further investigation.

The present study uses IMI and FPF because of their high water solubility and environmental persistence (Morrissey et al. 2015, Sanford and Prosser 2020). IMI is one of the most used insecticides worldwide (Macaulay et al. 2020). However, the European Union completely banned IMI for outdoor use in 2018 after studies showed its toxicity towards bees and its

5

consequences on bee populations globally (Carrington 2018). IMI is well known for its delayed or cumulative adverse effect caused by generating a bioactive metabolite, imidacloprid olefin (IMI-ole) (Huang et al. 2021). The new butenolide pesticide FPF is considered a safer alternative to IMI (Giorio et al. 2017b). However, several studies have found that FPF showed acute toxic effects on aquatic species (Bartlett et al. 2018, 2019a, Maloney et al. 2020), though at lower concentrations than IMI. Current knowledge of the biotransformation FPF suggests that it has no or less toxic metabolites (Jeschke et al. 2015a).

Gammarus pulex belongs to the family of amphipod crustaceans and is one of the most common and essential invertebrate species in streams of Northern Europe (Cold and Forbes 2004). As a detritivore, it plays a vital role in the degradation of leaf litter in aquatic systems (Olivier Dangles et al. 2004). A previous study has found that IMI could inhibit the feeding rate of *G. pulex* (Agatz et al. 2014). Moreover, *G. pulex* is a frequently used aquatic species in toxicity studies since it is sensitive to temperature and chemicals (Sutcliffe et al. 1981, Vellinger et al. 2012, Agatz and Brown 2014).

The objective of this study was to explore the influence of temperature on the effect of the two insecticides on *G. pulex*. As temperature influences on the TK may change the actual internal exposure to the chemical and, therefore, indirectly affect the apparent chemical's toxicity to the organism, we conducted both a systematic evaluation of the temperature influences on TK and toxicity. The choice of temperature ranges was based on the thermal windows of *G. pulex* (Maazouzi et al. 2011, Moenickes et al. 2011) and the yearly field temperature of the site where we collected the organisms (ranging from 7 to 24 °C, depending on exposure time). We hypothesised that temperature would enhance the effect of insecticides on both lethal and sublethal endpoints (immobility, food consumption, growth, fresh weight, dry weight, and water content).

5.2. Materials and methods

5.2.1 Chemicals and test organisms

Imidacloprid (IMI; CAS: 138261-41-3), its bioactive metabolite imidacloprid-olefin (IMI-ole; CAS: 115086-54-9), flupyradifurone (FPF; CAS: 951659-40-8) and its metabolite 6-chloronicotinic acid (6-CNA; CAS: 5326-23-8) were obtained from Sigma Aldrich. Stock solutions of IMI and FPF were dissolved into MiliQ water. Imidacloprid-d4 (IMI-d4; CAS:

1015855-75-0) was used as an internal standard during the analytical measurements of any organism samples. Stock solutions of IMI-d4 (200 µg · mL^{-1}) were dissolved into 2 % acetone (v:v) to ensure that the compound was fully dissolved.

Gammarus pulex was collected from an uncontaminated brook, the Heelsumse brook (coordinates 51.973400, 5.748697) in July (for TK experiments) and December (for chronic experiments of IMI and FPF) of 2020. This brook is groundwater-fed and cool in summer. That brook's yearly water temperature range is from 4 °C to 17 °C based on personal observation. The experimental temperatures 7, 11, 15, 18, and 24 °C are within the thermal tolerance of the organism, as *G. pulex* has a temperature optimum of 10-20 °C and an upper thermal limit of 27 - 33 °C (Sutcliffe et al. 1981, Maazouzi et al. 2011, Moenickes et al. 2011). The lower temperature limit is unknown to us, but temperatures of 7 °C or below are possible in streams in the Netherlands and should thus be within the organism's thermal tolerance.

5.2.2 Toxicokinetic (TK) experiments

Juvenile organisms with an average length of 6.87 mm (sd: 0.96 mm) were brought to the laboratory, counted, and separated into three groups. After 12 h acclimatization to the laboratory conditions at catchment temperature (14 °C) and a 12:12 h light:dark cycle, the individual water bath compartments were adjusted to 7, 18, and 24 °C at a rate of 0.5 °C per hour. The organisms were kept at these experimental temperatures for another minimum of 24 h. During the whole acclimatization procedure, the organisms were fed with *Populus* leaves ad libitum.

During the experiment, a replicate system consisted of ten individuals in a 1.5 L glass jar filled with 1 L groundwater retrieved from the *Sinderhoeve* experimental station (the Netherlands; www.sinderhoeve.org). We placed a piece of metal mesh in each jar as a substrate for the organisms to increase the surface area on which they can sit on or attach to, aiming to prevent cannibalistic behavior. During the uptake phase, the organisms were exposed to either 17.62 (sd: 0.49) µg · L^{-1} IMI or 18.24 (sd: 1.00) µg · L^{-1} FPF. The exposure concentrations were 0.1 times the 50 % effective concentration after 2 days of exposure (48h, EC$_{50}$) of *G .pulex* for IMI and FPF, respectively (Huang et al. 2021, Huang et al. 2022a).

Internal concentrations were measured after 6, 24, and 48 h in the uptake phase and after 72, 96, and 120 h in the elimination phase. After 48 h, all remaining organisms were transferred

to new jars with uncontaminated groundwater for the elimination phase. At each time point, three exposed replicates were sampled destructively. Organisms' survival was monitored throughout the whole experiment. At each time point, the respective jars were removed from the water bath, the organisms were washed with demineralized water, quickly dried on a paper towel, weighed to get the fresh weight, and frozen at -20 °C before further analysis of the internal concentration of the chemicals in the organisms.

5.2.3 Toxicokinetic (TK) modelling

Considering the generation of metabolites, different TK model types were used for IMI and FPF. As no metabolites were measured in the organisms samples exposed to FPF, a simple one-compartment first-order TK model was calibrated on the measured internal concentrations for each temperature (Supplementary data Text S1, Table S1, eq. 1). For the exposures to IMI, no metabolite was detected at 7 °C, so this data set was also calibrated to a simple one-compartment model. During the elimination phase in the experiments conducted at 18 and 24°C, IMI-ole was detected. Thus, these results were calibrated to a one-compartment TK model with metabolite, considering the biotransformation of IMI into IMI-olefin (Supplementary data Text S1, Table S1, eq. S2-3).

All model calibrations were performed in the software Matlab (2020b), starting from scripts available within the Bring Your Own Model (BYOM) modeling platform (www.debtox.info/byom.html, Version 5.2). Matlab scripts that were used can be downloaded from GitHub (https://github.com/NikaGoldring/Toxicokinetic-models-for-pesticides-in-Gammarus-pulex). The model parameters (Supplementary data Text S1, Table S1) and their confidence intervals were estimated based on the optimization algorithm provided in the BYOM platform, applying the likelihood region method.

5.2.4 Chronic experiments

Chronic experiments of 28 days were performed with *G. pulex*. After field collection, healthy juvenile individuals (without parasite seen as an orange dot on the back) with similar lengths (around 5 mm) were randomly selected and put into three buckets with a mixture of field water and pre-aerated groundwater from the *Sinderhoeve* experimental station (the Netherlands; www.sinderhoeve.org). *G. pulex* was acclimatized in three water bath sections at field temperature (11 °C) for two days. Afterward, the temperature in each section was

gradually increased or decreased to the experimental temperatures at a rate of 0.5 °C per hour. The intended temperatures were 7 ± 1 °C, 11 ± 1 °C and 15 ± 1 °C. After each section reached its experimental temperatures, *G. pulex* was acclimatized for at least two days. During the acclimation period, organisms were fed leached *Populus* leaves ad libitum. A light:dark regime of 12:12 hours was used.

Experiments were performed with three replicates per treatment level and five replicates for controls. At the start of the experiment, each replicate consisted of 11 individuals added to 1 L groundwater, after which a volume was dosed to reach a concentration of 0, 0.3, 1, 3, 10 or 30 µg · L-1 for both IMI and FPF. Gentle aeration was provided in the test systems. Immobility and mortality were monitored every 2 to 3 days during the experiment based on a method described in Roessink et al. (2013) (Roessink et al. 2013). Individuals were scored as immobile when no movement of any kind, except for the heart, was observed for a period of 20 s and were scored as dead when no response of any kind was observed during 3 to 5 s of gentle stimulation using a Pasteur's capillary pipette. Dead organisms were removed from the test vessels. Water samples were taken every week to measure the exposure concentrations of the analytes (section 2.5).

The food consumption of *G. pulex* was measured every two weeks in this study. The pre-treated (i.e., leached in water before use) *Populus* leaves were cut into circles with the same surface area (3.2 cm radius) using a cork borer and dried at 60 °C for at least 48 h (McGrath et al. 2007). Two pieces of dry leaf discs were provided for every replicate. The dry weight of the leaves of each replicate was recorded before adding them into the system. The dry leaves were added to each replicate 3 days before the organisms and the chemical to allow the leaves to soak in the water. The leaves in the test jars were changed every two weeks together with the refreshment of the system. The weight of the remaining leaves was recorded after drying at 60°C in the oven for at least 48 h. Two jars with only stainless-steel mesh and conditioned *Populus* leaves, and no *G. pulex,* were installed to estimate the microbial degradation of the leaves. The food consumption of each replicate was calculated as the difference between the initial leaf's weight and the remaining leaf's weight after the loss was corrected for microbial degradation (Eq. 1 and Eq. 2).

Dry mass (DM, mg) of leaves consumed by *G. pulex* per jar (L_e) after two weeks was calculated as:

$$L_e = L_i - L_f - Lc. \tag{Eq. 1}$$

Where L_i and L_f are the initial and final dry mass (mg) of leaves, Lc is the average dry mass loss of the control group accounting for microbiological degradation.

To obtain the food consumption per organism, we divided the total amount of food consumed per jar by the numeric mean of the remaining organisms at each observation time (Eq. 2). The food consumption per organism (F_{total}) after two weeks was calculated as:

$$F_{total} = \frac{L_e}{\frac{\sum(n_1 + n_2 + n_3 + n_4 + n_5 + n_6)}{6}} \tag{Eq. 2}$$

Where n is the number of remaining organisms at each observation time (1-6), observed on days 1, 4, 7, 9, 11, and 14 in the first two weeks and on days 16, 18, 21, 23, 25, and 28 for the last two weeks. To obtain the food consumption F per individual per day, we divided F_{total} by the two weeks period (Eq. 3).

$$F = \frac{F_{total}}{14} \tag{Eq.3}$$

The internal concentration, fresh weight, dry weight, and water content of the remaining organisms were measured at the end of the experiment (28 d). For fresh weight, individuals from the same jar were dabbed dry and weighed on a microbalance (0.1 mg). Then the samples were frozen for 12 h at -20 °C and freeze-dried for ≥24 h, after which dry weight was measured. The water content of the organisms from the same jar was calculated by the difference between the fresh and dry weights. The internal concentration measurement is described in section 2.5.

The physicochemical water parameters, dissolved oxygen, pH, electrical conductivity, and temperature were measured only in the control and the highest treatment at the beginning and end of the test. The results are provided in the raw data of water quality parameters in Mendeley data (Huang et al. 2022c).

5.2.5 Chemical analyses

Groundwater and surface water have been analysed by LC/MS-MS to confirm the absence of all the tested analytes. The light in the experiment did not contain ultraviolet light to prevent the photodegradation of FPF and IMI which was confirmed by the analytical measurement with LC/MS-MS.

All water and organism samples were analysed by reversed-phase liquid chromatography-tandem mass spectrometry (LC-MS/MS) based on the measurement of IMI as described by (Huang et al. 2021). The analyses were performed on an Agilent 1260 Infinity liquid chromatography coupled with a 6460 Triple quad mass spectrometer (Agilent Technologies, USA). Separations were carried out on an Agilent Eclipse Plus C18 column (4.6 × 150 mm, 5 µm) at 40 °C. The injection volume of the samples was set at 10 µL. The mobile phase used was MeOH + 0.1 % Formic acid (C) and Milli-Q water+ 0.1 % Formic acid (D) with the following multistep gradient: 0-1.5 min: 90/10 (C/D, v:v); 1.5-2.5 min: 90/10 (C/D, v:v) to 50/50 (C/D, v:v); 8 min: 50/50 (C/D, v:v); 8-8.1 min: 50/50 (C/D, v:v) to 0/100 (C/D, v:v); 9 min: 0/100 (C/D, v:v); 9-9.1 min: 0/100 (C/D, v:v) to 90/10 (C/D, v:v); 9.1-12 min: 90/10 (C/D, v:v) at a flow rate of 0.7 mL $\cdot$ min^{-1}. The mass spectrometer was operated using an Agilent jet stream electrospray ionization source in positive mode. Nitrogen was used both as nebulizer and collision gas, the capillary voltage was 5000 V, and the temperature of the ion source was set at 300 °C. The compounds were detected in the multiple reaction monitoring using two transitions per compound. The MS/MS transitions of all compounds are provided in Supplementary data in Text S2, Table S4.

Injected samples were quantified by peak area using the calibration curve constructed from the calibration standards included in the same sample sequence. Agilent Masshunter software (version 8.0) was used for instrument control and data acquisition. The extraction recovery of FPF and IMI in the organisms, evaluated at two concentrations by spiking them into the clean organisms, were acceptable based on recovery and repeatability (for further information on analysis methods and recovery results, see Supplementary data Text S2, Table S4-S7).

5.2.6 Data analysis

5.2.6.1 Data analysis for sublethal endpoints

Sublethal endpoints, such as food consumption and dry weight, were compared among concentration levels and temperatures. The assumption of normally distributed data was evaluated using the Shapiro-Wilk test, while the assumption of equal variance was assessed using a Spearman rank correlation between the residuals and the dependent variable. Data were expressed as mean ± standard deviation. A two-factor analysis of variance (ANOVA) was used to analyse the main effects of temperature and concentration and to detect an

interaction between these two variables. The Tukey procedure was used to compare individual means, and a p-value of *<0.05* was considered statistically significant. Post-hoc pairwise comparisons of significant interactions were made using Tukey contrasts with the TukeyHSD function in the package of "agricolae" in R (version 4.0.5).

5.2.6.2 Data analysis for mortality and immobility

The mortality and immobility observed during the IMI or FPF exposure period were analysed using generalized linear mixed models (GLMMs) with a binomial error structure (dead vs. alive and immobile vs. alive and mobile) and logistic regression function. Temperature and concentration were fixed factors, the exposure time was the covariate variable, and the jar number was the random factor. In addition, three types of interactions, temperature:concentration, temperature:time, and concentration:time, were included. The interaction of temperature:concentration:time was not significant in any case; thus, it was not included in the GLMM. $x2$ and *p-values* of each factor or interaction in generalized regressions were calculated with the 'car' package (Fox 2019) in open-source software R version 4.0.5 (Ritz et al. 2015).

In addition, the statistical analysis of NOEC at each temperature was based on the OECD guideline (OECD 2006). The dose-response relationship for lethal (mortality) and sublethal endpoint (immobility) of IMI and FPF at each temperature was fitted using the log-logistic regression, using GenStat (15th edition, Laws Agricultural Trust; VSN International) (Roessink et al. 2013).

5.3. Results and discussions

5.3.1. Toxicokinetics of IMI and FPF at different temperatures

All raw data of this study can be obtained from our Mendeley Data (Huang et al. 2022c). The measured internal concentrations of IMI and FPF in *G. pulex* showed a steep increase within the uptake phase (i.e., up to day 2) and decreased during the elimination phase (Figure 5.1). The internal concentration of IMI on day 2 was lowest in the 7 °C treatment (with an average concentration across replicates of 62 µg · kg^{-1}, compared to 89 µg · kg^{-1} at 18 °C) and highest in the 24 °C treatment (with 100 µg · kg^{-1}), suggesting an increased uptake with increasing temperature. The opposite trend was observed for FPF, however, with a smaller effect size, as average concentrations were of the same order of magnitude across temperatures, with

46 µg · kg^{-1}at 7 °C, 42 µg · kg^{-1}at 18 °C, and 40 µg · kg^{-1} at 24 °C. Additionally, the replicated measurements for the internal concentration of FPF at 7 °C showed a larger variation compared to the values measured at the other temperatures (Figure 5.1, B1, black triangles). The final internal concentration on day 5 (end of the elimination phase) did not differ much among temperatures for IMI (57 µg · kg^{-1}at 7 °C, 64 µg · kg^{-1} at 18 °C, and 59 µg · kg^{-1} at 24 °C). In contrast, it was lowest in the 24 °C treatment for FPF (with 15 µg · kg^{-1}, compared to 30 µg · kg^{-1}at 7 and 18 °C). From this, we observe that both compounds' elimination increased with increasing temperature.

The model calibration for each dataset separately (Figure 5.1) resulted in three parameter sets, one for each temperature (Supplementary data Text S1, Table S2-3). These parameters reflect the same pattern previously described by increasing uptake and elimination rate constants with increasing temperature for IMI and FPF. However, the temperature influence was different between parameters (i.e., for IMI, a 2 fold-difference for k_u and a 3.6 fold-difference for k_e) and between the two insecticides (with only a 1.3 fold-difference for k_u and a 3.1 fold-difference of k_e for FPF).

For IMI, increased uptake with increasing temperature was previously reported within a range of aquatic invertebrates(Camp and Buchwalter 2016). However, no elimination kinetics was evaluated in their study, leaving limited grounds for concluding statements about temperature's effect on the bioconcentration of IMI. In our study, the calibrated parameters could be used to calculate the kinetic bioconcentration factor (BCF$_{kin}$) by BCF$_{kin}$ = k_u/k_e for each temperature. For both insecticides, the BCF$_{kin}$ decreased with increasing temperature. However, the BCF$_{kin}$ for FPF at the lowest and the medium temperature was practically the same with 11.2 L·kg^{-1} at 7 °C and 11.0 L·kg^{-1} at 18 °C, while there was a more linear decrease observed for IMI (Supplementary data Text S1, Figure S1).

Another difference between the two insecticides concerns the presence of biotransformation products. No metabolite was detected in the organisms exposed to FPF at any temperature, whereas the metabolite IMI-olefin was detected during the elimination period of the exposures to IMI at 18 and 24 °C (Figure 5.2). The metabolite formation rate k_m increased from 0.023 L · kg^{-1} · d^{-1} at 18 °C to 0.051 L · kg^{-1} · d^{-1} at 24 °C. The metabolite elimination rate also increased with increasing temperature from 0.686 L · kg^{-1} · d^{-1} at 18 °C to 0.865 L · kg^{-1} · d^{-1} at 24 °C.

Interestingly, no metabolites were found in the organisms after the 28-day exposure of the chronic toxicity study at any concentration or temperature. For this, we see two possible explanations i) the metabolites are further degraded and thus not measured after 28 days, or ii) the metabolites are not produced at the temperatures used in the chronic experiments (i.e., 15 °C). With regards to the first consideration, to our knowledge, no studies have measured the internal concentrations of long-term exposure to IMI in aquatic species. A previous study found that IMI was biotransformed into IMI-ole in *G. pulex* (Huang et al. 2021). However, this study performed an acute (short time, i.e., 6 days) exposure. IMI-ole can be further biotransformed to 6-CNA in *G. pulex* (Huang et al. 2022g). In addition, IMI can be biotransformed to some intermediates which were not checked for in our LC-MS/MS analysis (Suchail. et al. 2001, Fusetto et al. 2017). In line with the second consideration, the temperature may influence biotransformation. While IMI-ole was detected in the TK experiments conducted at 18 and 24 °C, the highest temperature in our chronic study was 15 °C. We speculate that 15°C might inhibit or delay the biotransformation process of IMI. Nevertheless, we did not measure the internal concentration over time during the chronic exposure experiment. Thus, we are limited in interpreting the internal concentration measured at the end of the 28 days exposure.

Figure 5.1: *Internal concentrations and toxicokinetic models of imidacloprid (IMI) and flupyradifurone (FPF) at different temperatures in Gammarus pulex. Black dots for IMI (A1-A3) and triangles for FPF (B1-B3) are measured internal concentrations in µg · kg-1 at 7, 18, and 24 °C, respectively. Solid lines are the TK model fits with lower and upper confidence intervals (dotted lines). The grey vertical line represents the transition timepoint from the uptake to the elimination phase for each temperature and chemical.*

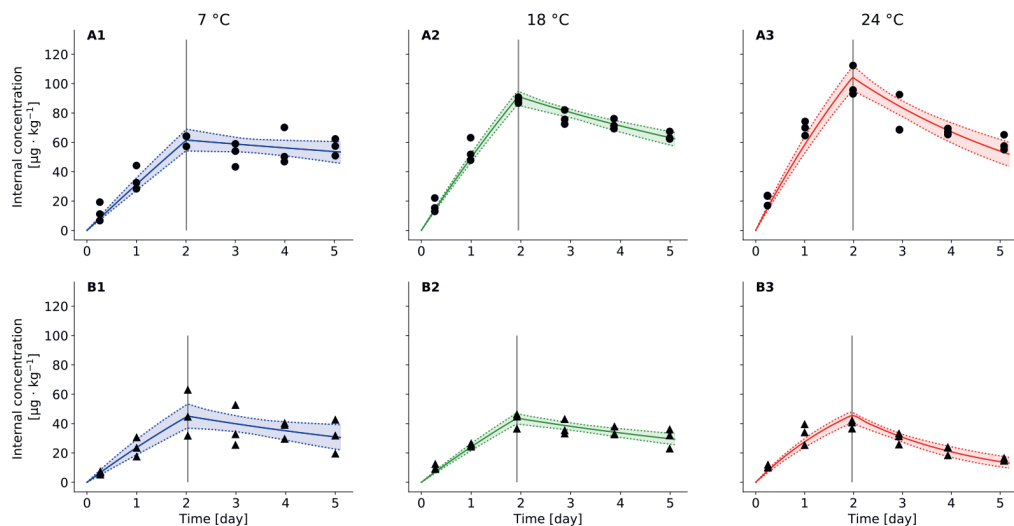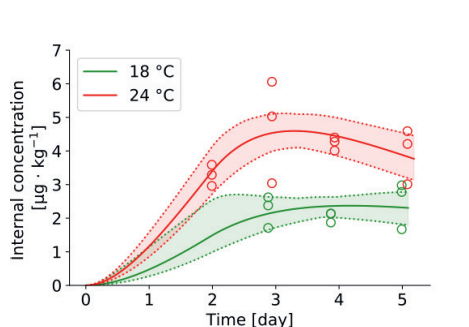**Figure 5.2**: *Internal concentration and toxicokinetic model of imidacloprid-olefin (IMI-ole) at different temperatures in Gammarus pulex. Empty green and red circles are measured internal concentrations of IMI-ole in µg · kg^{-1} at 18, and 24 °C, respectively. Solid lines are the TK model fits with lower and upper confidence intervals (dotted lines).*

5.3.2. Lethal effects of IMI and FPF at different temperatures

5.3.2.1 The chronic results after 28 days

In all chronic experiments, the water concentration of FPF and IMI was stable and within 20 % deviation with nominal concentration. Thus, the nominal concentration was used in reporting the result below.

The control mortality at each temperature was less than 20 %, and higher in higher temperatures (Figure 5.3). For the mortality caused by IMI, temperature, concentration, time, the interaction between temperature and concentration, and the interaction between concentration and time explain a significant part of the variation in the data (Table 5.1). The NOEC values for mortality and immobility were the same at each temperature; the values were 10 µg · L^{-1}, 0.3 µg · L^{-1} and <0.3 µg · L^{-1}, for 7 °C, 11 °C and 15 °C, respectively (Table 5.2). The LC$_{10}$ and LC$_{50}$ values were also presented in Table 5.2, which decreased with temperature. Regarding FPF, no significant influence of temperature on the lethal effects was detected by the GLMM model (Table 5.1). However, the LC$_{10}$ and LC$_{50}$ values decreased with temperature (Table 5.2). Similar to IMI, for FPF, the NOEC values for mortality and immobility were the same at each temperature; the values were 10 µg · L^{-1}, 3 µg · L^{-1} and 1 µg · L^{-1}, for 7 °C, 11 °C, and 15 °C, respectively (Table 5.2). Compared to previous studies which conducted chronic tests of IMI (Roessink et al. 2013) and FPF at 18 °C (Huang et al. 2022a), the LC$_{50}$ values at 18 °C were similar to our results at 15 °C in this study. To be specific, the LC$_{50}$ of IMI was 33.8 (20.9 – 54.6) µg/L, and the EC$_{50}$ of IMI was 15.4 (9.80 – 24.1) µg/L at 18 °C (Roessink et al. 2013); the LC$_{50}$ of FPF was 10.6 (2.4 – 18.8), the EC$_{50}$ of FPF was 10.6 (4.5 – 16.6) µg/L at 18 °C (Huang et al. 2022a).

Besides, based on the values of NOEC, LC$_{10}$, and LC$_{50}$ values at each temperature, the observed enhancement of the lethal effects through temperature increase was higher for IMI than for FPF. This finding is consistent with our internal concentration results after 28 days, as we found higher internal concentrations of IMI at higher temperatures (Supplementary data Text S3, Figure S3). An additional factor for the higher toxicity of IMI could lay in its increased biotransformation into the toxic metabolite IMI-ole. Although no IMI-ole was detected at the end of the chronic experiment, we cannot exclude its presence during the course of the experiment.

Our findings are in line with several studies which conducted acute tests. Previous studies have revealed that increased temperature increases the lethal effects of IMI on several aquatic species. For example, higher temperature decreased the time to immobility for *Isonychia bicolor* (Camp and Buchwalter 2016), and elevated toxicity of imidacloprid was found under the influence of increasing temperature for *Coloburiscus humeralis (Coloburiscidae)* and *Deleatidium spp* (Macaulay et al. 2019). Insecticides are not the only group of chemicals impacted by temperature. The toxic effects of other organic chemicals (Freitas et al. 2019), metals (Bednarska et al. 2017, Haque et al. 2020), and nano plastics (Sulukan et al. 2022) were enhanced by temperature. Together with many other studies, the temperature-enhanced toxicity observed in the present study emphasizes the need to consider this abiotic factor in toxicity testing, a growing concern in light of global climate change (Heye et al. 2019).

Table 5.1: *Generalized linear mixed models (GLMMs) of imidacloprid (IMI) and flupyradifurone (FPF) for mortality and immobility. Effects: tem = temperature, conc = concentration.*

Chemical	IMI						FPF					
	mortality			immobility			mortality			immobility		
Effect	$x2$	Df	*P*	$x2$	Df	*P*	$x2$	Df	*P*	$x2$	Df	*P*
tem	10.72	2	*4.70E-03*	18.90	2	*7.86E-05*	3.36	2	*0.19*	3.51	2	*0.17*
conc	23.47	5	*2.74E-04*	38.58	5	*2.88E-07*	15.92	5	*7.09E-03*	21.30	5	*7.10E-04*
day	15.32	1	*9.09E-05*	9.82	1	*1.72E-03*	25.37	1	*4.74E-07*	27.81	1	*1.34E-07*
tem : conc	29.28	10	*1.12E-03*	33.50	10	*2.25E-04*	16.96	10	*0.08*	18.46	10	*0.048*
tem : day	0.86	2	*0.65*	15.78	2	*3.75E-04*	1.79	2	*0.41*	1.04	2	*0.60*
conc : day	16.36	5	*5.88E-03*	8.32	5	*0.14*	11.86	5	*0.04*	8.84	5	*0.12*

Table 5.2: *Toxicity endpoints for imidacloprid (IMI) and flupyradifurone (FPF) at each temperature after 28 days of exposure. Lethal concentrations (LC_{10} and LC_{50}), effect concentrations(EC_{10} and EC_{50}) with their 95% confidence interval, and the NOEC values obtained for the endpoints mortality, immobility. Temp = temperature in °C and toxicity endpoints in µg · L-1.*

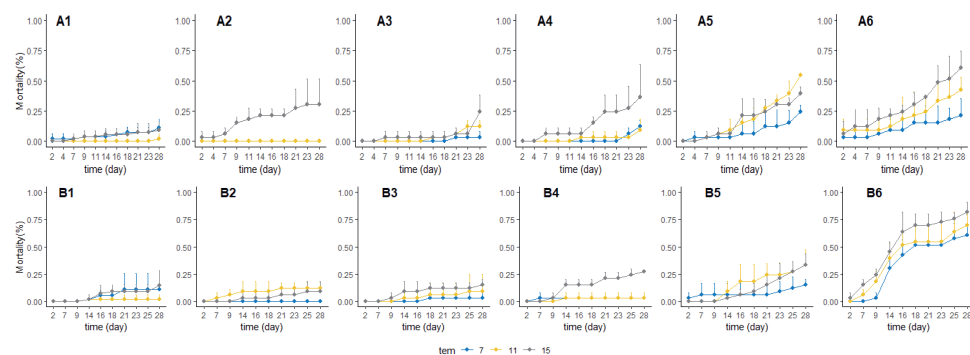| chemical	Temp	LC_{10}	LC_{50}	EC_{10}	EC_{50}		Mor-tality	Immo-bility
	7	9.8 (*)	163.2 (*)	7.8 (1.8 – 34.4)	93.2 (13.3 – 650.1)		10	10
IMI	11	1.5 (0.5 – 4.5)	24.3 (12.0 – 49.5)	1.5 (0.5 -4.3)	20.1 (11.0 – 36.8)		0.3	0.3
	15	0.1 (0.02 – 3.0)	30.1 (5.2 – 174.2)	0.03 (0.0-3.2)	34.5 (4.0 – 294.9)		<0.3	<0.3
	7	10.3 (4.6 – 22.9)	33.7 (21.8 – 52.1)	10.2 (4.7 – 21.9)	31.4 (21.3 – 46.3)		10	10
FPF	11	5.5 (2.6 – 11.7)	18.7 (13.4 – 26.2)	5.4 (2.6 – 10.9)	16.9 (12.2 – 23.3)		3	3
	15	5.1 (2.2 – 12.1)	16.3 (11.2 – 23.8)	5.9 (2.8 – 12.3)	15.9 (11.8 – 22.5)		1	1

Figure 5.3: *The mortality under imidacloprid (IMI, A) and flupyradifurone (FPF, B) exposure over time at 7, 11, and 15 °C. Tiles 1 to 6 represent the control group (0 µg · L-1) and the treatments (0.3, 1, 3, 10, 30 µg · L-1), respectively. Plotted are means + s.d. with n= 5 for control groups and n =3 for treatment groups. tem = temperature in °C.*

5.3.2.2 The temporal patterns of chronic toxicity

In addition, we also found differences in the temporal toxicity patterns between IMI and FPF. In general, the effects of IMI increased after 14 days of exposure, while the effects of FPF remained almost unchanged (Figure 5.3). Specifically, for IMI, we found that the difference between temperatures becomes more significant over time (Figure 5.3). For example, at all three temperatures, the effect of 1 µg · L^{-1} IMI was below 20 % on day 23 and reached nearly 30 % on day 28 at 15 °C, while the other temperatures remained below 20 % (Figure 5.3, A3). In the 30 µg · L^{-1} IMI treatment (Figure 5.3, A6), the mortality on day 14 at 7 °C, 11 °C, and 15 °C was 9 %, 18 %, and 24 %, respectively. However, these values increased to 21 %, 42 %, and 60 % on day 28, respectively.

To the best of our knowledge, only a few studies investigated the influence of temperature on toxicity in a chronic toxicity test (Macaulay et al. 2021). Macaulay et al. (2021) presented clear time-accumulative toxicity of IMI, which first affected mayfly's mobility after 12 days but eventually caused a strong effect (i.e., impairment) at the end of 36 days of exposure, and the heatwave increased the toxicity of IMI.

Our TK results on biotransformation can explain the observed difference in the temporal toxicity pattern between IMI and FPF. For IMI, the biotransformation rate was higher at higher temperatures, resulting in the formation of the toxic metabolite, IMI-ole. Thus, two compounds, the toxic parent compound IMI and its metabolite IMI-ole, which is less toxic but has a slower elimination rate (Huang et al. 2021), affected the organisms. This combined exposure resulted in an accumulating effect over time, also accelerating with increasing temperature. Since, for FPF, no toxic metabolites were detected, there was no such effect (Huang et al. 2022a). Our results indicated that it is essential to consider biotransformation in temperature assessment for toxicity testing, as also indicated in a recent study (Cerveny et al. 2021). In their study, they discovered that the water temperature affects the biotransformation and accumulation of a psychoactive pharmaceutical, temazepam, and its metabolite in aquatic organisms. They further found that the influence of temperature on accumulation and biotransformation was different in different species (Cerveny et al. 2021).

In conclusion, we observed that temperature enhanced the lethal effects of IMI and FPF, where the enhancement extent was greater for IMI than for FPF, and the influence of temperature on IMI became more significant with time due to its biotransformation.

5.3.3. Sublethal effects of IMI and FPF at different temperatures

5.3.3.1 The food consumption inhibition

Higher temperatures increased food consumption while IMI and FPF decreased it (Figure 5.4). Furthermore, higher temperatures exacerbated the food consumption inhibition of IMI and FPF (Figure 5.4). For IMI, in the first two weeks, at 15 °C, the food consumption at 1 µg · L^{-1} was significantly lower than in the control group, while it was 3 µg · L^{-1} at 11 °C, and there was no significant difference among concentrations at 7°C (Figure 5.4, A1). However, in the late two weeks, only 30 µg · L^{-1} IMI significantly inhibited food consumption compared to the control at 15 °C (Figure 5.4, A2). For FPF, the food inhibition was less than for IMI. Only 30 µg · L^{-1} significantly inhibited food consumption compared to the control at 15 °C, and only in the first two weeks (Figure 5.4, B1 and B2).

Feeding activity is a sensitive sublethal indicator at the individual level, impairing higher levels such as population, community, or ecosystem (Rinderhagen et al. 2000). The detritivorous activity of *G. pulex* is vital to aquatic systems (Olivier Dangles et al. 2004). The effects of temperature (Nilsson 1974) and pesticides have been explored separately in previous studies. Inhibition of food consumption by IMI and FPF has been found (Nyman et al. 2013, Agatz et al. 2014, Huang et al. 2022a). It was observed that the feeding rate of *G. pulex* was significantly reduced after continuous exposure to 30 µg · L^{-1} IMI for 4 days and 15 µg · L^{-1} IMI for 14 days at 13 °C (Nyman et al. 2013, Agatz et al. 2014). FPF inhibited the food consumption of *G. pulex* at concentrations higher than 0.3 µg · L^{-1} after 28 days of exposure at 18 °C (Huang et al. 2022a). Overall, our study showed the effect of temperature and IMI and FPF on food consumption and indicated that the interactive effect is higher for IMI than for FPF.

To the best of our knowledge, only a few studies have explored the interactive effects of temperature and chemicals on food consumption. In a recent study by Theys et al. (2020), the food consumption of another freshwater isopod, *Asellus aquaticus,* was measured under exposure to the pesticide chlorpyrifos, combined with increased mean temperature and in the presence or absence of daily temperature fluctuations (DTF) (Theys et al. 2020). They found

that organisms' food consumption decreased when exposed to chlorpyrifos and DTF simultaneously.

5.3.3.2 The influence of temperatures and chemicals on body weight of G. pulex

The dry weight results of *G. pulex* were consistent with the food consumption result (see section 5.3.3.1; Figure 5.4 and Figure 5.5). Higher temperature enhanced food consumption and increased the weight of organisms, whereas IMI and FPF exposure inhibited food consumption and decreased weight. The food consumption inhibition by FPF exposure in the last two weeks was not significant, which is consistent with the fresh weight results (Supplementary data Text S3, Figure S4 A and B). The water content increased with chemical treatment and temperature (Supplementary data Text S3, Figure S4 C and D). These results could be related to the physical characteristic of *G. pulex* as a previous study found that the water content of *G. pulex* was higher under higher temperature conditions (Maazouzi et al. 2011). They explained that the chitin exoskeleton fixes the body volume of crustaceans, and the lost tissue mass, used as a metabolic fuel, must be replaced with water to maintain the same body volume (Maazouzi et al. 2011). In line with their findings, we also did not find size differences between treatments at each temperature (Supplementary data Text S4).

5
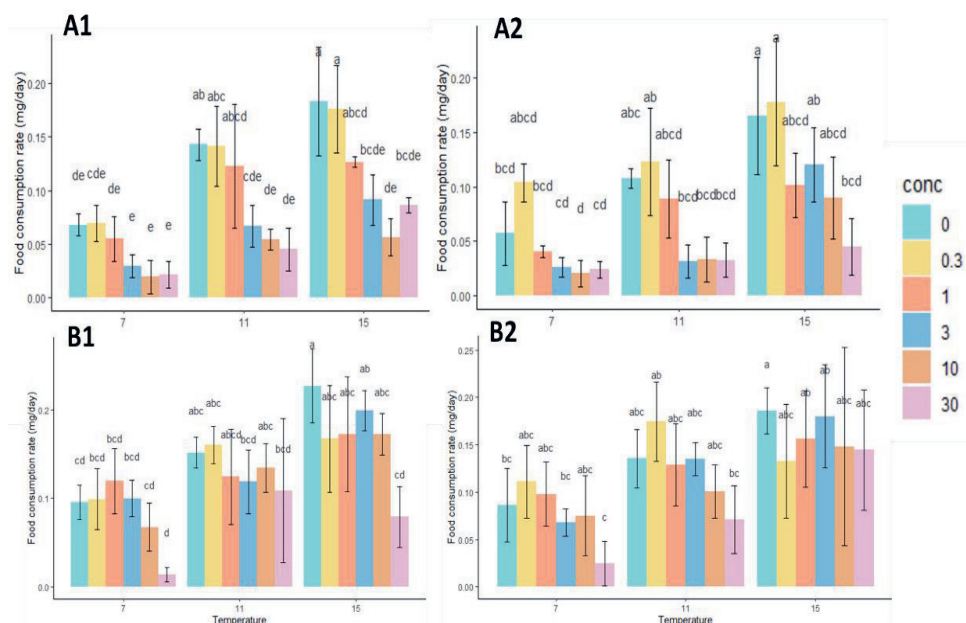
Figure 5.4: Food consumption rates per individual and day under imidacloprid (IMI, A) and flupyradifurone (FPF, B) exposure in the first two weeks (1) and the last two weeks (2). Different letters indicate significant differences between clones and treatments, using TukeyHSD (P < 0.05). conc = concentrations in µg · L-1, temperature in °C.
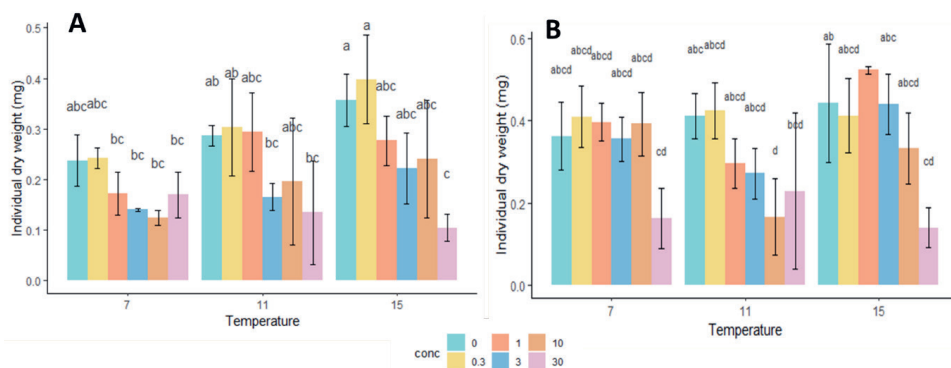
Figure 5.5: Dry weight result under imidacloprid (IMI, A) and flupyradifurone (FPF, B) exposure. Different letters indicate significant differences between clones and treatments, using TukeyHSD (P < 0.05). conc = concentrations in µg · L-1, temperature in °C.

5.4. Conclusion

We assessed the effect of temperature on the toxicokinetics and the chronic toxicity of IMI and FPF towards *G. pulex*. For both IMI and FPF, the uptake and elimination rate constants increased with temperature but in different magnitudes. In addition, temperature increased the biotransformation rate of IMI and thus accelerated the generation of the toxic metabolite IMI-ole. Furthermore, we found that higher temperatures increased the toxicity of IMI and FPF over time, where the increase was higher for IMI than for FPF. In addition, the adverse effects of insecticides on sublethal endpoints (i.e., food consumption and dry weight) were exacerbated by elevated temperatures. Overall, our results provided more evidence and understanding of the interaction between increasing temperatures and chemicals' lethal and sublethal effects. Our study indicated the importance of integrating temperature into future toxicity and risk assessments in light of global climate change.

5

Support Information

The support information of this chapter can be downloaded from:

https://www.sciencedirect.com/science/article/pii/S004896972205985X#s0110

6

CHAPTER 6.

Using a dynamic energy budget (DEB) model to analyze the sublethal and lethal effects of insecticides at different temperatures.

Anna Huang, Paul J. Van den Brink, Nico W. Van den Brink, Jan Baas

Graphical abstract: A graphic diagram of the experimental design and the results. Diagram created with BioRender (www.biorender.com).

Abstract

Temperature is an essential factor for aquatic life, influencing the metabolism and behaviours of organisms as well as the fate of various chemicals. Many previou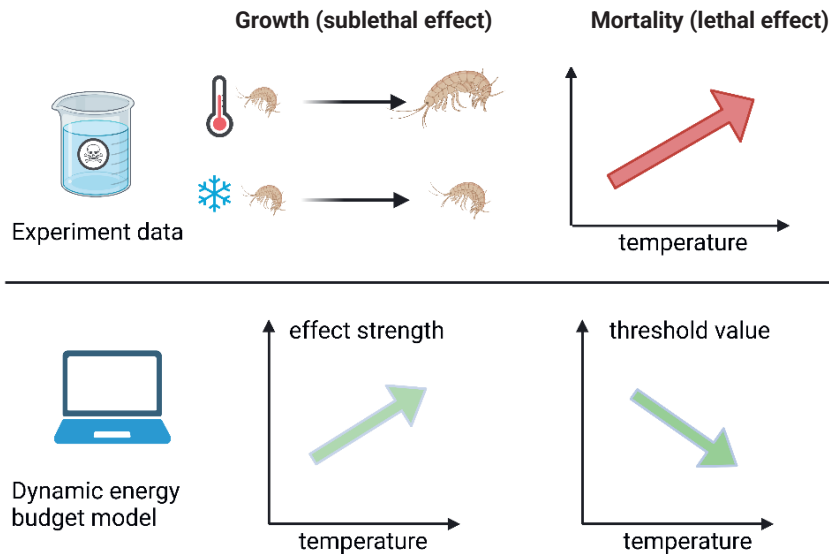s studies have found that the acute lethal toxicity of chemicals increases with temperature. However, the impact of temperature on chronic effects regarding both lethal and sublethal endpoints is rarely studied. Thus, more studies are needed to understand the impact of temperature on toxic effects to conduct better risk assessments of chemicals, especially in light of climate change. In this study, experimental data were applied to a dynamic energy budget (DEB) model to understand the sublethal and lethal mechanisms of toxic effects of pesticides at different temperatures. Firstly, individual growth experiments of *Gammarus pulex* were performed to explore the influence of temperature on the lethal and sublethal effects of temperature, resulting in the DEB-size model. However, lethal endpoints could not be integrated into this model due to the low and indifferent mortality in all treatment levels. Thus, experimental data from previous studies were collected to increase our understanding of the effect of temperature on the lethal effects of long term exposure, and this data was used for DEB-survival modelling. We have applied the DEB models to data on the lethal and sublethal effects of imidacloprid and flupyradifurone at different temperatures. Our results showed that for both insecticides, the dominant rate (kd) and threshold value (zs) tend to decrease with increasing temperature for both lethal and sublethal effects, while the effect strength (bs) and background mortality (hb) tend to increase with increasing temperature. DEB models revealed that temperature influences both the kinetic of chemicals and the intrinsic sensitivity of organisms. This present study deepens the understanding of the mechanism of temperature on pesticide toxicity, which can be used for future risk assessment when the temperature is integrated.

6.1. Introduction

Temperature is an important factor in biological processes, affecting growth, feeding and reproduction, especially for aquatic ectothermic species. Furthermore, temperature changes the behaviour of chemicals, such as their fate and bioavailability in the environment (Harwood et al. 2009, Camp and Buchwalter 2016). Lately, climate change has increased the concerns and awareness that temperature may enhance the toxicity of many pollutants to aquatic organisms (Noyes and Lema 2015, Polazzo et al. 2022). The call for integrating temperature into the conventional ecology risk assessment (ERA) has been increasing in recent publications (Wiles et al. 2020, Macaulay et al. 2021).

The effect of temperature on the toxicity of chemical substances can be divided into the effects on the kinetics of chemicals and the effect on the intrinsic sensitivity of organisms. Temperature affects the uptake of chemicals, and therefore (apparent) toxicity could be changed (Harwood et al. 2009). In addition, temperature may affect the intrinsic sensitivity of organisms by altering certain genes or enzymes (Hofmann and Todgham 2010). To separate these processes, toxicokinetic-toxicodynamic (TKTD) models (Jager et al. 2011) are needed, which can also benefit ecotoxicology and risk assessment (Jager et al. 2006). Toxicokinetics (TK) and toxicodynamics (TD) are concepts that explain the patterns of toxic effects on organisms over time by simulating the underlying processes (Ashauer et al. 2011a).

The TK part of the model describes the fate of a chemical from the surrounding environment to the internal body and may consist of uptake, absorption, excretion, and biotransformation (what the organism does with the chemical) (Kretschmann et al. 2011), depending on the complexity of the model used. Previous studies have found that temperature increases toxicokinetics (i.e., uptake and elimination) (Harwood et al. 2009, Dai et al. 2021).

The TD part describes the processes of how the toxic action at the target site propagates to effects on the individual organism (what the chemical does to the organism) (Ashauer et al. 2011a). The general unified threshold model of survival (GUTS) has been recognized as a suitable TKTD model to extrapolate lethality in laboratory tests to predict the effects resulting from realistic, time-variable exposure profiles (EFSA PPR Panel (Panel on Plant Protection Products and their Residues) et al. 2018). (Ashauer et al. 2011a, Jager et al. 2011). Besides mortality, insecticides may also affect sublethal endpoints, such as feeding rate (Nyman et al.

6

2013), growth, reproduction, and emergence (De França et al. 2017) and these processes are also likely to be temperature dependent. Thus, there is a clear need for models which can perform the same extrapolation for sublethal effects, i.e. models that translate a time-variable exposure concentrations to predicted effects on growth, development, and reproduction over time (Sherborne and Galic 2020). In addition, studies on the effect of temperature on TD, such as the intrinsic sensitivity (i.e. threshold and killing rate or effect strength) of tested organisms at different temperature regimes, are limited (Heugens et al. 2003).Two studies were found in literature, that have explored the influence of temperature on the toxicity of chemicals by using a mechanistic effect modelling approach (Heugens et al. 2003, Gergs et al. 2019). Heugens et al. (2003) performed an accumulation and acute cadmium toxicity test with *D. magna* at different temperatures, and they found that temperature influences both the kinetics of the compound and the intrinsic sensitivity of organisms. Increasing temperature lowered the threshold and increased the killing rate and the uptake rate of the metal (Heugens et al. 2003). The other study tested the acute toxicity of *D. magna* to chlorpyrifos at different temperatures, and they found that the threshold was not changed by temperature, and the killing rate was increased by temperature (Gergs et al. 2019). Both studies only focused on lethal endpoints (Heugens et al. 2003, Gergs et al. 2019).

To consider the effect on the sublethal endpoints, Dynamic Energy Budgets (DEB) models can be used. The theory of DEB provides a general framework for the metabolic organization and specifies the rules for the acquisition and use of energy of individual organisms over their entire life cycle, i.e., how organisms acquire and use resources for maintenance, growth, development and reproduction (Baas et al. 2010, Jager et al. 2015). The DEB model describes these processes with several specific parameters for each species. These parameter values are gathered in the Add-my-pet database, which is freely accessible and contains the physical characteristics of more than 2000 species (http://www.bio.vu.nl/thb/deb/deblab/add_my_pet/index.html). DEB models can identify where energy allocation has changed due to a stressor, affecting life cycle parameters like growth and/or reproduction – the physiological mode of action (pMoA) and the magnitude of the effect. The five commonly pMoA used in ecotoxicology are a decrease in assimilation, an increase in the costs for maintenance, growth or reproduction, and a direct hazard to the embryo (Jager and Zimmer 2012, Ashauer and Jager 2018). DEB models have been used

successfully in several ecotoxicological studies (Jager 2020, Sherborne and Galic 2020). However, the DEB model has often been applied for *Daphnia magna*, which is a fast reproducing, small lab-cultured species, while the application for other macroinvertebrate species which grow slower and have a longer life-cycle, such as *Gammarus pluex*, a common field aquatic crustaceans in Europe (Cold and Forbes 2004), is few. Only two studies were found that have explored the influence of temperature on *Gammaurs pulex'* growth (Moenickes et al. 2011).

In the present study, the research goal was to explore which parameters in the DEB model, regarding both lethal and sublethal effects, will be influenced by temperature. The experimental and modelling efforts focused on the effects of temperature and two insecticides on mortality and growth inhibition, as it was impossible to experimentally evaluate the effects on reproduction. We hypothesize that temperature will increase both the lethal and sublethal effects of insecticides, which could be explained by the DEB model for both toxicokinetic processes and intrinsic sensitivity.

6.2. Methods

6.2.1 Experimental setup

For the lethal endpoints, the 28 days toxicity data of the chronic experiment performed with two chemicals at three temperatures were derived from a previous study (Huang et al. 2022b). For the sublethal endpoints, a 90 days growth test was conducted which is described in the present paper.

6.2.1.1 Choice of chemicals, organisms and temperatures

Imidacloprid (IMI) and flupyradifurone (FPF) are widely used insecticides and have been detected in the aquatic environment widely due to their chemical characteristics, i.e., high solubility in water, low volatility and high DT50 values in water and soils (Bayer 2012, Nauen et al. 2015a, Pietrzak et al. 2020). The measured environmental concentration of IMI ranges from 0.002 to around 60 µg/L (Morrissey et al. 2015, Hladik et al. 2018), and the measured environmental concentration of FPF is up to 0.1 µg/L (Sanford and Prosser 2020).

We used *Gammarus pulex* in the present study, which belongs to the family of amphipod crustaceans and is one of the most common and essential invertebrate species in streams of

Northern Europe (Cold and Forbes 2004). Its diet is composed of a detritivorous basis, and it plays a vital role in the degradation of leaf litter in aquatic systems (Olivier Dangles et al. 2004). A previous study has found that IMI inhibits the feeding rate of *G. pulex* (Agatz et al. 2014). Moreover, *G. pulex* is a frequently used aquatic species since it is sensitive to temperature and pesticides (Sutcliffe et al. 1981, Vellinger et al. 2012, Agatz and Brown 2014).

6.2.1.2 Experimental design

The chronic 28 days toxicity data at 7, 11, and 15 °C originates from a previous study (Huang et al. 2022d). Briefly, during a 28 days experiment, *G. pulex* was exposed to 0, 0.3, 1, 3, 10, 30 µg/L of IMI or FPF at a temperature of 7, 11 or 15 °C. Enough food and aeration were provided. The mortality of the organisms was measured every two or three days. The chronic 28 days data at 18 °C of IMI was derived from (Roessink et al. 2013) at which *G. pulex* was exposed to 0, 1, 3, 10, 30, and 100 µg/L. The chronic 28 days data at 18 °C of FPF was derived from (Huang et al. 2022a), who exposed *G. pulex* to 0, 0.3, 1, 3, 10, and 30 µg/L of FPF. Enough food and aeration were provided. 11 individuals were present in each jar.

The temperature range from 7 to 18 °C was selected since *G. pulex* would suffer from temperature stress when it exceeds 20 °C (Moenickes et al. 2011).

The chronic 90 days experiment was performed at two temperatures, 11 and 15 °C. A single *G. pulex* individual was added to a 100 mL jar which contains 0.01, 0.1 and 0.3 µg/L IMI or FPF. A piece of conditioned Populus leave (Ø 17 mm) was provided in each jar as food.

All experiments met the quality requirements, being: (1) the mortality in the control group was less than 20%; and (2) the measured water concentration was within 80% - 120% of the nominal water concentration. A summary of these data is provided in Table S1.

6.2.2 DEB model calibration

We used the BYOM MATLAB package (available at debtox.info/byom.html) to fit the model parameters to the experimental data. We used two classes of DEB models, the DEB-size and DEB-survival model, which only fit either the size or survival data, respectively, for each temperature. The DEB standard framework is described in detail in Jager (2018) and Jager et al. (2013). However, a summary of the current application is provided in the supporting

information. The supporting information also contains the full derivation of the model in compound parameters. The symbols used are explained in Table S2.

The measured average water concentrations in the experiments were used as parameter values of *Cw* in the models.

6.2.2.1 DEB-size model

In the DEB-size model, only the size results from the 90 days experiment test were used to calibrate the model parameters (Table S2). In detail, the control data was first fitted to estimate the growth rate (*rB*) of *G. pulex.* Then, *rB* was fixed to this estimate and the treatment data were fitted to estimate the parameters of *kd* (dominate rate), *zb* (the threshold for sublethal effects) and *bb* (effect strength for sublethal effects).

The mode of action on feeding, assimilation or growth was tested by switching the stress options. Our models were modified based on DEBtox2019 (Version 4.5b, 2022) from the BYOM platform (https://www.debtox.info/debtoxm.html). Specifically, the modification was to exclude reproduction and survival, as we did not measure reproduction, and no significant mortality relative to the controls occur at all treatment levels. The mode of action with the smallest Akaike information criterion (*AIC)* value was selected.

6.2.2.2 DEB-survival model

The DEB-survival model, was similar to those above, but only the survival results from the 28 days experiment test were used to calibrate the model parameters (Table S2). In detail, the control and the treatment data were fitted together to estimate the *hb* (background mortality), *kd* (dominate rate), *zs* (the threshold for lethal effect) and *bs* (effect strength for lethal effect) parameters (Table 6.1).

For both DEB-size and DEB-survival models, the Normalized Root Mean Square Error (NRMSE) was used in our study to evaluate model performance (EFSA PPR Panel (Panel on Plant Protection Products and their Residues) et al. 2018).

For the parameter estimates boundary conditions are required as input for the model. With the standard setting (Jager 2019) it was not possible to get plausible parameter values as estimates tended to go to either 0 or infinity. Therefore the lower boundary for zs was set to

the lowest experimental concentration that showed no significant effect when compared to the control group. For more discussion, see supporting information Text S2.

6.2.3 Data analysis

Significant differences in sublethal endpoints, *e.g.*, the size among treatments at each temperature and each time point, and the fresh weight of males and females at each temperature at the end of the experiment, were assessed. The assumptions of normality were evaluated using a Shapiro-Wilk test, and the assumption of equal variance was evaluated using a Spearman rank correlation between the residuals and the dependent variable. If the assumptions of normality and equal variance were passed, a one-way analysis of variance (ANOVA) with α=0.05 and a post-hoc Tukey's test was conducted. If assumptions failed, a Kruskal-Wallis test, with α=0.05, and a post-hoc Dunn's test were used. A two-tailed p-value (p < 0.05) was considered to be statistically significant. A Bonferroni correction approach was adopted when multiple comparisons were made.

Table 6.1*: The overview of parameters*

Model	Parameter	Definition
DEB-size	Lm	maximum body length (mm)
	rB	von B growth rate constant (1/d)
	kd	dominant rate constant (1/d)
	zb	no-effect threshold energy budget (μg/L)
	bb	effect strength energy budget (L/μg)
DEB-survival	hb	background hazard rate (1/d)
	kd	dominant rate constant (1/d)
	zs	no-effect threshold survival (μg/L)
	bs	effect strength survival (L/μg)

6.3. Results and discussion

6.3.1 DEB-size model for IMI and FPF

Overall, the mortality in all treatments was less than 20% at the end of the 90 days test, while *G. pulex* kept growing during the test (Figure S1 and Figure S2). After 90 days of the experiment, in the control group of 15 °C, the organisms grew from 4.6 (± 0.3) mm to 8.3 (± 0.7) mm; while for the 11 °C control group, the organisms grew from 4.4 (± 0.4) mm to 7.0 (± 1.0) mm (Figure 6.1). We only fitted the growth data in DEB-size models since no significant mortality could be captured.

6.3.1.1 The growth of G. pulex in the control group at different temperatures

We fitted the control size results of 11 and 15 °C, and the growth difference in different temperatures was clear (Figure 6.1). Our result showed that *G. pulex* grew faster at higher temperatures (Figure 6.1). These results are consistent with other studies (Welton and Clarke 1980, Sutcliffe et al. 1981, Moenickes et al. 2011), which also found that *G. pulex* grew faster at higher temperatures. We did not find the sex-related difference in growth (Figures S1 and S2) and the fresh weight after 90 days (Figures S3 and S4). Sutcliffe et al. (1981), however, showed that male *G. pulex* grows faster than females. It could be due to the limited experimental duration of our study, not being long enough to show the difference. For example, in Sutcliffe et al. (1981), the sex difference was not shown until 100 days.
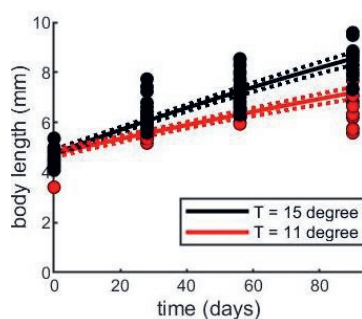

Figure 6.1: *The growth of G. pulex in the control group at different temperatures. Solid lines represented the fitting, and dash lines represented the 95% confidence interval of estimated fittings.. The dots represented the experimental data (n = 20).*

6.3.1.2 The growth of G. pulex with chemicals at different temperatures

In the present study, we calibrated the DEB-size model successfully based on the NRMSE values (Table S2 and Table 6.2). However, the chemical-induced reduction in growth was not significant, especially between the control, 0.01 µg/L and 0.1 µg/L treatments (Table 6.2), which resulted in a wide confidence interval of the effect strength parameter (*bb*) in both types of model (Table S2). Overall, the chemical effects on growth were not significant compared to the control, even in the highest exposure concentration (Table S2).

Another limitation of the present study was that the maximum length was not obtained within our experiment period. At the end of the test, the average size at 15 °C was only 8.3 ± 0.7 mm. Although we could take the maximum length of 13.8 mm from *add my pet database* (http://www.bio.vu.nl/thb/deb/deblab/add_my_pet/index.html), we selected 20 mm as the maximum length based on two reasons. The first reason was based on the lab observation (data was not shown); the maximum length of *G. pulex* from the same pond was around 20 mm. The second reason was based on a previous study, which modelled the length of *G. pulex* at different temperatures and used 20 mm as the maximum length (Moenickes et al. 2011).

The observed effects on growth at different treatments were rather small, and basically, only a limited effect was observed at the highest concentration. The fitting of the model to the experimental data resulted in wide confidence intervals in the parameter values. Therefore, we cautiously conclude (based on a set maximum length and small effects at the highest concentration) that there is no substantial effect of the chemical on growth.
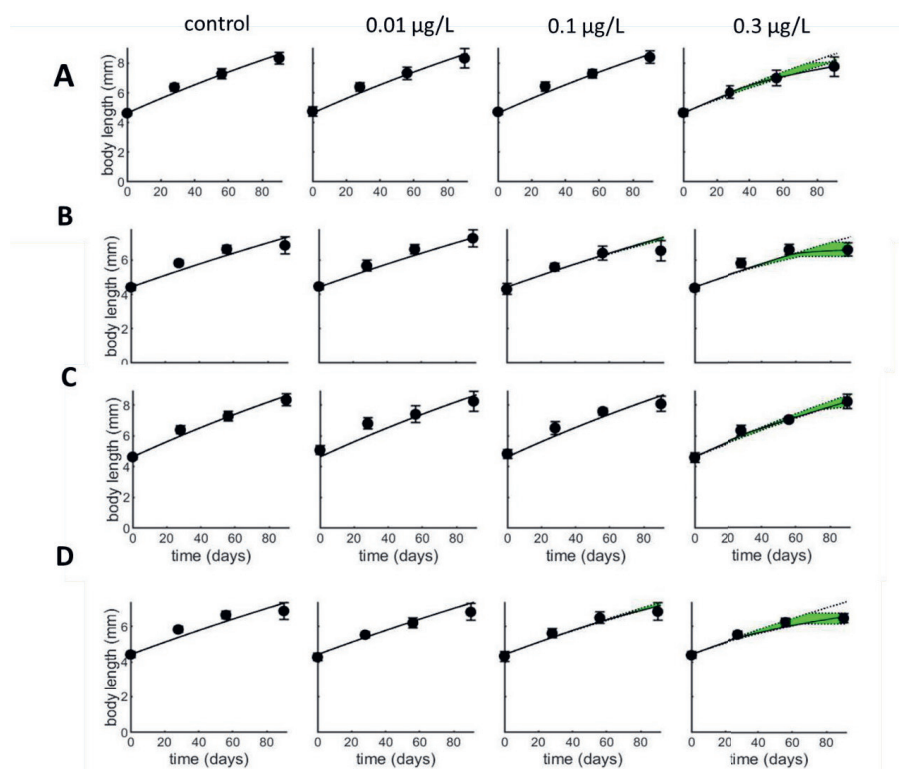
Figure 6.2: The calibration of DEB-size type 2 models of G. pulex with IMI at 15 °C (A) and 11 °C (B) and with FPF at 15 °C (C) and 11 °C (D). The dots represented the experimental data (n = 20 for control, n=15 for treatment). The dots represent the measured size data from the experiment; bars represent Wilson score confidence intervals. The line and the green area represent the calibration and the 95 % confidence interval of the calibration, respectively.

6.3.2 DEB-survival model of IMI and FPF for each temperature

In the present study, results showed that temperature impacted the kinetics of the chemicals (kd) and the intrinsic sensitivity of organisms (zs, bs and hb) (Figure 6.3 and Figure 6.4). For both IMI and FPF, the hb increase with temperature; the kd decreased with temperature, especially for IMI; the bs increased with temperature, especially for IMI; the zs decreased with temperature, especially for FPF (Figure 6.3 and Figure 6.4). Our results are consistent with a previous study with *D. magna* (Heugens et al. 2003). They performed an accumulation and acute Cadmium toxicity test at different temperatures and found that temperature influences

both the kinetics of chemicals and the intrinsic sensitivity of organisms (Heugens et al. 2003). The discussion of each parameter (kd, zs, bs and hb) is presented below.

A previous study explored the kinetic process (uptake rate constant and elimination rate constant) of IMI and FPF with *G. pulex* at 7 °C, 18°C and 24 °C, and found that both uptake and elimination rate constant increased with temperature (Huang et al. 2022d), which resulted in a decrease of kinetic Bioaccumulation factor (*BCFk*) with temperature. In our study, kd is a "lumped" parameter, which is supposed to incorporate the most dominant processes of chemical elimination and damage recovery (EFSA PPR Panel (Panel on Plant Protection Products and their Residues) et al. 2018, Brock et al. 2021). The decreasing pattern of *kd* of IMI with temperature indicates that the damage recovery decreases with temperature since the elimination rate constant increases with temperature based on that previous study (Huang et al. 2022d). The damage recovery decreases with temperature, indicating the potential delay effect since slow damage recovery may cause the time-accumulative toxicity (EFSA PPR Panel (Panel on Plant Protection Products and their Residues) et al. 2018).

The increase in effect strength (bs) of IMI could be attributed to the higher biotransformation rate of IMI at higher temperatures (Huang et al. 2022d). In *G. pulex*, IMI is metabolized into a toxic metabolite, IMI-olefin (Huang et al. 2021). The generation of such a bioactive metabolite complicates the influence of temperature on the toxicity of IMI since temperature usually influences the biotransformation process (Huang et al. 2022d). Huang et al. (2022b) performed toxicokinetic tests with *G. pulex* and IMI at different temperatures and found that the metabolite generation occurred earlier and was higher at higher temperatures. However, no toxic metabolite has been found for FPF so far (Huang et al. 2022a).

Only one previous study was found in literature that has determined the relationship of GUTS parameters with temperatures (Gergs et al. 2019). In their study, they conducted acute toxicity tests (96h) evaluating the toxicity of chlorpyrifos to *D. magna* at different temperatures. They found the dominant rate and the effect strength to increase with temperature. In contrast, the threshold was independent of temperature (Gergs et al. 2019). However, our study found that the threshold decreased with increasing temperature. This result indicated that the tolerance of organisms was decreased by temperature, which was supported by the increase in background mortality (*hb*). In addition, the current results indicate that the relationship between each parameter and temperature might vary with

species and chemicals; therefore, more studies need to be conducted to get a general and
clearer picture.

kd: dominant rate constant (1/d)

hb: background hazard rate (1/d)

zs: no-effect threshold survival (µg/L)

bs: effect strength survival (L/µg)
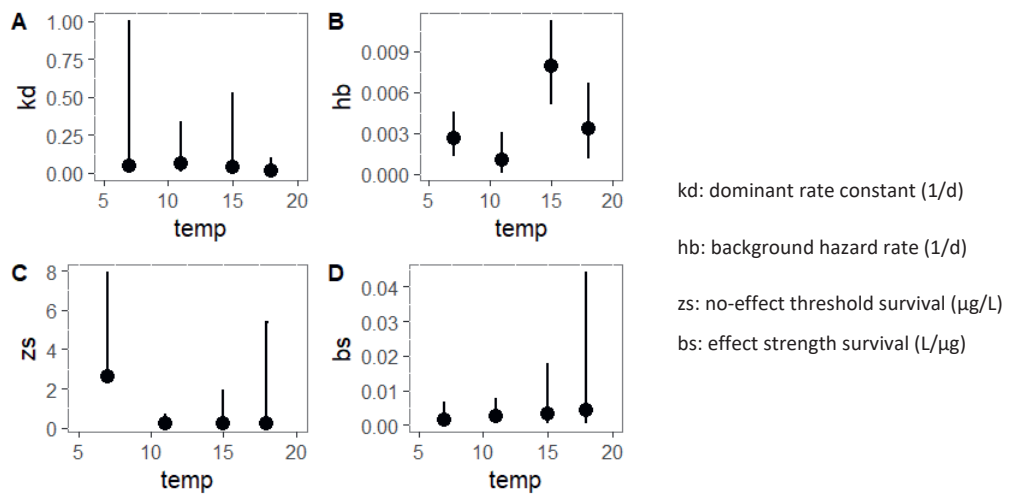
Figure 6.3: The parameter fits by the DEB model IMI for each temperature. The dot represents the mean value; the vertical bar represents the confidence interval of the parameter fit.

kd: dominant rate constant (1/d)

hb: background hazard rate (1/d)

zs: no-effect threshold survival (µg/L)

bs: effect strength survival (L/µg)
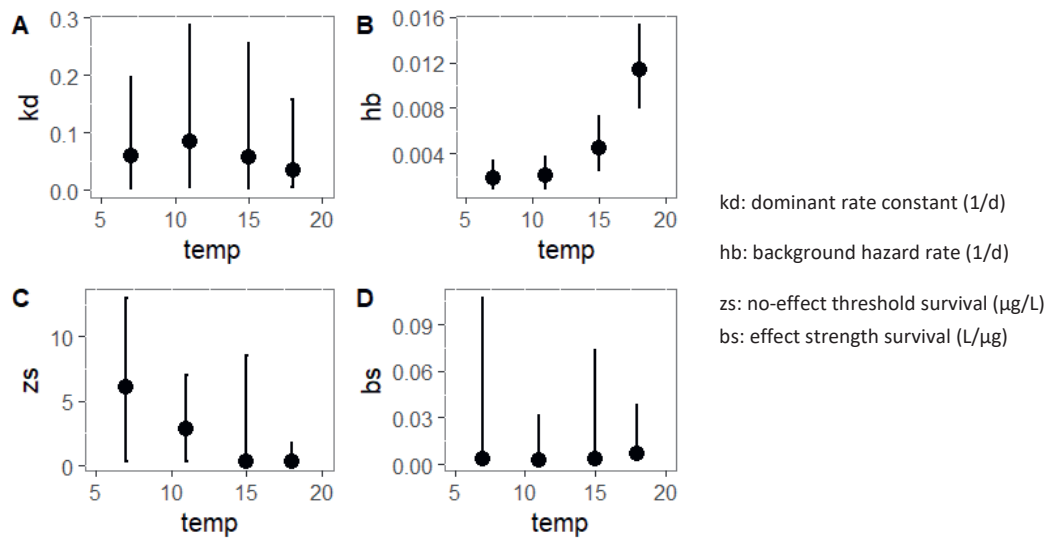
Figure 6.4: The parameter of DEB model FPF in each temperature. The dot represents the mean value; the vertical bar represents the confidence interval of the parameter fit.

6.4. Conclusion

In the present study, we have successfully applied DEB models to both lethal and sublethal effect data of IMI and FPF at different temperatures. For model calibration, putative threshold values provided prior information resulting in a more realistic and better model fits (finite confidence interval). Our results reveal that for both insecticides, no effects of chemicals on sublethal endpoints were found, while for lethal effects, the dominant rate and threshold values decreased with temperature and the effect strength tended to increase with temperature. The present study deepens the understanding of the mechanism of temperature on the effect of insecticides, which can be used for future risk assessment.

Chapter 6 Supporting information:

Table of Contents:

6

Table S1. *The overview of data for model calibration*

experimental data	chemical	concentration level (µg/L)	temperature level	model	source
	IMI	0, 0.3, 1, 3, 10, 30	7, 11, 15	DEB-survival	(Huang et al.
	FPF	0, 0.3, 1, 3, 10, 30	7, 11, 15	DEB-survival	2022d)
28 days chronic	IMI	0, 1, 3, 10, 30, 100	18	DEB-survival	(Roessink et al. 2013)
	FPF	0, 0.3, 1, 3, 10, 30	18	DEB-survival	(Huang et al. 2022a)
90 days long term	IMI	0, 0.01, 0.1, 0.3	11 and 15	DEB-size	
experiment	FPF	0, 0.01, 0.1, 0.3	11 and 15	DEB-size	Present study

Text S2. *Two parameter settings*

We used two different parameters estimation settings, the point is that the estimation procedure for the parameter values easily runs into boundary problems. Where one parameter has a tendency to go to zero and another to infinity with the standard settings for the boundaries of the parameter estimates. When this happens the survival matrix is the starting point to set the boundaries in the estimation procedure to narrow the range of the parameter values in the estimation procedure.

For DEB-size models, although the range of *bb* was not finite in either parameter's setting, the dedicated setting outperformed the standard settings because the confidence intervals for *kd* and *zs* had narrower ranges in the dedicated settings than that in standard settings (Table S2).

For DEB-survival models, in terms of fitting performance, there was not much difference between these two parameter settings (Table S3). However, the dedicated setting with a putative threshold setting outperformed the standard setting in terms of confidence intervals. Furthermore, the dedicated setting makes more realistic sense than the infinite parameter of bs in the standard setting, i.e. the threshold seems unlikely to be close to zero. Likewise, a previous study found that prior knowledge about parameters, such as using the lowest and highest tested concentrations as lower and upper thresholds, could increase the robustness of the fit (Delignette-Muller et al. 2017). Nevertheless, such prior information must also be carefully considered (Jager 2017a).

Table S2: The overview of the growth related parameters in the DEB model

Chemical	Temp	Parameters estimation setting	L0	Lm	rB	kd	zb	bb	AIC	R2	NRMSE
MI	11	1	4.4	20	2.30E-03	3.20E-03 (<1.1E-04 - 0.02)	5.00E-02 (8.1E-03 - 0.09)	313.9 (15.85 - >1000)	1453.1	0.89	10.1%
		2				3.20E-03 (5.0E-04 – 0.02)	5.00E-02 (<0.01 – 0.088)	313.9 (15.85 - >1000)	1453.1	0.89	10.1%
	15	1	4.6	20	3.30E-03	4.10E-04 (1.3E-04 - 0.66)	8.90E-03 (0- 0.3)	109.4 (0.9 - >1000)	1435.4	0.97	3.2%
		2				2.1E-03 (5.2E-4 – 0.29)	0.01 (<0.01 – 0.3)	20.23 (0.8 - >1000)	1435.0	0.97	3.2%
FPF	11	1	4.4	20	2.30E-03	1.10E-04 (<1.1E-04 - 0.03)	3.7E-04 (0 - 0.05)	441.3 (3.4 - >1000)	1329.4	0.92	4.5%
		2				0.003 (4.8E-4 – 0.03)	0.01 (<0.01 – 0.3)	19.3 (2- >1000)	1329.8	0.92	4.6%
	15	1	4.6	20	3.30E-03	2.70E-03 (<1.1E-04 - >143.8)	0.02 (0 - 0.3)	9.26 (0.25 - >1000)	1316.4	0.92	5.3%
		2				0.24 (4.5E-03 - >143.8)	0.3 (0.1 – 0.3)	693.9 (0.8 – 1000)	1317.1	0.92	5.3%

note: For parameters estimation setting, 1 represents standard setting and 2 represents dedicated setting

6

Table S3: The overview of the survival-related parameters and the fitting performance in the DEB model

chemical	Temperature	Parameters estimation setting	hb (mean + 95% CIs)		kd (mean + 95% CIs)		zs (mean + 95% CIs)		bs (mean + 95% CIs)		AIC	r²	NRMSE
IMI	7	1	2.1E-03	9.8E-04 - 4.1E-03	1.6E-03	<1.2E-02 - 0.3	1.7E-02	<5.5E-5 - 1.3	2.4E-02	4.2E-4 - 4.9E-2	239.5	0.79	0.03
		2	2.6E-03	1.4E-03 - 4.5E-03	4.2E-02	1.5E-02 – 1.0	2.6	<2.6 - 7.9	1.7E-03	3.6E-4 – 6.4E-3	241.5	0.73	0.03
	11	1	8.6E-04	7.0E-05 - 2.7E-3	8.8E-03	<1.2E-02 - 0.2	5.5E-05	<5.5E-5 - 0.5	1.2E-02	2.6E-3 - 8.3E-2	351.1	0.76	0.06
		2	1.1E-03	1.1E-4 - 3.0E-3	6.2E-02	1.4E-2 - 0.3	0.2	<0.2 - 0.7	2.5E-03	1.2E-3 - 7.5E-3	352.8	0.74	0.07
	15	1	7.5E-03	5.1E-3 - 1.1E-2	1.6E-03	<1.2E-02 - 0.4	5.5E-05	<5.5E-5 - 1.3	5.3E-02	2.8E-2 - 8.0E-2	568.1	0.83	0.07
		2	7.9E-03	5.2E-3 - 1.1E-2	3.5E-02	5.3E-3 - 0.52	0.2	<0.2 - 1.9	3.2E-03	8.8E-4 - 1.8E-2	569.1	0.82	0.07
	18	1	2.7E-03	1.0E-3 - 5.3E-3	1.6E-03	<1.2E-02 - 0.8	1.3E-04	<5.5E-5 - 1.3	2.8E-02	9.3E-4 - 3.8E-2	308.9	0.93	0.06
		2	3.3E-03	1.2E-3 - 6.6E-3	1.1E-02	<1.2E-02 - 0.9	0.2	<0.2 - 5.4	4.4E-03	8.2E-4 - 4.4E-2	309.8	0.93	0.07
FPF	7	1	1.9E-03	9.0E-4 - 3.3E-3	6.0E-02	<1.2E-02 - 0.2	6.1	0.2 - >13.0	3.5E-03	1.6E-3 - 0.1	270.2	0.94	0.04
		2	1.9E-03	9.0E-4 - 3.3E-3	6.0E-02	<1.2E-02 - 0.2	6.1	<0.3 - >13.0	3.5E-03	1.6E-3 - 0.1	270.2	0.94	0.04
	11	1	2.1E-03	1.0E-3 - 3.7E-3	8.4E-02	<1.2E-02 - 0.3	2.9	3.0E-2 - 7.0	2.8E-03	1.4E-3 - 5.0E-2	339.1	0.95	0.04
		2	2.1E-03	1.0E-3 - 3.7E-3	8.4E-02	5.0E-3 - 0.3	2.9	<0.3 - 7.0	2.8E-03	1.4E-3 - 3.1E-2	339.2	0.95	0.04
	15	1	4.3E-03	2.3E-3 - 7.2E-3	4.6E-02	<1.2E-02 - 0.2	0.1	<5.5E-5 - 8.5	3.9E-03	1.6E-3 - 0.1	493.4	0.90	0.08
		2	4.5E-03	2.6E-3 - 7.3E-3	5.7E-02	2.6E-3 - 0.3	0.3	<0.29 - 8.5	3.4E-03	1.5E-3 - 7.3E-2	493.5	0.90	0.07
	18	1	1.0E-02	7.3E-3 - 1.4E-2	1.6E-03	<1.2E-02 - 0.1	5.5E-05	<5.5E-5 - 0.5	0.1	7.1E-2 - 0.1	550.7	0.93	0.08
		2	1.1E-02	8.1E-3 - 1.5E-2	3.3E-02	5.5E-3 - 0.2	0.3	<0.3 - 1.8	6.7E-03	2.3E-3 - 3.8E-2	553.1	0.92	0.08

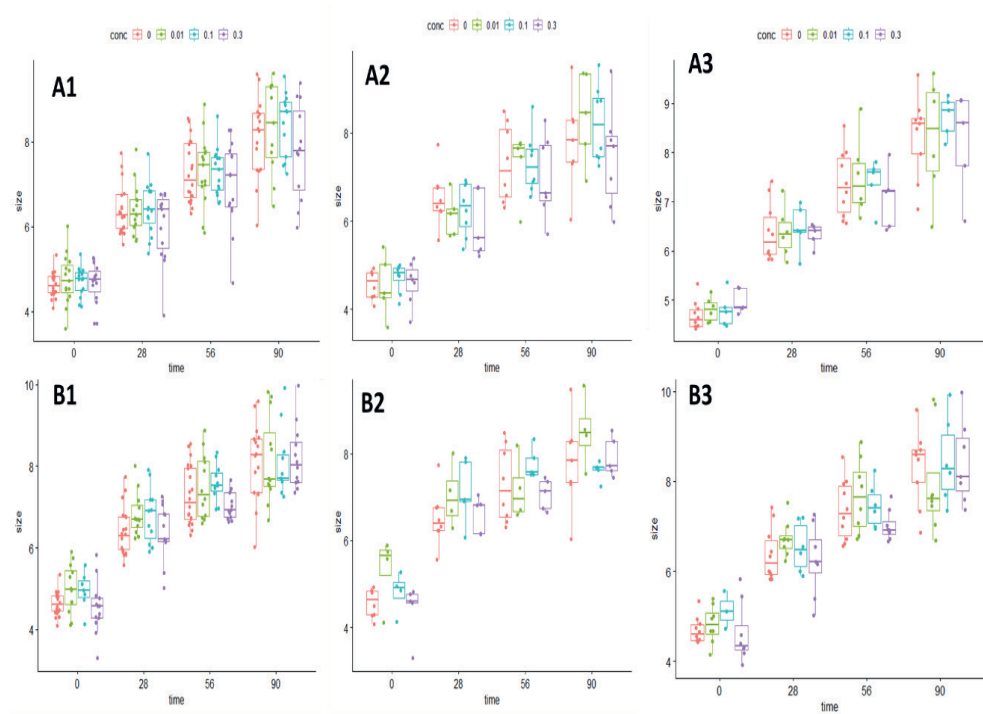*note: For parameters estimation setting, 1 represents standard setting and 2 represents dedicated setting*

Figure S1: The measured size of Gammarus pule in IMI exp (A) and FPF exp (B) at 15 °C. Panel 1 means the size for all individuals, panel 2 means the female individuals, and panel 3 means the male individuals.
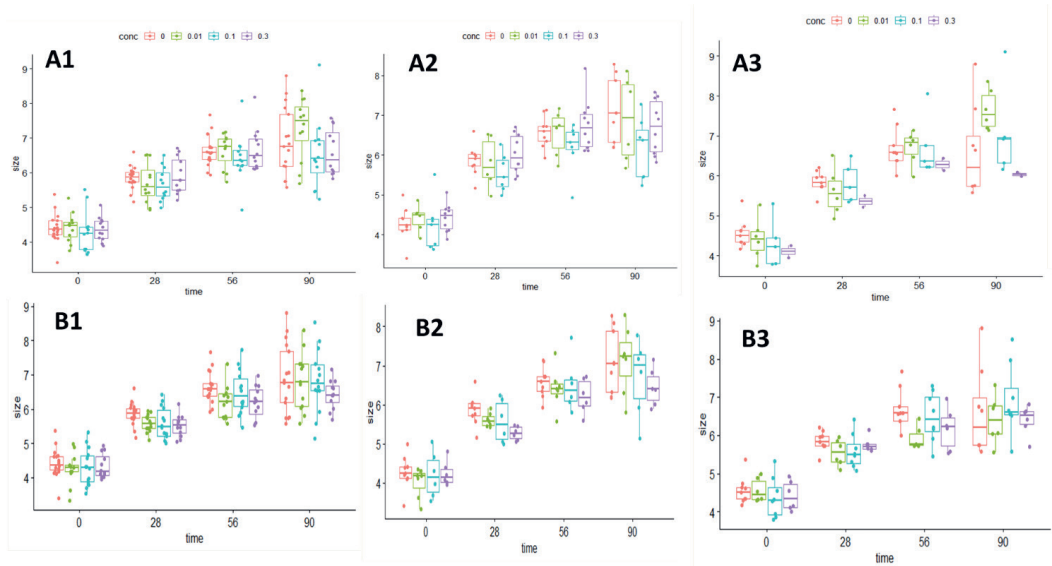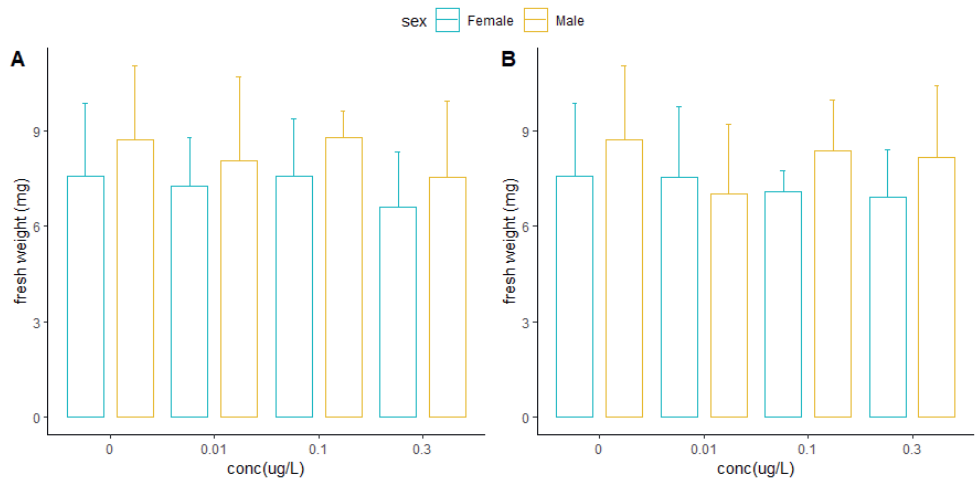
Figure S2: The measured size of Gammarus pule in IMI exp (A) and FPF exp (B) at 11 °C. Panel 1 means the size for all individuals, panel 2 means the female individuals, and panel 3 means the male individuals.

Figure S3:The fresh weight of Gammarus pulex at 15 °C under IMI exposure (left figure) and FPF exposure (right figure).
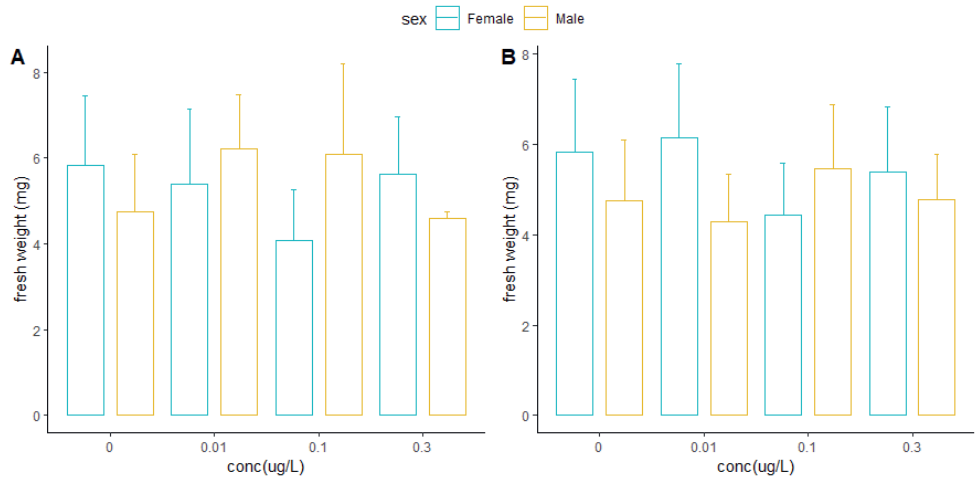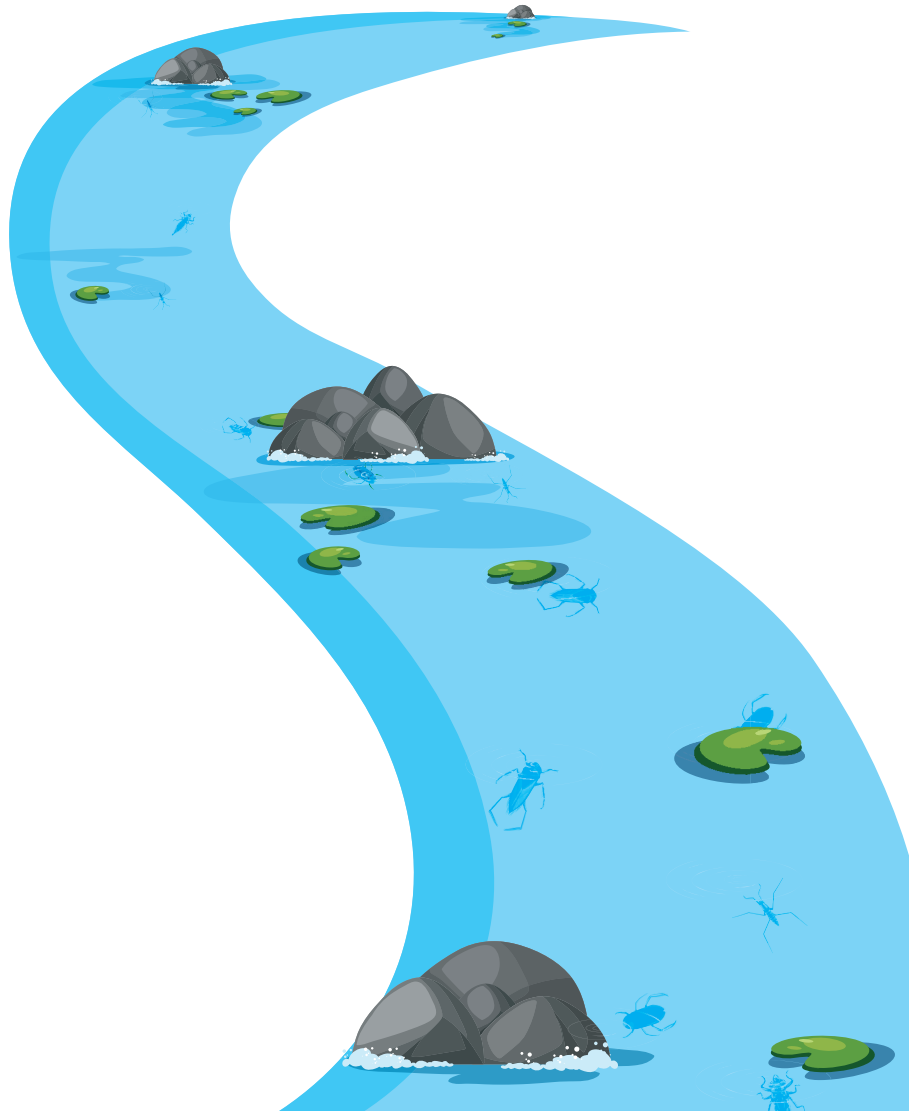

Figure S4: The fresh weight of Gammarus at 11 °C under IMI exposure (left figure) and FPF exposure (right figure).

7

CHAPTER 7.

Synthesis and general discussion.

7.1. Overview

Neonicotinoids (NNIs) are among the most used insecticides in the world to protect crops from harmful insects. However, the widespread use of NNIs causes a number of environmental issues, particularly for pollinators. Many studies have found that NNIs are causing declines in both managed and wild bee populations (Commission 2018). In addition, they also raise environmental concerns about aquatic systems since they have been detected in many water systems due to their high water solubility and persistence (Morrissey et al. 2015, Hladik et al. 2018).

Compared to the number of bee studies, the number of studies about the effects of NNIs on aquatic systems is limited. In addition, scientific questions and knowledge gaps have emerged from our current understanding of the impact of neonicotinoids on aquatic systems and on protecting our environment. These questions and gaps include (1) why are some aquatic arthropods more sensitive to imidacloprid (IMI), which is the most used NNI, than other species?, (2) how can we explain differences in intraspecific sensitivity?, and (3) does flupyradifurone (FPF, an alternative to IMI) also show time-accumulative toxicity to some aquatic arthropods like IMI?

The present work is carried out to address these three research questions by investigating the interspecies and intraspecies sensitivity differences of aquatic macro-invertebrates for two insecticides, imidacloprid and flupyradifurone. The main findings of this thesis are summarized in Figure 7.1, and in-depth reflections on biotransformation and temperature will be discussed later.

The main conclusions of the individual papers are:

a. the formation of the toxic metabolite, IMI-ole, (partly) accounts for the observed interspecies and intraspecies differences in sensitivity to IMI (**chapter 2** and **chapter 3**) (Figure 7.1 A).

b. different size or sex of individuals of the same species should be used for toxicity testing (**Chapter 3**) (Figure 7.1 B).

c. FPF has a relative lower uptake rate constant than IMI, which resulted in lower toxicity (**Chapter 4**) (Figure 7.1 C).

b. FPF does not hold the time-accumulative toxicity effect as IMI (**Chapter 4**) (Figure 7.1 D).

e. Temperature influences both toxicokinetic (**Chapter 5**) and toxicodynamic processes (**Chapter 6**) of IMI and FPF in *Gammarus pulex* (Figure 7.1 E).
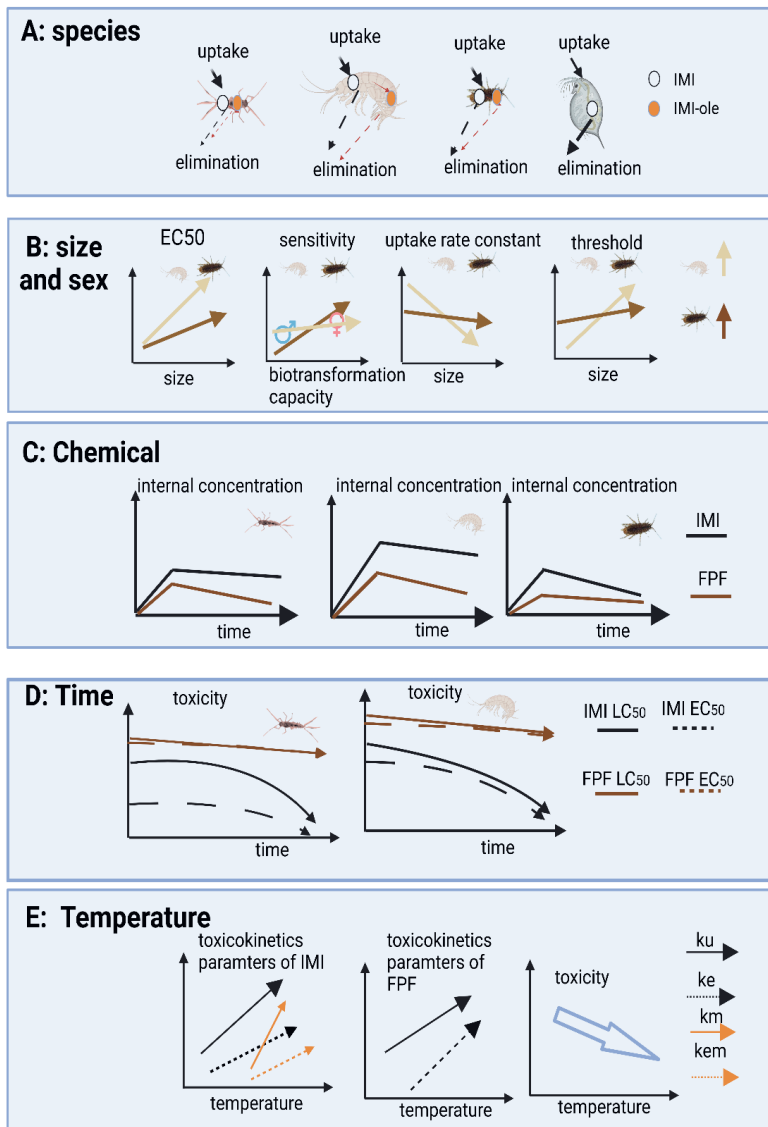

Figure 7.1: *Schematic overview of the intra- and interspecies sensitivity differences of aquatic arthropods found in this thesis. This figure was created with BioRender (https://biorender.com/).*

In this chapter, I reflect on the newly extended knowledge gathered from this thesis and discuss future challenges. All this knowledge contributes to a better assessment of the ecological risks of pesticides to protect our environment.

7.2. The importance of biotransformation in the overall toxicity

7.2.1. The biotransformation of IMI and FPF by organisms

Biotransformation of chemicals by animals and/or microorganisms, or degradation caused by environmental factors such as light, pH, etc., can affect the effects chemicals have on aquatic ecosystems (Lushchak et al. 2018). The metabolism of neonicotinoids is facilitated mostly by enzymes of the CYP450 family (Casida 2011). Nevertheless, the knowledge of the biotransformation of IMI and FPF in aquatic arthropods is limited.

Based on the results in **Chapter 2** and **Chapter 3,** we conclude that among the four selected metabolites (IMI-ole, 5-OH-IMI, IMI-urea, 6-CNA), only IMI-ole was generated within *Cloeon dipterum*, *Gammarus pulex* and *Asellus aquaticus* once they were exposed to IMI for 1 or 2 days (**Chapter 2)** while only 6-CNA was detected in the water and the organisms when *Gammarus pulex* and *Asellus aquaticus* were exposed to IMI-ole (**Chapter 2** and **Chapter 3**) (Figure 7.2). No metabolites (6-CNA) were found for FPF (**Chapter 4**).

Researchers have proved that P450 enzymes are responsible for the biotransformation of NNIs in bee studies (Casida 2011). Thiacloprid is efficiently detoxified by the P450 enzyme CYP9Q3 in the bumblebee *Bombus terrestris*, but imidacloprid is only poorly metabolized (Feyereisen 2018, Haas et al. 2022). For terrestrial insect species other than bees, CYP6G1 in the fruit fly *Drosophila melanogaster* (Hoi et al. 2014, Fusetto et al. 2017) and CYP6CM1vQ in the pest species *Bemisia tabaci* (Karunker et al. 2009) were identified as responsible for the biotransformation of IMI (Figure 7-2). Three P450 enzymes: CYP6AQ1, CYP9Q2 and CYP9Q3, were identified to be involved in the biotransformation of FPF in the honey bee, *A. mellifera,* to detoxify FPF into non-toxic metabolites (Haas et al. 2021) (Figure 7.2). However, the biotransformation of NNIs in aquatic arthropods is less studied, and the exact CYP genes of aquatic arthropods which are responsible for the potential biotransformation remain unknown. The knowledge of the exact CYP genes of aquatic arthropods to chemicals could improve our understanding of the biological mechanism of the defence of organisms against xenobiotics in evolution, and also shed light on why some organisms do biotransform IMI,

while some other organisms (e.g., Daphnia) do not (Figure 7.1 A). These genes can subsequently also be used as potential biomarkers in environmental biomonitoring (Han and Lee 2021, Barrick et al. 2022).
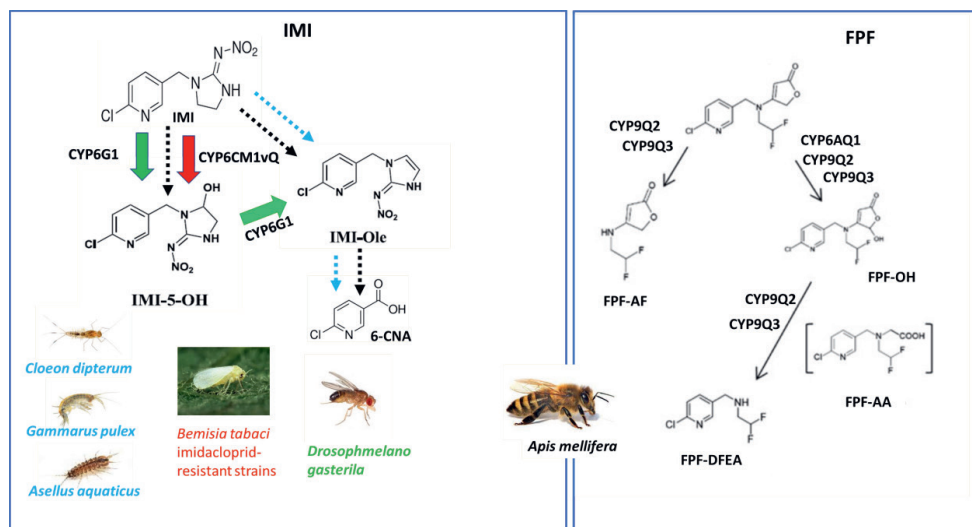

Figure 7.2: The biotransformation pathway of IMI (left) and FPF (right) in this thesis and literature information. For IMI, the green arrows summarise the information available for Drosophmelano gasterila, adapted from (Fusetto et al. 2017); the red lines concern Bemisia tabaci, adapted from (Karunker et al. 2009), while the black line concerns Apis mellifera, adapted from (Zaworra et al. 2019). The blue line summarises the pathways for aquatic arthropods, adapted from this thesis. For FPF, all pathways are adapted from (Haas et al. 2021). Dash lines represent the case that no exact CYP genes have been identified.

7.2.2. The toxic metabolite of IMI, IMI-ole

In this thesis, the formation of the toxic metabolite, IMI-ole, (partly) accounts for the observed interspecies and intraspecies differences in sensitivity to IMI (**Chapter 2** and **Chapter 3**, Figure 7.1 A, B). The biotransformation pathways of the parent NNIs, IMI and FPF, and their metabolites in different arthropod species are presented in Figure 7.2. The extent to which biotransformation of IMI to IMI-ole contributes to its overall toxicity is different for different species and individuals (Figure 7.1 A and B). **Chapter 2** confirms that the formation of a bioactive metabolite, IMI-olefin (IMI-ole), contributes to the overall time-accumulative

toxicity of IMI. IMI-ole showed similar toxicity as IMI to aquatic arthropods but was eliminated slower (**Chapter 2** and **Chapter 3**).

Similarly, previous bee studies found that in addition to the toxicity of the parent compound of NNIs, some metabolites of IMI were found to be toxic to terrestrial insects. Bees can eat pollen contaminated with IMI, which means IMI will enter the organism and be further biotransformed (Nauen et al. 2001). Some studies have demonstrated that some metabolites of IMI display similar or even higher neurotoxicity than the parent compound in locusts (Parkinson and Gray 2019) and bees (Nauen et al. 2001). In addition, IMI-ole shows a slightly greater affinity to nAChRs than IMI in the bee species *Apis mellifera* (Nauen et al. 2001, Casida 2011).

The formation of such a toxic and persistent metabolite causes time-accumulative effects of IMI, it also caused a mismatch between the parameterisation of the GUTS model on acute data and its validation using chronic data when biotransformation was not included in the toxicokinetics model (**Chapter 2**). No time-accumulative effect of FPF was found, however, since no bio-active metabolites were detected (**Chapter 4**).

When assessing the toxicity of parent compounds together with toxic metabolites, the overall toxicity is a result of a mixture. The development of TK-TD models including such mixture exposure needs to be considered for improving the GUTS fitting on IMI effect data (Focks et al. 2018). Usually, for mixture toxicity, the mode of action of different chemicals needs to be determined, for example, the independent mode of action or the addition mode of action. To start, we can assume concentration addition for this mixture because the chemical structure of the parent compound and metabolite is quite similar (Figure 7.3). Not only the toxicity of the metabolite is important, but also its fate within the organisms. The toxic metabolite, IMI-ole, appears to be eliminated slower than the parent compound IMI (**Chapter 2** and **Chapter 3**), which results in extended toxicity. Lately, a parent-metabolite-GUTS model has been developed; this model integrates the toxicokinetic and toxicity of the parent compound and potential active metabolites. Inclusion of the toxicity related to the metabolite improved the predicted long term toxicity of the chemical in a pulse exposure compared to when only the parent compound was considered (Huang et al. 2022e).
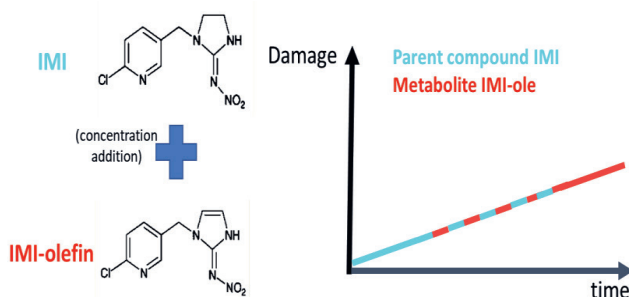
Figure 7.3: *Scheme of the concentration addition for the parent and toxic metabolite with regard to damage.*

7.3. Influence of the temperature on effects of chemicals

Temperature affects the functioning of all living species, especially cold-blooded animals like aquatic arthropods. Previous studies have indicated that the temperature should be integrated into the environmental risk assessment (Noyes and Lema 2015, Ricupero et al. 2020) because increased toxicity with temperature increase has been found for several species and chemicals combinations (Camp and Buchwalter 2016, Macaulay et al. 2019). The present thesis also recommends this consideration based on our findings.

Chapter 5 reports that an increase in temperature increases the uptake rate constant and biotransformation rate of IMI, as well as the elimination rate constant, which resulted in a lower BCF at a higher temperature for both IMI and FPF (Figure 7.4). **Chapter 5** also reveals that temperature increased the lethal and sublethal toxicity of IMI and FPF to *G. pulex.* Furthermore, **Chapter 5** finds that the biotransformation rate of IMI increases with temperature, which may lead to an increase in the toxicity of IMI with temperature because the production of the active metabolite IMI-ole is higher at higher temperatures. This increase in biotransformation rate has also been reported for organophosphorus insecticides (chlorpyrifos and m-parathion) and the insect *Chironomus tentans* (Lydy et al. 1999).

Moreover, temperature also influences the toxicodynamic process. **Chapter 6** reveals that the background mortality tended to increase with increasing temperature, while the threshold tended to decrease with increasing temperature, especially for FPF. **Chapter 5** and **Chapter 6** together prove the influence of temperature on both toxicokinetics and toxicodynamics processes. **Chapter 6** explains the mechanism by which toxicity increases, although the overall

accumulation of chemicals decreases with increasing temperature, i.e., the intrinsic susceptibility of the organism increases.

Based on our experimental data and the literature and when we assume that the toxicodynamics process is independent of temperature, we can hypothesise that the effect of temperature on toxicity may have two different outcomes by changing its toxicokinetics: 1) temperature reduces toxicity, 2) temperature enhances toxicity (Fig. 7.4 F). Temperature increases each process of toxicokinetics, such as uptake rate, biotransformation rate and the elimination rates of the parent compound and its metabolite(s), while the extent of the influence of temperature on each process of toxicokinetics is different. For example, in the case of permethrin, the toxicity was higher at the lower temperature due to the much slower elimination rate at lower temperatures (Harwood et al. 2009) (Figure 7.4, yellow one). The toxicity of chlorpyrifos (CPF) was lower at lower temperatures due to lower formation of the more toxic metabolite (CPF-oxon) (Harwood et al. 2009) (Figure 7.4, blue one). However, our IMI and FPF toxicity results were inconsistent with previous hypotheses, suggesting that toxicodynamics are also affected by temperature. The toxicity of IMI and FPF in this study was higher at higher temperatures, while the overall accumulation of IMI and FPF was lower at higher temperatures (**Chapter 5**), suggesting that toxicodynamics processes are also affected by temperature, with intrinsic sensitivities being higher at higher temperatures (**Chapter 6**) (Figure 7.4, orange and grey).
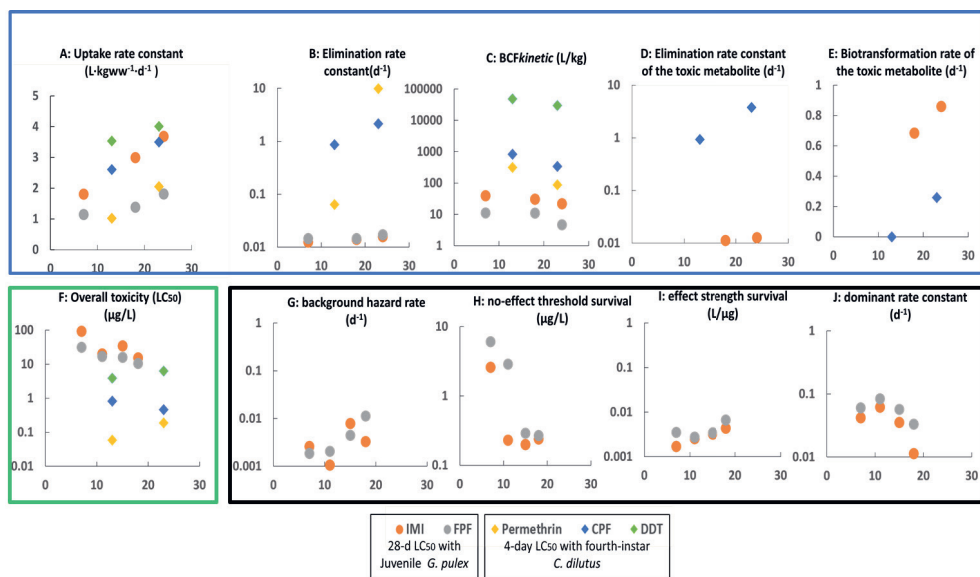
Figure7.4: *The influence of temperature on the parameters of toxicokinetic models and the toxicity of five insecticides (For all plots, the x-axis is temperature. And the y-axis corresponds to the respective title in each figure). IMI and FPF data are adapted from this thesis, and permethrin, CPF and DDT data are adapted from (Harwood et al. 2009). The Blue Frame includes the toxicokinetic process, the black frame includes the toxicodynamics process, and the green frame includes the overall toxicity.*

For future studies, considering the temperature in the risk assessment of chemicals is essential to better assess the risks of chemicals in a world under global warming (Noyes and Lema 2015). The effect of temperature on the sensitivity of organisms is also different between species and chemicals (**Chapter 6**); thus, more studies on the effect of temperature on the toxicodynamics of chemicals are needed. In addition, the toxicokinetics of metabolites, especially toxic metabolites (such as IMI-ole for IMI, CPF-oxon for CPF), should be considered in future studies (e.g., internal concentrations need to be analysed) because these toxic metabolites also contribute to the overall toxicity, as discussed in section 7.2 (Figure 7.3).

7.4. Implications for future research

Lately, there has been an increasing interest and number of publications on using ecotoxicological models (such as toxicokinetic and toxicodynamic models) in ERA to account for intra- and interspecies sensitivity differences of chemicals (EFSA PPR Panel (Panel on Plant Protection Products and their Residues) et al. 2018). Toxicokinetic models focus on the kinetics

of chemicals, and the toxicodynamic models focus on the damage of chemicals caused to the organisms. This thesis, especially **Chapters 2, 3, 4,** and **6**, contributes to these efforts. **Chapter 2** supports that incorporating biotransformation into toxicokinetics is needed to understand the acute and chronic toxicity of IMI to some aquatic arthropods. **Chapter 3** indicates that the intraspecies sensitivity difference can be better understood using toxicokinetic modelling while toxicodynamic modelling is also needed. **Chapter 4** provides evidence that a TKTD model, parameterised on acute toxicity data, predicts the chronic effects of FPF well. **Chapter 5** and **Chapter 6** demonstrate the use of toxicokinetics and TKTD models which includes the effects on sublethal endpoints and aims to understand the interactive effects of chemicals and temperature (Figure 7.1).

The advantages of TKTD models are numerous; however, the exact requirements of the experimental setup to satisfy model calibration are unclear. I developed some criteria based on previous recommendations (Products et al. 2018) and the main findings of this thesis (Figure 7.5). For example, **Chapter 3** reveals that the biotransformation rate of IMI to IMI-ole varies between sizes and/or sexes of organisms, leading to intraspecies sensitivity differences (Figure 7.1 B). Combining this knowledge allows us to better protect entire aquatic species populations rather than individuals at certain life stages, such as juveniles used in most current ERA standard toxicity tests:

Chemicals		a. The treatment levels should cause full effects, e.g. 0% to 100% survival b. Measured water concentration should be used into models.
Time		a. Raw observation data for at least five time-points including day 0. b. If it is possible, both acute test (48 hours or 98 hours) and chronic test (28 days) should be conducted to check the time-accumulative toxicity.
Species		a. The initial size of animals is needed to to be known. b. If it is possible, the sex of animals is needed to be known. c. If it is possible, a toxicokinetics test and analysis of the internal concentration and biotransformation should be performed.

Figure 7.5: *General guidelines for experimental setup for the TKTD model based on the findings of the present thesis. This figure created with BioRender (https://biorender.com/).*

Moreover, an adverse-outcome- pathway (AOP) could be built and used to understand the selected pesticides' toxicity in a more biological mechanism manner. To build AOPs, processes

at sub-individual levels of organisms need to be characterized (molecular interactions and responses at the cell, organ, organism and population level), thereby providing mechanistic information that can be used for interspecies and intraspecies extrapolation of sensitivity. For example, the difference in the biotransformation capacity related to the CYP enzyme among different species (toxicokinetics) and the receptor affinity among different aquatic arthropods (toxicodynamics) need to be assessed (Ashauer 2010, Spurgeon et al. 2020) (Figure 7.6). The differences in biotransformation regulated by enzymes are summarized in Figure 7.2, and as discussed earlier, more studies exploring the differences in the presence of enzyme systems in aquatic arthropods are needed. Although receptor differences were not explored in this thesis, we did find that the intrinsic sensitivities differ between individuals of different size or sex or at different temperatures (**Chapters 2** and **6**), which can be hypothesised to be related to differences in receptor affinity.
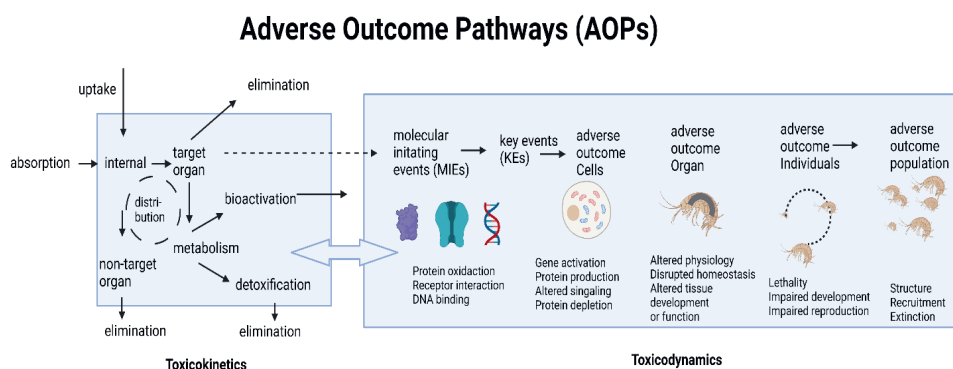

Figure 7.6: *Scheme of the adverse outcome pathways, including the toxicokinetics (uptake, absorption, metabolization, distribution and elimination) and the toxicodynamic (effect on receptor, enzyme, protein, DNA, organisms and population). This figure created with BioRender (https://biorender.com/).*

Concluding, in this thesis, we have explored differences in the sensitivity of individuals to chemicals as a result of differences in species identity, size, sex, temperature and time. Using toxicokinetic-toxicodynamic models, the important role of biotransformation, the kinetic differences of chemicals and the intrinsic sensitivity differences of tested organisms are determined. This study supports the use of TKTD models in the risk assessment and recommends considering differences in sizes, sex and temperature in the standard toxicity test strategies so these factors can be included into future risk assessment.

References

o   Abubakar, Y., H. Tijjani, C. Egbuna, C. O. Adetunji, S. Kala, T. L. Kryeziu, J. C. Ifemeje, and K. C. Patrick-Iwuanyanwu. 2020. Pesticides, History, and Classification. Pages 29-42 Natural Remedies for Pest, Disease and Weed Control.

o   Agatz, A., R. Ashauer, and C. D. Brown. 2014. Imidacloprid perturbs feeding of Gammarus pulex at environmentally relevant concentrations. Environ Toxicol Chem **33**:648-653.

o   Agatz, A., and C. D. Brown. 2014. Variability in feeding of Gammarus pulex: moving towards a more standardised feeding assay. Environ Sci Eur **26**:15.

o   Anderson., K. P. B. a. D. R. 2002. Model selection and miltimodel inference. A practical information-theoretic approach. Springer-Verlag, New York, second edition.

o   Andreazza, F., K. Haddi, S. D. Nornberg, R. N. C. Guedes, D. E. Nava, and E. E. Oliveira. 2020. Sex-dependent locomotion and physiological responses shape the insecticidal susceptibility of parasitoid wasps. Environ Pollut **264**:114605.

o   Ashauer, R. 2010. Toxicokinetic–toxicodynamic modelling in an individual based context—Consequences of parameter variability. Ecological Modelling **221**:1325-1328.

o   Ashauer, R., A. Agatz, C. Albert, V. Ducrot, N. Galic, J. Hendriks, T. Jager, A. Kretschmann, I. O'Connor, M. N. Rubach, A. M. Nyman, W. Schmitt, J. Stadnicka, P. J. van den Brink, and T. G. Preuss. 2011a. Toxicokinetic-toxicodynamic modeling of quantal and graded sublethal endpoints: a brief discussion of concepts. Environ Toxicol Chem **30**:2519-2524.

o   Ashauer, R., C. Albert, S. Augustine, N. Cedergreen, S. Charles, V. Ducrot, A. Focks, F. Gabsi, A. Gergs, B. Goussen, T. Jager, N. I. Kramer, A. M. Nyman, V. Poulsen, S. Reichenberger, R. B. Schafer, P. J. Van den Brink, K. Veltman, S. Vogel, E. I. Zimmer, and T. G. Preuss. 2016. Modelling survival: exposure pattern, species sensitivity and uncertainty. Sci Rep **6**:29178.

o   Ashauer, R., I. Caravatti, A. Hintermeister, and B. I. Escher. 2010. Bioaccumulation kinetics of organic xenobiotic pollutants in the freshwater invertebrate Gammarus pulex modeled with prediction intervals. Environmental Toxicology and Chemistry **29**:1625-1636.

o   Ashauer, R., and B. I. Escher. 2010. Advantages of toxicokinetic and toxicodynamic modelling in aquatic ecotoxicology and risk assessment. J Environ Monit **12**:2056-2061.

o   Ashauer, R., A. Hintermeister, I. O'Connor, M. Elumelu, J. Hollender, and B. I. Escher. 2012. Significance of xenobiotic metabolism for bioaccumulation kinetics of organic chemicals in Gammarus pulex. Environ Sci Technol **46**:3498-3508.

o   Ashauer, R., A. Hintermeister, E. Potthoff, and B. I. Escher. 2011b. Acute toxicity of organic chemicals to Gammarus pulex correlates with sensitivity of Daphnia magna across most modes of action. Aquatic Toxicology **103**:38-45.

o   Ashauer, R., and T. Jager. 2018. Physiological modes of action across species and toxicants: the key to predictive ecotoxicology. Environ Sci Process Impacts **20**:48-57.

o   Baas, J., T. Jager, and B. Kooijman. 2010. A review of DEB theory in assessing toxic effects of mixtures. Science of The Total Environment **408**:3740-3745.

- Barrick, A., O. Laroche, M. Boundy, J. K. Pearman, T. Wiles, J. Butler, X. Pochon, K. F. Smith, and L. A. Tremblay. 2022. First transcriptome of the copepod Gladioferens pectinatus subjected to chronic contaminant exposures. Aquat Toxicol **243**:106069.
- Bartlett, A. J., A. M. Hedges, K. D. Intini, L. R. Brown, F. J. Maisonneuve, S. A. Robinson, P. L. Gillis, and S. R. de Solla. 2018. Lethal and sublethal toxicity of neonicotinoid and butenolide insecticides to the mayfly, Hexagenia spp. Environmental Pollution **238**:63-75.
- Bartlett, A. J., A. M. Hedges, K. D. Intini, L. R. Brown, F. J. Maisonneuve, S. A. Robinson, P. L. Gillis, and S. R. de Solla. 2019a. Acute and chronic toxicity of neonicotinoid and butenolide insecticides to the freshwater amphipod, Hyalella azteca. Ecotoxicol Environ Saf **175**:215-223.
- Bartlett, A. J., A. M. Hedges, K. D. Intini, L. R. Brown, F. J. Maisonneuve, S. A. Robinson, P. L. Gilliss, and S. R. de Solla. 2019b. Acute and chronic toxicity of neonicotinoid and butenolide insecticides to the freshwater amphipod, Hyalella azteca. Ecotoxicology and Environmental Safety **175**:215-223.
- Bass, C., I. Denholm, M. S. Williamson, and R. Nauen. 2015. The global status of insect resistance to neonicotinoid insecticides. Pesticide Biochemistry and Physiology **121**:78-87.
- Bayer. 2012. Flupyradifurone Technical Information.
- Bednarska, A. J., M. Choczynski, R. Laskowski, and M. Walczak. 2017. Combined effects of chlorpyriphos, copper and temperature on acetylcholinesterase activity and toxicokinetics of the chemicals in the earthworm Eisenia fetida. Environmental Pollution **220**:567-576.
- Benton, E. P., J. F. Grant, R. J. Webster, R. J. Nichols, R. S. Cowles, A. F. Lagalante, and C. I. Coots. 2015. Assessment of Imidacloprid and Its Metabolites in Foliage of Eastern Hemlock Multiple Years Following Treatment for Hemlock Woolly Adelgid, Adelges tsugae (Hemiptera: Adelgidae), in Forested Conditions. J Econ Entomol **108**:2672-2682.
- Bertin, A., and F. Cezilly. 2003. Sexual selection, antennae length and the mating advantage of large males in Asellus aquaticus. Journal of Evolutionary Biology **16**:698-707.
- Bloor, M. C. 2010. Animal standardisation for mixed species ecotoxicological studies: Establishing a laboratory breeding programme for Gammarus pulex and Asellus aquaticus. Zool. Baetica **21**:179-190.
- Bonmatin, J. M., C. Giorio, V. Girolami, D. Goulson, D. P. Kreutzweiser, C. Krupke, M. Liess, E. Long, M. Marzaro, E. A. Mitchell, D. A. Noome, N. Simon-Delso, and A. Tapparo. 2015. Environmental fate and exposure; neonicotinoids and fipronil. Environ Sci Pollut Res Int **22**:35-67.
- Bottger, R., J. Schaller, and S. Mohr. 2012. Closer to reality--the influence of toxicity test modifications on the sensitivity of Gammarus roeseli to the insecticide imidacloprid. Ecotoxicol Environ Saf **81**:49-54.
- Brock, T., M. Arena, N. Cedergreen, S. Charles, S. Duquesne, A. Ippolito, M. Klein, M. Reed, I. Teodorovic, P. J. van den Brink, and A. Focks. 2021. Application of General Unified Threshold Models of Survival Models for Regulatory Aquatic Pesticide Risk Assessment Illustrated with an Example for the Insecticide Chlorpyrifos. Integr Environ Assess Manag **17**:243-258.

- Cairns, J., Jr. 1986. The Myth of the Most Sensitive Species: Multispecies testing can provide valuable evidence for protecting the environment. BioScience **36**:670-672.
- Camp, A. A., and D. B. Buchwalter. 2016. Can't take the heat: Temperature-enhanced toxicity in the mayfly Isonychia bicolor exposed to the neonicotinoid insecticide imidacloprid. Aquat Toxicol **178**:49-57.
- Campbell, J. W., A. R. Cabrera, C. Stanley-Stahr, and J. D. Ellis. 2016. An evaluation of the honey bee (Hymenoptera: Apidae) safety profile of a new systemic insecticide, flupyradifurone, under field conditions in Florida. Journal of economic entomology **109**:1967-1972.
- Carleton, J. 2014. Environmental Fate and Ecological Risk Assessment for Foliar, Soil Drench, and Seed Treatment Uses of the New Insecticide Flupyradifurone (BYI 02960). Licensee MDPI, Basel, Switzerland. This article is an open access article distributed under the terms and conditions of the Creative Commons Attribution (CC BY) license (http://creativecommons. org/licenses/by/4.0/).
- Carr, G., and S. Belanger. 2019. SSDs revisited: Part I—a framework for sample size guidance on species sensitivity distribution analysis. Environmental Toxicology and Chemistry **38**:1514-1525.
- Carrington, D. 2018. EU agrees total ban on bee-harming pesticides. The Guardian.
- Carter, L. J., R. Ashauer, J. J. Ryan, and A. B. Boxall. 2014. Minimised bioconcentration tests: a useful tool for assessing chemical uptake into terrestrial and aquatic invertebrates? Environ Sci Technol **48**:13497-13503.
- Carvalho, F. P. 2017. Pesticides, environment, and food safety. Food and Energy Security **6**:48-60.
- Casida, J. E. 2011. Neonicotinoid metabolism: compounds, substituents, pathways, enzymes, organisms, and relevance. J Agric Food Chem **59**:2923-2931.
- Casillas, A., A. de la Torre, I. Navarro, P. Sanz, and M. L. A. Martinez. 2022. Environmental risk assessment of neonicotinoids in surface water. Sci Total Environ **809**:151161.
- Cerveny, D., J. Fick, J. Klaminder, E. S. McCallum, M. G. Bertram, N. A. Castillo, and T. Brodin. 2021. Water temperature affects the biotransformation and accumulation of a psychoactive pharmaceutical and its metabolite in aquatic organisms. Environ Int **155**:106705.
- Codling, G., Y. Al Naggar, J. P. Giesy, and A. J. Robertson. 2016. Concentrations of neonicotinoid insecticides in honey, pollen and honey bees (Apis mellifera L.) in central Saskatchewan, Canada. Chemosphere **144**:2321-2328.
- Cold, A., and V. E. Forbes. 2004. Consequences of a short pulse of pesticide exposure for survival and reproduction of Gammarus pulex. Aquat Toxicol **67**:287-299.
- Commission, E. 2004. Review report for the active substance thiacloprid.
- Commission, E. 2005. Review report for the active substance clothianidin, finalised in the Standing Committee on the Food Chain and Animal Health at its meeting on 27 January 2006 in view of the inclusion of clothianidin in Annex I of Directive 91/414/EEC.
- Commission, E. 2006. Review report for the active substance thiamethoxam, finalised in the Standing Committee on the Food Chain and Animal Health at its meeting on 14 July 2006 in view of the inclusion of thiamethoxam in Annex I of Directive 91/414/EEC.

o   Commission, E. 2008. Review report for the active substance imidacloprid. Finalised in the Standing Committee on the Food Chain and Animal Health at its meeting on 26 September 2008 in view of the inclusion of imidacloprid in Annex I of Directive 91/414/EEC.

o   Commission, E. 2018. Commission Implementing Regulation (EU) 2018/783 of 29 May 2018 amending Implementing Regulation (EU) no 540/2011 as regards the conditions of approval of the active substance imidacloprid. Pages 31-34 Off. J. Eur. Union.

o   Coots, C., P. Lambdin, J. Grant, and R. Rhea. 2013. Spatial and temporal distribution of residues of imidacloprid and its insecticidal 5-hydroxy and olefin and metabolites in eastern hemlock (Pinales: Pinaceae) in the southern Appalachians. J Econ Entomol **106**:2399-2406.

o   Crayton, S. M., P. B. Wood, D. J. Brown, A. R. Millikin, T. J. McManus, T. J. Simpson, K.-M. Ku, and Y.-L. Park. 2020. Bioaccumulation of the pesticide imidacloprid in stream organisms and sublethal effects on salamanders. Global Ecology and Conservation **24**.

o   Dai, W., S. Slotsbo, C. A. M. van Gestel, and M. Holmstrup. 2021. Temperature-Dependent Toxicokinetics of Phenanthrene in Enchytraeus albidus (Oligochaeta). Environ Sci Technol **55**:1876-1884.

o   Dalhoff, K., M. Gottardi, Å. Rinnan, J. J. Rasmussen, and N. Cedergreen. 2018. Seasonal sensitivity of Gammarus pulex towards the pyrethroid cypermethrin. Chemosphere **200**:632-640.

o   Dalhoff, K., A. M. B. Hansen, J. J. Rasmussen, A. Focks, B. W. Strobel, and N. Cedergreen. 2020. Linking Morphology, Toxicokinetic, and Toxicodynamic Traits of Aquatic Invertebrates to Pyrethroid Sensitivity. Environ Sci Technol.

o   De França, S. M., M. O. Breda, D. R. Barbosa, A. M. Araujo, and C. A. Guedes. 2017. The sublethal effects of insecticides in insects. Biological control of pest and vector insects:23-39.

o   de Lima, E. S. C., C. van Haren, G. Mainardi, W. de Rooij, M. Ligtelijn, N. M. van Straalen, and C. A. M. van Gestel. 2021. Bringing ecology into toxicology: Life-cycle toxicity of two neonicotinoids to four different species of springtails in LUFA 2.2 natural soil. Chemosphere **263**:128245.

o   De Zwart, D., and L. Posthuma. 2005. Complex mixture toxicity for single and multiple species: proposed methodologies. Environ Toxicol Chem **24**:2665-2676.

o   Delignette-Muller, M. L., P. Ruiz, and P. Veber. 2017. Robust Fit of Toxicokinetic-Toxicodynamic Models Using Prior Knowledge Contained in the Design of Survival Toxicity Tests. Environ Sci Technol **51**:4038-4045.

o   Di Lorenzo, T., W. D. Di Marzio, B. Fiasca, D. M. P. Galassi, K. Korbel, S. Iepure, J. L. Pereira, A. Reboleira, S. I. Schmidt, and G. C. Hose. 2019. Recommendations for ecotoxicity testing with stygobiotic species in the framework of groundwater environmental risk assessment. Sci Total Environ **681**:292-304.

o   EFSA, E. F. S. A. 2016. Setting of new maximum residue levels for flupyradifurone in strawberries, blackberries and raspberries. EFSA Journal **14**:4423.

o   EFSA PPR Panel (Panel on Plant Protection Products and their Residues), P. Adriaanse, P. Berny, T. Coja, S. Duquesne, A. Focks, M. Marinovich, M. Millet, and O. Pelkonen. 2022. Statement on the active substance flupyradifurone. EFSA Journal **20**:e07030.

o   EFSA PPR Panel (Panel on Plant Protection Products and their Residues), Ockleford C, Adriaanse P, Berny P, T. c. Bro, and e. a. S. Duquesne. 2018. Scientific Opinion on the

state of the art of Toxicokinetic/Toxicodynamic (TKTD) effect models for regulatory risk assessment of pesticides for aquatic organisms. EFSA Journal **16**:e05377.

o EPA, U. 2016. Species Sensitivity Distribution Generator. Internet: Available online at: https://www.epa.gov/chemical-research/species-sensitivity-distribution-ssd-toolbox

o EPA, U. S. E. P. A. 2015. Notice of pesticide registration: flupyradifurone TC. Bayer Crop Science, Virginia, USA.

o Erban, T., B. Sopko, P. Talacko, K. Harant, K. Kadlikova, T. Halesova, K. Riddellova, and A. Pekas. 2019. Chronic exposure of bumblebees to neonicotinoid imidacloprid suppresses the entire mevalonate pathway and fatty acid synthesis. J Proteomics **196**:69-80.

o Escher, B. I., R. Ashauer, S. Dyer, J. L. Hermens, J. H. Lee, H. A. Leslie, P. Mayer, J. P. Meador, and M. S. Warne. 2011. Crucial role of mechanisms and modes of toxic action for understanding tissue residue toxicity and internal effect concentrations of organic chemicals. Integr Environ Assess Manag **7**:28-49.

o European Commission. 2018a. Commission implementing regulation (EU) 2018/783 of 29 May 2018 amending implementing regulation (EU) no 540/2011 as regards the conditions of approval of the active substance imidacloprid. Off. J. Eur. Union **132**:31.

o European Commission. 2018b. Commission implementing regulation (EU) 2018/784 of 29 May 2018 amending implementing regulation (EU) no 540/2011 as regards the conditions of approval of the active substance clothianidin. Off. J. Eur. Union **132**:35.

o European Commission. 2018c. Commission implementing regulation (EU) 2018/785 of 29 May 2018 amending implementing regulation (EU) no 540/2011 as regards the conditions of approval of the active substance thiamethoxam. Off. J. Eur. Union **132**:40.

o Ewere, E. E., D. Powell, D. Rudd, A. Reichelt-Brushett, P. Mouatt, N. H. Voelcker, and K. Benkendorff. 2019. Uptake, depuration and sublethal effects of the neonicotinoid, imidacloprid, exposure in Sydney rock oysters. Chemosphere **230**:1-13.

o Feyereisen, R. 2018. Toxicology: Bee P450s Take the Sting out of Cyanoamidine Neonicotinoids. Curr Biol **28**:R560-R562.

o Focks, A., D. Belgers, M. C. Boerwinkel, L. Buijse, I. Roessink, and P. J. Van den Brink. 2018. Calibration and validation of toxicokinetic-toxicodynamic models for three neonicotinoids and some aquatic macroinvertebrates. Ecotoxicology **27**:992-1007.

o Fox, J., Weisberg, S. 2019. An {R} Companion to Applied Regression, Third Edition. . Sage, Thousand Oaks CA. .

o Freitas, R., F. Coppola, S. Costa, C. Pretti, L. Intorre, V. Meucci, A. Soares, and M. Sole. 2019. The influence of temperature on the effects induced by Triclosan and Diclofenac in mussels. Sci Total Environ **663**:992-999.

o Fu, Q., A. Rosch, D. Fedrizzi, C. Vignet, and J. Hollender. 2018. Bioaccumulation, Biotransformation, and Synergistic Effects of Binary Fungicide Mixtures in Hyalella azteca and Gammarus pulex: How Different/Similar are the Two Species? Environ Sci Technol **52**:13491-13500.

o Fusetto, R., S. Denecke, T. Perry, R. A. J. O'Hair, and P. Batterham. 2017. Partitioning the roles of CYP6G1 and gut microbes in the metabolism of the insecticide imidacloprid in Drosophila melanogaster. Sci Rep **7**:11339.

o Gao, Y., Z. Xie, M. Feng, J. Feng, and L. Zhu. 2020. A biological characteristic extrapolation of compound toxicity for different developmental stage species with toxicokinetic-toxicodynamic model. Ecotoxicol Environ Saf **203**:111043.

- Gao, Y., Y. Zhang, J. Feng, and L. Zhu. 2019. Toxicokinetic-toxicodynamic modeling of cadmium and lead toxicity to larvae and adult zebrafish. Environ Pollut **251**:221-229.
- Gergs, A., F. Gabsi, A. Zenker, and T. G. Preuss. 2016. Demographic Toxicokinetic-Toxicodynamic Modeling of Lethal Effects. Environ Sci Technol **50**:6017-6024.
- Gergs, A., J. Hager, E. Bruns, and T. G. Preuss. 2021. Disentangling Mechanisms Behind Chronic Lethality through Toxicokinetic-Toxicodynamic Modeling. Environ Toxicol Chem **40**:1706-1712.
- Gergs, A., D. Kulkarni, and T. G. Preuss. 2015. Body size-dependent toxicokinetics and toxicodynamics could explain intra- and interspecies variability in sensitivity. Environ Pollut **206**:449-455.
- Gergs, A., K. J. Rakel, D. Liesy, A. Zenker, and S. Classen. 2019. Mechanistic Effect Modeling Approach for the Extrapolation of Species Sensitivity. Environ Sci Technol **53**:9818-9825.
- Giorio, C., A. Safer, F. Sánchez-Bayo, A. Tapparo, A. Lentola, V. Girolami, M. B. van Lexmond, and J.-M. Bonmatin. 2017a. An update of the Worldwide Integrated Assessment (WIA) on systemic insecticides. Part 1: new molecules, metabolism, fate, and transport. Environmental Science and Pollution Research.
- Giorio, C., A. Safer, F. Sanchez-Bayo, A. Tapparo, A. Lentola, V. Girolami, M. B. van Lexmond, and J. M. Bonmatin. 2017b. An update of the Worldwide Integrated Assessment (WIA) on systemic insecticides. Part 1: new molecules, metabolism, fate, and transport. Environ Sci Pollut Res Int.
- Goodhue, R., K. Mace, T. Tolhurst, D. Tregeagle, H. Wei, J. Rudder, B. Grafton-Cardwell, I. Grettenberger, H. Wilson, and R. Van Steenwyk. 2020. Economic and Pest Management Evaluation of Nitroguanidine-substituted Neonicotinoid Insecticides: Eight Major California Commodities.
- Haas, J., A. Hayward, B. Buer, F. Maiwald, B. Nebelsiek, J. Glaubitz, C. Bass, and R. Nauen. 2022. Phylogenomic and functional characterization of an evolutionary conserved cytochrome P450-based insecticide detoxification mechanism in bees. Proc Natl Acad Sci U S A **119**:e2205850119.
- Haas, J., M. Zaworra, J. Glaubitz, G. Hertlein, M. Kohler, A. Lagojda, B. Lueke, C. Maus, M. T. Almanza, T. G. E. Davies, C. Bass, and R. Nauen. 2021. A toxicogenomics approach reveals characteristics supporting the honey bee (Apis mellifera L.) safety profile of the butenolide insecticide flupyradifurone. Ecotoxicol Environ Saf **217**:112247.
- Han, J., and K. W. Lee. 2021. Identification and response of cytochrome P450 genes in the brackish water flea Diaphanosoma celebensis after exposure to benzo[alpha]pyrene and heavy metals. Mol Biol Rep **48**:657-664.
- Haque, M. N., S. E. Nam, B. M. Kim, K. Kim, and J. S. Rhee. 2020. Temperature elevation stage-specifically increases metal toxicity through bioconcentration and impairment of antioxidant defense systems in juvenile and adult marine mysids. Comp Biochem Physiol C Toxicol Pharmacol **237**:108831.
- Harwood, A. D., J. You, and M. J. Lydy. 2009. Temperature as a Toxicity Identification Evaluation Tool for Pyrethroid Insecticides: Toxicokinetic Confirmation. Environmental Toxicology and Chemistry **28**:1051-1058.
- Hazell, P., and S. Wood. 2008. Drivers of Change in Global Agriculture. Philosophical Transactions: Biological Sciences **363**:495-515.

- Heugens, E. H. W., T. Jager, R. Creyghton, M. H. S. Kraak, A. J. Hendriks, N. M. Van Straalen, and W. Admiraal. 2003. Temperature-dependent effects of cadmium on Daphnia magna: Accumulation versus sensitivity. Environmental Science & Technology **37**:2145-2151.
- Heye, K., T. Lotz, A. Wick, and J. Oehlmann. 2019. Interactive effects of biotic and abiotic environmental stressors on carbamazepine toxicity in the non-biting midge Chironomus riparius. Water Res **156**:92-101.
- Hladik, M. L., A. R. Main, and D. Goulson. 2018. Environmental Risks and Challenges Associated with Neonicotinoid Insecticides. Environ Sci Technol **52**:3329-3335.
- Hofmann, G. E., and A. E. Todgham. 2010. Living in the now: physiological mechanisms to tolerate a rapidly changing environment. Annu Rev Physiol **72**:127-145.
- Hoi, K. K., P. J. Daborn, P. Battlay, C. Robin, P. Batterham, R. A. J. O'Hair, and W. A. Donald. 2014. Dissecting the Insect Metabolic Machinery Using Twin Ion Mass Spectrometry: A Single P450 Enzyme Metabolizing the Insecticide Imidacloprid in Vivo. Analytical Chemistry **86**:3525-3532.
- Hommen, U., J. M. Baveco, N. Galic, and P. J. van den Brink. 2010. Potential application of ecological models in the European environmental risk assessment of chemicals. I. Review of protection goals in EU directives and regulations. Integr Environ Assess Manag **6**:325-337.
- Hooper, M. J., G. T. Ankley, D. A. Cristol, L. A. Maryoung, P. D. Noyes, and K. E. Pinkerton. 2013. Interactions between chemical and climate stressors: A role for mechanistic toxicology in assessing climate change risks. Environmental Toxicology and Chemistry **32**:32-48.
- Horion, S., J. P. Thome, and E. Gismondi. 2015. Changes in antitoxic defense systems of the freshwater amphipod Gammarus pulex exposed to BDE-47 and BDE-99. Ecotoxicology **24**:959-966.
- Huang, A., A. Mangold-Döring, A. Focks, C. Zhang, and P. van den Brink. 2022a. Comparison of the acute and chronic toxicity of flupyradifurone and imidacloprid to non-target aquatic arthropod species Under review.
- Huang, A., A. Mangold-Döring, A. Focks, C. Zhang, and P. van den Brink. 2022b. Data for: Comparing the acute and chronic toxicity of flupyradifurone and imidacloprid to non-target aquatic arthropod species. Mendeley Data, V1, doi: 10.17632/52bfvs5vyn.1.
- Huang, A., A. Mangold-Döring, H. Guan, M.-C. Boerwinkel, D. Belgers, A. Focks, and P. Van den Brink. 2022c. Data for: The effect of temperature on toxicokinetics and the chronic toxicity of insecticides towards Gammarus pulex. Mendeley Data, V2, doi: 10.17632/6dbgkhzxvx.2.
- Huang, A., A. Mangold-Döring, H. Guan, M.-C. Boerwinkel, D. Belgers, A. Focks, and P. J. Van den Brink. 2022d. The effect of temperature on toxicokinetics and the chronic toxicity of insecticides toward Gammarus pulex Under review.
- Huang, A., A. Mangold-Doring, and P. Van den Brink. 2022e. Modelling the Contribution of Metabolites in the Overall Aquatic Toxicity of Imidacloprid. SETAC EUROPE 32ND ANNUAL MEETING, Copenhagen, Denmark.
- Huang, A., I. Roessink, N. Van den Brink, and P. Van den Brink. 2022f. Data for: Size- and sex-related sensitivity differences of aquatic crustaceans to imidacloprid. Mendeley Data, V1, doi: 10.17632/fst4m6s3ms.1.

o Huang, A., I. Roessink, N. W. van den Brink, and P. J. van den Brink. 2022g. Size- and sex-related sensitivity differences of aquatic crustaceans to imidacloprid. Ecotoxicology and Environmental Safety **242**:113917.

o Huang, A., N. W. van den Brink, L. Buijse, I. Roessink, and P. J. van den Brink. 2021. The toxicity and toxicokinetics of imidacloprid and a bioactive metabolite to two aquatic arthropod species. Aquat Toxicol **235**:105837.

o Hynes, H. 1970. The ecology of stream insects. Annual Review of Entomology **15**:25-42.

o Jactel, H., F. Verheggen, D. Thiéry, A. J. Escobar-Gutiérrez, E. Gachet, N. Desneux, and N. W. Group. 2019. Alternatives to neonicotinoids. Environment international **129**:423-429.

o Jager, T. 2011. Some good reasons to ban ECx and related concepts in ecotoxicology. Environ Sci Technol **45**:8180-8181.

o Jager, T. 2017a. Comment on "Robust Fit of Toxicokinetic–Toxicodynamic Models Using Prior Knowledge Contained in the Design of Survival Toxicity Tests". Environmental Science & Technology **51**:8200-8201.

o Jager, T. 2017b. Making sense of chemical stress. Application of Dynamic Energy Budget Theory in Ecotoxicology and Stress Ecology. Version **2**.

o Jager, T. 2019. Design document for openGUTS. DEBtox Research, De Bilt, The Netherlands.

o Jager, T. 2020. Revisiting simplified DEBtox models for analysing ecotoxicity data. Ecological Modelling **416**.

o Jager, T. 2021. Robust Likelihood-Based Approach for Automated Optimization and Uncertainty Analysis of Toxicokinetic-Toxicodynamic Models. Integr Environ Assess Manag **17**:388-397.

o Jager, T., C. Albert, T. G. Preuss, and R. Ashauer. 2011. General unified threshold model of survival--a toxicokinetic-toxicodynamic framework for ecotoxicology. Environ Sci Technol **45**:2529-2540.

o Jager, T., D. Altin, C. Miljeteig, and B. H. Hansen. 2016. Stage-dependent and sex-dependent sensitivity to water-soluble fractions of fresh and weathered oil in the marine copepod Calanus finmarchicus. Environ Toxicol Chem **35**:728-735.

o Jager, T., E. H. Heugens, and S. A. Kooijman. 2006. Making sense of ecotoxicological test results: towards application of process-based models. Ecotoxicology **15**:305-314.

o Jager, T., I. B. Overjordet, R. Nepstad, and B. H. Hansen. 2017. Dynamic Links between Lipid Storage, Toxicokinetics and Mortality in a Marine Copepod Exposed to Dimethylnaphthalene. Environ Sci Technol **51**:7707-7713.

o Jager, T., I. Salaberria, and B. H. Hansen. 2015. Capturing the life history of the marine copepod Calanus sinicus into a generic bioenergetics framework. Ecological Modelling **299**:114-120.

o Jager, T., and E. I. Zimmer. 2012. Simplified Dynamic Energy Budget model for analysing ecotoxicity data. Ecological Modelling **225**:74-81.

o Jeschke, P., and R. Nauen. 2008. Neonicotinoids—from zero to hero in insecticide chemistry. Pest Management Science: formerly Pesticide Science **64**:1084-1098.

o Jeschke, P., R. Nauen, O. Gutbrod, M. E. Beck, S. Matthiesen, M. Haas, and R. Velten. 2015a. Flupyradifurone (Sivanto) and its novel butenolide pharmacophore: Structural considerations. Pestic Biochem Physiol **121**:31-38.

- Jeschke, P., R. Nauen, O. Gutbrod, M. E. Beck, S. Matthiesen, M. Haas, and R. Velten. 2015b. Flupyradifurone (Sivanto™) and its novel butenolide pharmacophore: Structural considerations☆. Pesticide Biochemistry and Physiology **121**:31-38.
- Jeschke, P., R. Nauen, M. Schindler, and A. Elbert. 2011. Overview of the status and global strategy for neonicotinoids. Journal of agricultural and food chemistry **59**:2897-2908.
- Johnson, R. K., T. Wiederholm, and D. M. Rosenberg. 1993. Freshwater biomonitoring using individual organisms, populations, and species assemblages of benthic macroinvertebrates. Freshwater biomonitoring and benthic macroinvertebrates:40-158.
- Kamel, A. 2010. Refined methodology for the determination of neonicotinoid pesticides and their metabolites in honey bees and bee products by liquid chromatography-tandem mass spectrometry (LC-MS/MS). J Agric Food Chem **58**:5926-5931.
- Kandie, F. J., M. Krauss, L. M. Beckers, R. Massei, U. Fillinger, J. Becker, M. Liess, B. Torto, and W. Brack. 2020. Occurrence and risk assessment of organic micropollutants in freshwater systems within the Lake Victoria South Basin, Kenya. Sci Total Environ **714**:136748.
- Karunker, I., E. Morou, D. Nikou, R. Nauen, R. Sertchook, B. J. Stevenson, M. J. Paine, S. Morin, and J. Vontas. 2009. Structural model and functional characterization of the Bemisia tabaci CYP6CM1vQ, a cytochrome P450 associated with high levels of imidacloprid resistance. Insect Biochem Mol Biol **39**:697-706.
- Kretschmann, A., R. Ashauer, T. G. Preuss, P. Spaak, B. I. Escher, and J. Hollender. 2011. Toxicokinetic model describing bioconcentration and biotransformation of diazinon in Daphnia magna. Environ Sci Technol **45**:4995-5002.
- Lahr, J., C. Moermond, M. Montforts, A. Derksen, N. Bondt, L. Puister-Jansen, T. de Koeijer, and P. Hoeksma. 2019. Diergeneesmiddelen in het milieu: een synthese van de huidige kennis. Stowa.
- Lamichhane, J. R. 2017. Pesticide use and risk reduction in European farming systems with IPM: An introduction to the special issue. Crop Protection **97**:1-6.
- Legierse, K. C. H. M., H. J. M. Verhaar, W. H. J. Vaes, J. H. M. De Bruijn, and J. L. M. Hermens. 1999. Analysis of the Time-Dependent Acute Aquatic Toxicity of Organophosphorus Pesticides: The Critical Target Occupation Model. Environmental Science & Technology **33**:917-925.
- Lewis, K. A., J. Tzilivakis, D. J. Warner, and A. Green. 2016. An international database for pesticide risk assessments and management. Human and Ecological Risk Assessment: An International Journal **22**:1050-1064.
- Li, H., Q. Zhang, H. Su, J. You, and W. X. Wang. 2021. High Tolerance and Delayed Responses of Daphnia magna to Neonicotinoid Insecticide Imidacloprid: Toxicokinetic and Toxicodynamic Modeling. Environ Sci Technol **55**:458-467.
- Li, Y., L. Long, J. Ge, H. Li, M. Zhang, Q. Wan, and X. Yu. 2019. Effect of Imidacloprid Uptake from Contaminated Soils on Vegetable Growth. J Agric Food Chem **67**:7232-7242.
- Lushchak, V. I., T. M. Matviishyn, V. V. Husak, J. M. Storey, and K. B. Storey. 2018. Pesticide toxicity: a mechanistic approach. EXCLI journal **17**:1101.

- Lydy, M. J., J. B. Belden, and M. A. Ternes. 1999. Effects of temperature on the toxicity of m-parathion, chlorpyrifos, and pentachlorobenzene to Chironomus tentans. Arch Environ Contam Toxicol **37**:542-547.
- Ma, Y., S. Zhai, S. Y. Mao, S. L. Sun, Y. Wang, Z. H. Liu, Y. J. Dai, and S. Yuan. 2014. Co-metabolic transformation of the neonicotinoid insecticide imidacloprid by the new soil isolate Pseudoxanthomonas indica CGMCC 6648. J Environ Sci Health B **49**:661-670.
- Maazouzi, C., C. Piscart, F. Legier, and F. Hervant. 2011. Ecophysiological responses to temperature of the "killer shrimp" Dikerogammarus villosus: is the invader really stronger than the native Gammarus pulex? Comp Biochem Physiol A Mol Integr Physiol **159**:268-274.
- Macaulay, S. J., D. B. Buchwalter, and C. D. Matthaei. 2019. Water temperature interacts with the insecticide imidacloprid to alter acute lethal and sublethal toxicity to mayfly larvae. New Zealand Journal of Marine and Freshwater Research.
- Macaulay, S. J., D. B. Buchwalter, and C. D. Matthaei. 2020. Water temperature interacts with the insecticide imidacloprid to alter acute lethal and sublethal toxicity to mayfly larvae. New Zealand Journal of Marine and Freshwater Research **54**:115-130.
- Macaulay, S. J., K. J. Hageman, J. J. Piggott, and C. D. Matthaei. 2021. Time-cumulative effects of neonicotinoid exposure, heatwaves and food limitation on stream mayfly nymphs: A multiple-stressor experiment. Science of The Total Environment **754**.
- Mach, B. M., S. Bondarenko, and D. A. Potter. 2018. Uptake and dissipation of neonicotinoid residues in nectar and foliage of systemically treated woody landscape plants. Environ Toxicol Chem **37**:860-870.
- Main, A. R., E. B. Webb, K. W. Goyne, R. Abney, and D. Mengel. 2021. Impacts of neonicotinoid seed treatments on the wild bee community in agricultural field margins. Science of The Total Environment **786**:147299.
- Maloney, E. M., C. A. Morrissey, J. V. Headley, K. M. Peru, and K. Liber. 2017. Cumulative toxicity of neonicotinoid insecticide mixtures to Chironomus dilutus under acute exposure scenarios. Environ Toxicol Chem **36**:3091-3101.
- Maloney, E. M., H. Sykes, C. Morrissey, K. M. Peru, J. V. Headley, and K. Liber. 2020. Comparing the Acute Toxicity of Imidacloprid with Alternative Systemic Insecticides in the Aquatic Insect Chironomus dilutus. Environ Toxicol Chem **39**:587-594.
- Maltby, L., N. Blake, T. C. Brock, and P. J. van den Brink. 2005. Insecticide species sensitivity distributions: importance of test species selection and relevance to aquatic ecosystems. Environ Toxicol Chem **24**:379-388.
- Martin, O. V., J. Adams, A. Beasley, S. Belanger, R. L. Breton, T. Brock, V. A. Buonsante, M. Galay Burgos, J. Green, and P. D. Guiney. 2019. Improving environmental risk assessments of chemicals: Steps towards evidence-based ecotoxicology. Environment International **128**.
- McCahon, C., and D. Pascoe. 1988. Culture techniques for three freshwater macroinvertebrate species and their use in toxicity tests. Chemosphere **17**:2471-2480.
- McCarty, L. S., P. F. Landrum, S. N. Luoma, J. P. Meador, A. A. Merten, B. K. Shephard, and A. P. van Wezel. 2011. Advancing environmental toxicology through chemical

dosimetry: external exposures versus tissue residues. Integr Environ Assess Manag **7**:7-27.

o McClellan-Green, P., J. Romano, and E. Oberdorster. 2007. Does gender really matter in contaminant exposure? A case study using invertebrate models. Environ Res **104**:183-191.

o McGrath, K. E., E. T. H. M. Peeters, J. A. J. Beijer, and M. Scheffer. 2007. Habitat-mediated cannibalism and microhabitat restriction in the stream invertebrate Gammarus pulex. Hydrobiologia **589**:155-164.

o Merga, L. B., A. A. Mengistie, M. T. Alemu, and P. J. Van den Brink. 2021. Biological and chemical monitoring of the ecological risks of pesticides in Lake Ziway, Ethiopia. Chemosphere **266**:129214.

o Metcalfe, C. D., P. Helm, G. Paterson, G. Kaltenecker, C. Murray, M. Nowierski, and T. Sultana. 2019. Pesticides related to land use in watersheds of the Great Lakes basin. Sci Total Environ **648**:681-692.

o Miller, T. H., G. L. McEneff, L. C. Stott, S. F. Owen, N. R. Bury, and L. P. Barron. 2016. Assessing the reliability of uptake and elimination kinetics modelling approaches for estimating bioconcentration factors in the freshwater invertebrate, Gammarus pulex. Science of The Total Environment **547**:396-404.

o Moe, S. J., K. De Schamphelaere, W. H. Clements, M. T. Sorensen, P. J. Van den Brink, and M. Liess. 2013. Combined and interactive effects of global climate change and toxicants on populations and communities. Environ Toxicol Chem **32**:49-61.

o Moenickes, S., A. K. Schneider, L. Muhle, L. Rohe, O. Richter, and F. Suhling. 2011. From population-level effects to individual response: modelling temperature dependence in Gammarus pulex. J Exp Biol **214**:3678-3687.

o Moermond, C. T., R. Kase, M. Korkaric, and M. Agerstrand. 2016. CRED: Criteria for reporting and evaluating ecotoxicity data. Environ Toxicol Chem **35**:1297-1309.

o Morrissey, C. A., P. Mineau, J. H. Devries, F. Sanchez-Bayo, M. Liess, M. C. Cavallaro, and K. Liber. 2015. Neonicotinoid contamination of global surface waters and associated risk to aquatic invertebrates: a review. Environ Int **74**:291-303.

o Motohiro Tomizawa, D. L. L., and John E. Casida. 2000. Neonicotinoid Insecticides: Molecular Features Conferring Selectivity for Insect versus Mammalian Nicotinic Receptors. J. Agric. Food Chem. **48**:6016−6024.

o Murphy, P. M., and M. A. Learner. 1982. The life history and production ofAsellus aquaticus (Crustacea: Isopoda) in the River Ely, South Wales. Freshwater Biology **12**:435-444.

o Na, J., Y. Kim, J. Song, T. Shim, K. Cho, and J. Jung. 2021. Evaluation of the combined effect of elevated temperature and cadmium toxicity on Daphnia magna using a simplified DEBtox model. Environ Pollut **291**:118250.

o Nauen, R., U. Ebbinghaus-Kintscher, and R. Schmuck. 2001. Toxicity and nicotinic acetylcholine receptor interaction of imidacloprid and its metabolites in Apis mellifera (Hymenoptera: Apidae). Pest Manag Sci **57**:577-586.

o Nauen, R., P. Jeschke, R. Velten, M. E. Beck, U. Ebbinghaus-Kintscher, W. Thielert, K. Wolfel, M. Haas, K. Kunz, and G. Raupach. 2015a. Flupyradifurone: a brief profile of a new butenolide insecticide. Pest Manag Sci **71**:850-862.

o Nauen, R., P. Jeschke, R. Velten, M. E. Beck, U. Ebbinghaus-Kintscher, W. Thielert, K. Wölfel, M. Haas, K. Kunz, and G. Raupach. 2015b. Flupyradifurone: a brief profile of a new butenolide insecticide. Pest management science **71**:850-862.

- Nilsson, L. M. 1974. Energy budget of a laboratory population of Gammarus pulex (Amphipoda). Oikos:35-42.
- Nishiwaki, H., K. Sato, Y. Nakagawa, M. Miyashita, and H. Miyagawa. 2004. Metabolism of imidacloprid in houseflies. Journal of Pesticide Science **29**:110-116.
- Noyes, and S. C. Lema. 2015. Forecasting the impacts of chemical pollution and climate change interactions on the health of wildlife. Current Zoology **61**:669-689.
- Nyman, A. M., A. Hintermeister, K. Schirmer, and R. Ashauer. 2013. The insecticide imidacloprid causes mortality of the freshwater amphipod Gammarus pulex by interfering with feeding behavior. PLoS One **8**:e62472.
- OECD. 2004. Test No. 202: Daphnia sp. Acute Immobilisation Test, OECD Guidelines for the Testing of Chemicals, Section 2. OECD Publishing, Paris.
- OECD. 2006. Current Approaches in the Statistical Analysis of Ecotoxicity Data.
- OECD. 2012. Test No. 211: Daphnia magna Reproduction Test, OECD Guidelines for the Testing of Chemicals, Section 2. OECD Publishing, Paris.
- Olivier Dangles, Mark O. Gessner, François Guerold, and E. Chauvet. 2004. Impacts of stream acidification on litter breakdown: implications for assessing ecosystem functioning. Journal of Applied Ecology **41**:365-378.
- Parkinson, R. H., and J. R. Gray. 2019. Neural conduction, visual motion detection, and insect flight behaviour are disrupted by low doses of imidacloprid and its metabolites. Neurotoxicology **72**:107-113.
- Pietrzak, D., J. Kania, E. Kmiecik, G. Malina, and K. Wątor. 2020. Fate of selected neonicotinoid insecticides in soil–water systems: Current state of the art and knowledge gaps. Chemosphere **255**:126981.
- PMRA, P. M. R. A. 2015. Flupyradifurone. Registration Decision RD2015-24.
- Polazzo, F., S. K. Roth, M. Hermann, A. Mangold-Doring, A. Rico, A. Sobek, P. J. Van den Brink, and M. C. Jackson. 2022. Combined effects of heatwaves and micropollutants on freshwater ecosystems: Towards an integrated assessment of extreme events in multiple stressors research. Glob Chang Biol **28**:1248-1267.
- Pörtner, H.-O. 2010. Oxygen- and capacity-limitation of thermal tolerance: a matrix for integrating climate-related stressor effects in marine ecosystems. J Exp Biol **213**:881-893.
- Poteat, M. D., and D. B. Buchwalter. 2014. Phylogeny and size differentially influence dissolved Cd and Zn bioaccumulation parameters among closely related aquatic insects. Environ Sci Technol **48**:5274-5281.
- Products, E. P. o. P. P., R. their, C. Ockleford, P. Adriaanse, P. Berny, T. Brock, S. Duquesne, S. Grilli, A. F. Hernandez-Jerez, S. H. Bennekou, M. Klein, T. Kuhl, R. Laskowski, K. Machera, O. Pelkonen, S. Pieper, R. H. Smith, M. Stemmer, I. Sundh, A. Tiktak, C. J. Topping, G. Wolterink, N. Cedergreen, S. Charles, A. Focks, M. Reed, M. Arena, A. Ippolito, H. Byers, and I. Teodorovic. 2018. Scientific Opinion on the state of the art of Toxicokinetic/Toxicodynamic (TKTD) effect models for regulatory risk assessment of pesticides for aquatic organisms. EFSA J **16**:e05377.
- Raby, M., M. Nowierski, D. Perlov, X. Zhao, C. Hao, D. G. Poirier, and P. K. Sibley. 2018. Acute toxicity of 6 neonicotinoid insecticides to freshwater invertebrates. Environ Toxicol Chem **37**:1430-1445.
- Rauch, N., and R. Nauen. 2003. Identification of biochemical markers linked to neonicotinoid cross resistance in Bemisia tabaci (Hemiptera: Aleyrodidae). Archives of Insect Biochemistry and Physiology **54**:165-176.

o   Rico, A., A. Arenas-Sanchez, J. Pasqualini, A. Garcia-Astillero, L. Cherta, L. Nozal, and M. Vighi. 2018. Effects of imidacloprid and a neonicotinoid mixture on aquatic invertebrate communities under Mediterranean conditions. Aquatic Toxicology **204**:130-143.

o   Ricupero, M., K. Abbes, K. Haddi, A. Kurtulus, N. Desneux, A. Russo, G. Siscaro, A. Biondi, and L. Zappala. 2020. Combined thermal and insecticidal stresses on the generalist predator Macrolophus pygmaeus. Sci Total Environ **729**:138922.

o   Rinderhagen, M., J. Ritterhoff, and G.-P. Zauke. 2000. Crustaceans as bioindicators. Pages 161-194 *in* Biomonitoring of Polluted Water-Reviews on Actual Topics. Trans Tech Publications-Scitech Publications, Environmental Research Forum.

o   Ritz, C., F. Baty, J. C. Streibig, and D. Gerhard. 2015. Dose-Response Analysis Using R. PLoS One **10**:e0146021.

o   Ritz, C., and J. C. Streibig. 2005. Bioassay analysis using R. Journal of Statistical Software **12**:1-22.

o   Roessink, I., L. B. Merga, H. J. Zweers, and P. J. Van den Brink. 2013. The neonicotinoid imidacloprid shows high chronic toxicity to mayfly nymphs. Environ Toxicol Chem **32**:1096-1100.

o   Rondeau, G., F. Sánchez-Bayo, H. A. Tennekes, A. Decourtye, R. Ramírez-Romero, and N. Desneux. 2014. Delayed and time-cumulative toxicity of imidacloprid in bees, ants and termites. Scientific Reports **4**:5566.

o   Rubach, M. N., R. Ashauer, S. J. Maund, D. J. Baird, and P. J. Van den Brink. 2010. Toxicokinetic variation in 15 freshwater arthropod species exposed to the insecticide chlorpyrifos. Environmental Toxicology and Chemistry **29**:2225-2234.

o   Rubach, M. N., D. J. Baird, M.-C. Boerwinkel, S. J. Maund, I. Roessink, and P. J. Van den Brink. 2012. Species traits as predictors for intrinsic sensitivity of aquatic invertebrates to the insecticide chlorpyrifos. Ecotoxicology **21**:2088-2101.

o   Sanford, M., and R. S. Prosser. 2020. High-Frequency Sampling of Small Streams in the Agroecosystems of Southwestern Ontario, Canada, to Characterize Pesticide Exposure and Associated Risk to Aquatic Life. Environ Toxicol Chem **39**:2570-2587.

o   Schaefer, K. 2013. Science-Policy Linkages in Ecotoxicology. Pages 997-1002 *in* J.-F. Férard and C. Blaise, editors. Encyclopedia of Aquatic Ecotoxicology. Springer Netherlands, Dordrecht.

o   Schuijt, L. M., F. J. Peng, S. J. P. van den Berg, M. M. L. Dingemans, and P. J. Van den Brink. 2021. (Eco)toxicological tests for assessing impacts of chemical stress to aquatic ecosystems: Facts, challenges, and future. Sci Total Environ **795**:148776.

o   Shahid, N., J. M. Becker, M. Krauss, W. Brack, and M. Liess. 2018. Pesticide Body Burden of the Crustacean Gammarus pulex as a Measure of Toxic Pressure in Agricultural Streams. Environ Sci Technol **52**:7823-7832.

o   Sherborne, N., and N. Galic. 2020. Modeling Sublethal Effects of Chemicals: Application of a Simplified Dynamic Energy Budget Model to Standard Ecotoxicity Data. Environ Sci Technol **54**:7420-7429.

o   Simon-Delso, N., V. Amaral-Rogers, L. P. Belzunces, J.-M. Bonmatin, M. Chagnon, C. Downs, L. Furlan, D. W. Gibbons, C. Giorio, and V. Girolami. 2015. Systemic insecticides (neonicotinoids and fipronil): trends, uses, mode of action and metabolites. Environmental Science and Pollution Research **22**:5-34.

- Siviter, H., S. K. Richman, and F. Muth. 2021. Field-realistic neonicotinoid exposure has sub-lethal effects on non-Apis bees: A meta-analysis. Ecology Letters **24**:2586-2597.
- Spurgeon, D., E. Lahive, A. Robinson, S. Short, and P. Kille. 2020. Species Sensitivity to Toxic Substances: Evolution, Ecology and Applications. Frontiers in Environmental Science **8**.
- Stark, J. D., J. E. Banks, and S. Acheampong. 2004. Estimating susceptibility of biological control agents to pesticides: influence of life history strategies and population structure. Biological Control **29**:392-398.
- Starner, K., and K. S. Goh. 2012. Detections of the neonicotinoid insecticide imidacloprid in surface waters of three agricultural regions of California, USA, 2010-2011. Bull Environ Contam Toxicol **88**:316-321.
- Suchail, S., G. De Sousa, R. Rahmani, and L. P. Belzunces. 2004a. In vivo distribution and metabolisation of 14C-imidacloprid in different compartments of Apis mellifera L. Pest Manag Sci **60**:1056-1062.
- Suchail, S., L. Debrauwer, and L. P. Belzunces. 2004b. Metabolism of imidacloprid in Apis mellifera. Pest Management Science **60**:291-296.
- Suchail., S., D. Guez., and L. P. Belzunces. 2001. Discrepancy Between Acute and Chronic Toxicity Induced by Imidacloprid and Its Metabolites in Apis Mellifera.
- Sulukan, E., A. Baran, O. Senol, S. Yildirim, A. Mavi, H. A. Ceyhun, E. Toraman, and S. B. Ceyhun. 2022. The synergic toxicity of temperature increases and nanopolystrene on zebrafish brain implies that global warming may worsen the current risk based on plastic debris. Sci Total Environ **808**:152092.
- Sumon, K. A., A. K. Ritika, E. Peeters, H. Rashid, R. H. Bosma, M. S. Rahman, M. K. Fatema, and P. J. Van den Brink. 2018. Effects of imidacloprid on the ecology of sub-tropical freshwater microcosms. Environ Pollut **236**:432-441.
- Sutcliffe, D. W. 1992. Reproduction in Gammarus (Crustacea, Amphipoda) Basic processes.
- Sutcliffe, D. W., T. R. Carrick, and L. G. Willoughby. 1981. Effects of diet, body size, age and temperature on growth rates in the amphipod Gammarus pulex. Freshwater Biology **11**:183-214.
- Taillebois, E., A. Cartereau, A. K. Jones, and S. H. Thany. 2018. Neonicotinoid insecticides mode of action on insect nicotinic acetylcholine receptors using binding studies. Pesticide Biochemistry and Physiology **151**:59-66.
- Taylor, L. N., and R. P. Scroggins. 2013. Biological Test Methods in Ecotoxicology. Pages 197-204 *in* J.-F. Férard and C. Blaise, editors. Encyclopedia of Aquatic Ecotoxicology. Springer Netherlands, Dordrecht.
- Tennekes, H. A. 2011. The significance of the Druckrey–Küpfmüller equation for risk assessment—The toxicity of neonicotinoid insecticides to arthropods is reinforced by exposure time: Responding to a Letter to the Editor by Drs. C. Maus and R. Nauen of Bayer CropScience AG. Toxicology **280**:173-175.
- Theys, C., J. Verheyen, N. Tuzun, and R. Stoks. 2020. Higher mean and fluctuating temperatures jointly determine the impact of the pesticide chlorpyrifos on the growth rate and leaf consumption of a freshwater isopod. Chemosphere:128528.
- Thunnissen, N. W., L. S. Lautz, T. W. G. van Schaik, and A. J. Hendriks. 2020a. Ecological risks of imidacloprid to aquatic species in the Netherlands: Measured and

estimated concentrations compared to species sensitivity distributions. Chemosphere **254**:126604.

o Thunnissen, N. W., L. S. Lautz, T. W. G. van Schaik, and A. J. Hendriks. 2020b. Ecological risks of imidacloprid to aquatic species in the Netherlands: Measured and estimated concentrations compared to species sensitivity distributions. Chemosphere **254**.

o Tomalski, M., W. Leimkuehler, C. Schal, and E. L. Vargo. 2010. Metabolism of Imidacloprid in Workers of Reticulitermes flavipes (Isoptera: Rhinotermitidae). Annals of the Entomological Society of America **103**:84-95.

o Tosi, S., J. C. Nieh, A. Brandt, M. Colli, J. Fourrier, H. Giffard, J. Hernandez-Lopez, V. Malagnini, G. R. Williams, and N. Simon-Delso. 2021. Long-term field-realistic exposure to a next-generation pesticide, flupyradifurone, impairs honey bee behaviour and survival. Commun Biol **4**:805.

o Tran, T. T., K. Dinh Van, L. Janssens, and R. Stoks. 2020. The effect of warming on pesticide toxicity is reversed between developmental stages in the mosquito Culex pipiens. Sci Total Environ **717**:134811.

o Van de Perre, D., K. S. Yao, D. Li, H. J. Lei, P. J. Van den Brink, and G. G. Ying. 2021. Imidacloprid treatments induces cyanobacteria blooms in freshwater communities under sub-tropical conditions. Aquat Toxicol **240**:105992.

o Van den Berg, S. J. P., H. Baveco, E. Butler, F. De Laender, A. Focks, A. Franco, C. Rendal, and P. J. Van den Brink. 2019. Modeling the Sensitivity of Aquatic Macroinvertebrates to Chemicals Using Traits. Environ Sci Technol **53**:6025-6034.

o Van den Brink, P. J., D. J. Baird, H. Baveco, and A. Focks. 2013. The use of traits-based approaches and eco(toxico)logical models to advance the ecological risk assessment framework for chemicals. Integrated Environmental Assessment and Management **9**:e47-e57.

o Van den Brink, P. J., A. B. A. Boxall, L. Maltby, B. W. Brooks, M. A. Rudd, T. Backhaus, D. Spurgeon, V. Verougstraete, C. Ajao, G. T. Ankley, S. E. Apitz, K. Arnold, T. Brodin, M. Canedo-Arguelles, J. Chapman, J. Corrales, M. A. Coutellec, T. F. Fernandes, J. Fick, A. T. Ford, G. Gimenez Papiol, K. J. Groh, T. H. Hutchinson, H. Kruger, J. V. K. Kukkonen, S. Loutseti, S. Marshall, D. Muir, M. E. Ortiz-Santaliestra, K. B. Paul, A. Rico, I. Rodea-Palomares, J. Rombke, T. Rydberg, H. Segner, M. Smit, C. A. M. van Gestel, M. Vighi, I. Werner, E. I. Zimmer, and J. van Wensem. 2018. Toward sustainable environmental quality: Priority research questions for Europe. Environ Toxicol Chem **37**:2281-2295.

o Van den Brink, P. J., J. M. Van Smeden, R. S. Bekele, W. Dierick, D. M. De Gelder, M. Noteboom, and I. Roessink. 2016. Acute and chronic toxicity of neonicotinoids to nymphs of a mayfly species and some notes on seasonal differences. Environ Toxicol Chem **35**:128-133.

o van Hagen, A. 2020. Bijengif Imidacloprid vergiftigt het oppervlaktewater. Algemene Waterschapspartij.

o van Leeuwen, C. J., and T. G. Vermeire. 2007. Risk assessment of chemicals: an introduction. Springer.

o Vellinger, C., V. Felten, P. Sornom, P. Rousselle, J. N. Beisel, and P. Usseglio-Polatera. 2012. Behavioural and physiological responses of Gammarus pulex exposed to cadmium and arsenate at three temperatures: individual and combined effects. PLoS One **7**:e39153.

- Vijver, M. G., and P. J. van den Brink. 2014. Macro-invertebrate decline in surface water polluted with imidacloprid: a rebuttal and some new analyses. PLoS One **9**:e89837.
- Wan, Y., Q. Han, Y. Wang, and Z. He. 2020. Five degradates of imidacloprid in source water, treated water, and tap water in Wuhan, central China. Sci Total Environ **741**:140227.
- Wang, Y., Y. Han, P. Xu, B. Guo, W. Li, and X. Wang. 2018. The metabolism distribution and effect of imidacloprid in chinese lizards (Eremias argus) following oral exposure. Ecotoxicology and Environmental Safety **165**:476-483.
- Wang., Y. Zhang, W. Li, Y. T. Han, and B. Y. Guo. 2019. Study on neurotoxicity of dinotefuran, thiamethoxam and imidacloprid against Chinese lizards (Eremias argus). Chemosphere **217**:150-157.
- Welton, J. S., and R. T. Clarke. 1980. Laboratory Studies on the Reproduction and Growth of the Amphipod, Gammarus Pulex. Journal of Animal Ecology **49**.
- Wiles, S. C., M. G. Bertram, J. M. Martin, H. Tan, T. K. Lehtonen, and B. B. M. Wong. 2020. Long-Term Pharmaceutical Contamination and Temperature Stress Disrupt Fish Behavior. Environ Sci Technol **54**:8072-8082.
- Williams, K., D. Green, and D. Pascoe. 1984. Toxicity testing with freshwater macroinvertebrates: Methods and application in environmental management. Pages 81-91 Freshwater biological monitoring. Elsevier.
- Woodcock, B. A., J. M. Bullock, R. F. Shore, M. S. Heard, M. G. Pereira, J. Redhead, L. Ridding, H. Dean, D. Sleep, and P. Henrys. 2017. Country-specific effects of neonicotinoid pesticides on honey bees and wild bees. Science **356**:1393-1395.
- Woodcock, B. A., N. J. Isaac, J. M. Bullock, D. B. Roy, D. G. Garthwaite, A. Crowe, and R. F. Pywell. 2016. Impacts of neonicotinoid use on long-term population changes in wild bees in England. Nature Communications **7**:1-8.
- Xu, F.-L., Y.-L. Li, Y. Wang, W. He, X.-Z. Kong, N. Qin, W.-X. Liu, W.-J. Wu, and S. E. Jorgensen. 2015. Key issues for the development and application of the species sensitivity distribution (SSD) model for ecological risk assessment. Ecological Indicators **54**:227-237.
- Zabar, R., D. Dolenc, T. Jerman, M. Franko, and P. Trebse. 2011. Photolytic and photocatalytic degradation of 6-chloronicotinic acid. Chemosphere **85**:861-868.
- Zaworra, M., H. Koehler, J. Schneider, A. Lagojda, and R. Nauen. 2019. Pharmacokinetics of Three Neonicotinoid Insecticides upon Contact Exposure in the Western Honey Bee, Apis mellifera. Chem Res Toxicol **32**:35-37.
- Zhong, K., Y. Meng, J. Wu, Y. Wei, Y. Huang, J. Ma, and H. Lu. 2021. Effect of flupyradifurone on zebrafish embryonic development. Environ Pollut **285**:117323.

Summary

Neonicotinoids (NNIs) are among the most used insecticides in the world to protect crops from harmful insects. The intensive use of NNIs, however, also brings many environmental concerns about aquatic systems since they have been detected in many water systems due to their high water solubility and persistence. In addition, scientific questions and knowledge gaps have emerged from our current understanding of the impact of neonicotinoids on aquatic systems and on protecting our environment. These questions and gaps include (1) why are some aquatic arthropods more sensitive to imidacloprid (IMI), which is the most used NNI, than other species?, (2) how can we explain differences in intraspecific sensitivity?, and (3) does flupyradifurone (FPF, an alternative to IMI) also show time-accumulative toxicity to some aquatic arthropods like IMI?

The present work is carried out to address these three research questions by investigating the interspecies and intraspecies sensitivity differences of aquatic macro-invertebrates for two insecticides, IMI and FPF.

In **Chapter 2,** we assess the toxicity and toxicokinetics of imidacloprid and a bioactive metabolite to two aquatic arthropod species, a mayfly species *Cloeon dipterum* (sensitive to IMI) and an amphipod species *Gammarus pulex* (less sensitive to IMI). Of the four tested metabolites, only imidacloprid-olefin (IMI-ole) is readily biotransformed from the parent IMI and showed similar toxicity as IMI to both species. Our results on internal kinetics of IMI and IMI-ole, and biotransformation of IMI indicate that the metabolite IMI-ole is toxic and is rather persistent inside the body tissue of both invertebrate species, especially for *C. dipterum*. In conclusion, as IMI and IMI-ole have similar toxicity and IMI is replaced by IMI-ole which in turn is poorly eliminated by *C. dipterum*, the overall toxicity is a function of dose and time. As a result, no long-term threshold of effects of IMI may exist for *C. dipterum* as the poor elimination results in an ongoing increase of toxicity over time for mayflies as also found experimentally in previously published papers.

In **Chapter 3**, we investigate the size- and sex-related sensitivity differences of aquatic crustaceans to imidacloprid. We perform standard acute toxicity and toxicokinetic tests with *Gammarus pulex* and *Asellus aquaticus*. For both species, neonates, juveniles and male and female adults are investigated. For both species, the neonates are the most sensitive group.

For *G. pulex*, the sensitivity decreases linearly with size, which can be explained by the size-related uptake rate constant in the toxicokinetic process and size-related threshold value in the toxicodynamic process. For *A. aquaticus*, female adults are least sensitive to imidacloprid, which could be explained by low internal biotransformation of IMI to IMI-ole. Besides, IMI-ole is more toxic than IMI to *A. aquaticus*, with differences being 8.4 times for females and 2.7 times for males. In conclusion, we establish size-related sensitivity differences for *G. pulex* and sex-related sensitivity for *A. aquaticus*, and intraspecies differences can be explained by both toxicokinetic and toxicodynamic processes. Our findings suggest that to protect populations in the field, we should consider the size and sex of focal organisms and that a pragmatic selection of test organisms of equal size and/or sex can underestimate the sensitivities of populations in the field.

In **Chapter 4**, We assess the acute and chronic toxicity of FPF to aquatic arthropod species and compared it with the toxicity of IMI. We find that compared to IMI, *C. dipterum* and *G. pulex* show a slower uptake and faster elimination rates for FPF. FPF is less acutely toxic than IMI based on the HC_{05} values for aquatic arthropods. The chronic 28d EC_{50} and EC_{10} values of FPF were higher or similar to those of IMI. However, FPF inhibited the food consumption of *G. pulex* at a concentration at the same order of magnitude as the current environmental realistic concentration (NOEC = 0.3 µg/L). More environmental monitoring studies of FPF should be performed to know the environmental concentration of FPF better. In addition, a toxicokinetic-toxicodynamic (TKTD) model parameterised on the acute toxicity data predicted the observed chronic effects of FPF on *G. pulex* well, indicating that toxicity mechanisms of FPF did not change with prolonged exposure time, which is not the case for IMI.

In **Chapter 5** and **Chapter 6**, we explore the sensitivity differences of IMI and FPF to *Gammarus pulex* at different temperatures. In **Chapter 5**, we assess the effect of temperature on the toxicokinetics and the chronic toxicity of IMI and FPF towards *G. pulex*. For both IMI and FPF, the uptake and elimination rate constants increase with temperature but in different magnitudes. In addition, temperature increases the biotransformation rate of IMI and thus accelerates the formation of the toxic metabolite IMI-ole. Furthermore, we find that higher temperatures increases the toxicity of IMI and FPF over time, where the increase is higher for IMI than for FPF. In addition, the adverse effects of insecticides on sublethal endpoints (i.e., food consumption and dry weight) are exacerbated by elevated temperatures. In **Chapter 6**,

DEB models are calibrated to understand the influence of temperature on the effect of IMI and FPF on the growth and survival of *Gammarus pulex*. Our results show that for both IMI and FPF, the dominant rate and threshold value tend to decrease with increasing temperature for both lethal and sublethal effects, while the effect strength and background mortality tend to increase with increasing temperature.

Chapter 5 and **Chapter 6** reveal that temperature influences both the toxicokinetic and toxicodynamic processes. For future studies, taking the temperature into consideration in the risk assessment of chemicals is essential in order to better assess the risks of chemicals in a world under global warming. In addition, the effect of temperature on the sensitivity of organisms is also different between species and chemicals. Thus, more studies on the effect of temperature on the toxicokinetics and toxicodynamics of chemicals are needed.

Finally, in **Chapter 7,** I discuss the findings of my thesis, especially the importance of biotransformation in explaining the interspecies and intraspecies sensitivity differences, emphasising the important need to consider the toxic metabolite as well as the temperature in toxicity assessment. The final chapter also provides an outlook on the adverse-outcome-pathway (AOP), which links the toxicokinetic-toxicodynamic models to a deeper biological perspective, to gain more understanding of the intra- and inter-species sensitivity differences in future studies.

Acknowledgement

"Time flies", people say so, let us enjoy this flight then.

I do not how to start this acknowledgement, so much gratitude poured into my chest, and so many faces flashed through my mind. At this moment, I just want to say "thank you" to everyone.

But the loudest thank you goes to my family. I am deeply grateful to my family for their support and love over the years. My mom, my dad, my younger sister and my little brother. I have not seen you for over 3 years due to the covid pandemic. I miss you all deeply, but I can feel you are always there for me. Our daily small talk and weekly video calls make me feel like I am always surrounded by you. Doing a PhD abroad was an exciting decision for me, but a worrying one for my parents. They care a lot about me, but if something bad happens, they cannot help me in time. I want to say thank you and let you know that I am also proud of your support. Also, over the years I have gained more experience with the tough parts of life because I do go through tough time. And the more I understand the hardships of life, the more I admire my parents, who overcome many difficulties in life and set many good examples for me. Their perseverance and optimism illuminated the path of my life, especially during some hard time of my PhD. Again, my dear family, thank you for always being with me!

Next, I would like to thank my supervisors, Paul, Nico and Ivo. Having three supervisors, although two of them are brothers, is not easy to have discussions with. At the beginning of my PhD, I recorded the meetings with my supervisors because I could not follow them, I barely understand my PhD topic yet, let alone follow the intense discussion among three experts from different perspectives. But I need to emphasize that I have the best team of supervisors, they are always, at least one of them, reachable to support me and give me help whenever I ask for it. Ivo, you are very sweet and supportive, you notice my stress during the meeting and comfort me after the meeting, encouraging me with your big smile. I often meet you in the lab, your smile gives me energy. Nico, whose office is in Helix, is not around me as often as Paul and Ivo, but it does not reduce his supervision. Nico, we have many meetings in person and I learn a lot about toxicokinetics, biotransformation and enzyme from you, thanks! Last but not least, my respected supervisor Paul. Paul, I am so lucky with you. In addition to your significant help with my academic performance, I have benefited hugely from your attitude to

work and life. Your positive and flexible attitude has inspired me, and your encouragement and support have helped me through many difficult times. Your insights into turning bad things like failed experiments, paper rejections, etc. into good things motivate me to keep going. Now, I can proudly say that I also have this turning ability to focus on the positive things in my life. I think that is the greatest skill I ever learnt in my PhD. After all, life is too short to be unhappy. Again, I am so appreciative that I have these three best supervisors as my belayers while I was climbing my PhD's project mountains.

I am so grateful to be part of some great teams and I would like to thank our AEW and ERA teams.

When I started my PhD project at AEW in 2018, I mentioned that my goal at AEW was "AEW: Academic Achievement, Enjoyable Work, and Worldwide Friendship". There is no doubt that 4 years later, I have achieved this with the nice people of the AEW Group. We have a lot of good times and countless laughs during our happy hours, like at the coffee machine corner, in the lab, in the aquarium lunchroom, at hangout events, and in the climbing gym. Of all the nice people at AEW, I am very grateful to Lara, Markus, Annika, Hazi, Vera, and Li. Vera and Lara invited me to the Christmas family party. It is touching to be invited to your big family, Vera. Lara, a huge thank you for saving me from a kayak fall, and a great BBQ night afterwards. Also, we have many sweet memories of biking, hiking and nice dinners, Lara, you are a sister to me. Annika, we interact a lot with each other, we even have a paper where we are co-first author. "A" team, you use this to describe us, not only because both of our names start with "A", but also because our collaboration is the best, "A" class. Annika, having you on my PhD project has accelerated my process and I have got enormous help from you on modelling aspects. I appreciate your honesty and thoughtfulness. Hazi, thank you for taking me to the top of the wall, I enjoy climbing very much. Li, thank you for many nice dinners and your cute cat, Tiger. Last but not least, Markus, hi Bro, I have nothing to say because words cannot express how grateful I am to you, you are always so cheerful and supportive! Again, It is not easy to do a PhD, I am very happy and thankful to have such a warm AEW family, with great support from all aspects, for example, Frits, Marlies, Dorine, Wendy, Annie from the lab; Nancy from the paperwork; Louis from the finance; and so much fun from wonderful PhD fellows.

Also, I am fortunate to be involved in ERA and have the opportunity to work with these wonderful people. My PhD project has benefited from the free use of LC-MS/MS. I especially thank Laura for guiding me through the use of LC-MS/MS, you are so kind and welcoming. I also thank Andres and Jan for guiding my modelling skills. You are very kind and patient with my endless questions. Also, thank you so much, Jasper, Marie-Claire and Dick, it is a pleasure working with you.

I have another team that has nothing to do with my PhD project but has brought considerable joy and fulfilment to my PhD life, and that is the WIMEK PhD council. Kim, my teammates who organized events together, and I enjoy working with you, you are kind and good at organizing things. Kim, also thanks for your nice suggestion of my A2 project! The other members, such as Peter, Mo, Ivonne, Martin and Fanrong, I would like to tell you again that I am proud that we have made the PhD guideline, especially thanks to Fanrong and Mo.

I would like to thank the many people I know at conferences or just from journal papers. I contacted many scientists with questions or details in their papers. I am grateful for their quick responses and inspiring discussions that have motivated me to continue to enjoy research and enjoy being a part of this wonderful scientific community.

Outside of work, I would like to thank my friends, such as Jin, Nana, Shanshan, Merel, Vaibhav, Marjolein, Jessie and many others for their sweet company. For sure, I will see some people again and let us do some exercise or have dinner or have a good time as usual. In particular, I would like to thank old friends who have known me for more than 5 years or even more than 10 years. Although we can only contact online most of the time, our friendship is deep-rooted and vivid. Year after year, we gossip about each other, make fun of each other, and also have each other's back. Having you and the constant jokes, especially in the tough and unpredictable period of the covid time, making my life under control with a sense of familiarity. Siqi, Yingying, Xianglin, having you is the blessing of my life!

At the end of this acknowledgement, I would like to express my deep gratitude to two companions who have given me great support. One is Doudou, he was the cutest and coolest rabbit, I learnt the relaxation philosophy from him. The other is Xixi, she is the most beautiful and smartest person. Dear Xixi, thank you for your tremendous support and love, I am really lucky and happy to have you in my life. Thank you for your company and comfort during the

last two years of my PhD, especially through all the ups and downs with me. Not much to say, just want to hug you.

Before wrapping up this acknowledgement, I would like to add a bit more. As I write this acknowledgement, time flies and I still feel that overwhelming sense of gratitude. I am sure I forgot to mention some people. For these people, you have a good excuse to ask me to buy you a drink, and I would love to do so. For all of you who are reading this, our paths may have been or will be crossed, I wish you all the best and see you around.

About the author

Anna Huang was born on the 13th of February in China. In 2010, she studied Environmental Science for her bachelor's study. Her interest in experimental research on environmental chemistry and biology made her continue her education in a Master's program at Nanjing University. During her master's study, she was involved in a project to assess the effect of microplastics. During this project, she performed several experiments, including toxicity tests, bioaccumulation and biotransformation measurement, and adsorption tests. After her master's study, she worked for a year in a new environment to explore her capability and embrace new challenges.

In the year 2018, she started her PhD on the toxic effects of insecticides under the supervision of Paul van den Brink, Nico van den Brink and Ivo Roessink. Her PhD project focuses on the mechanisms of toxicity of neonicotinoid to aquatic arthropods. During her PhD project, she not only performed experiments, such as toxicity tests, internal concentration and biotransformation measurement, but she also applied toxicokinetic and toxicodynamic models to explore the mechanisms. Her work offers insights of the inter- and intra-species sensitivity difference of aquatic arthropods to imidacloprid and flupyradifurone. These insights can be used to better assess the risk of insecticides. After proudly completing her PhD project, she looks forward to more challenges and using her skills to contribute to a better world.

Scientific publications

Huang, A., van den Brink, N.W., Buijse, L., Roessink, I. and van den Brink, P.J., 2021. The toxicity and toxicokinetics of imidacloprid and a bioactive metabolite to two aquatic arthropod species. Aquatic Toxicology, 235, p.105837.
https://doi.org/10.1016/j.aquatox.2021.105837

Huang, A., Roessink, I., van den Brink, N.W. and van den Brink, P.J., 2022. Size-and sex-related sensitivity differences of aquatic crustaceans to imidacloprid. Ecotoxicology and Environmental Safety, 242, p.113917. https://doi.org/10.1016/j.ecoenv.2022.113917

Huang, A., Mangold-Döring, A., Focks, A., Zhang, C. and Van den Brink, P.J., 2022. Comparing the acute and chronic toxicity of flupyradifurone and imidacloprid to non-target aquatic arthropod species. Ecotoxicology and Environmental Safety, 243, p.113977.
https://doi.org/10.1016/j.ecoenv.2022.113977

Huang, A., Mangold-Döring, A., Guan, H., Boerwinkel, M.C., Belgers, D., Focks, A. and Van den Brink, P.J., 2022. The effect of temperature on toxicokinetics and the chronic toxicity of insecticides towards Gammarus pulex. Science of The Total Environment, p.158886.
https://doi.org/10.1016/j.scitotenv.2022.158886

Mangold-Döring, A., **Huang, A.**, van Nes, E.H., Focks, A. and Van den Brink, P.J., 2022. Explicit consideration of temperature improves predictions of toxicokinetic-toxicodynamic models for flupyradifurone and imidacloprid in *Gammarus pulex*. Environmental Science & Technology, https://doi.org/10.1021/acs.est.2c04085

Netherlands Research School for the
Socio-Economic and Natural Sciences of the Environment

D I P L O M A

for specialised PhD training

The Netherlands research school for the
Socio-Economic and Natural Sciences of the Environment
(SENSE) declares that

Anna Huang

born on 2 January 1992, in Anhui, China

has successfully fulfilled all requirements of the
educational PhD programme of SENSE.

Wageningen, 16 November 2022

Chair of the SENSE board

Prof. dr. Martin Wassen

The SENSE Director

Prof. Philipp Pattberg

The SENSE Research School has been accredited by the Royal Netherlands Academy of Arts and Sciences (KNAW)

K O N I N K L I J K E   N E D E R L A N D S E
A K A D E M I E   V A N   W E T E N S C H A P P E N

The SENSE Research School declares that **Anna Huang** has successfully fulfilled all
requirements of the educational PhD programme of SENSE with a
work load of 57.6 EC, including the following activities:

SENSE PhD Courses

o   Environmental research in context (2018)
o   Multivariate Analysis, co-organised with PE&RC (2019)
o   Research in context activity: 'Communicating and sharing the PhD research in
    Environmental toxicology through a personal research blog' (2022)

Other PhD and Advanced MSc Courses

o   Advanced Statistics, Wageningen University (2018)
o   R for statistics, Wageningen University (2019)
o   Research Data Management, Wageningen University (2018)
o   Ecotoxicology, PET (2019)
o   Risk Assessment, PET (2019)
o   Scientific Writing, Wageningen Graduate Schools (2020)
o   Bridging across cultural differences, Wageningen Graduate Schools (2018)
o   Dynamic Modelling of Toxic Effects, PhD School of Science, University of Copenhagen
    (2021)
o   Career Perspectives, Wageningen Graduate Schools (2022)

Management and Didactic Skills Training

o   Active member of WIMEK PhD council (2019-2022)
o   Supervising two MSc students with thesis entitled 'Chronic Toxicity of Flupyradifurone to
    the Freshwater Invertebrates *Cloeon dipterum* (Ephemeroptera) and *Gammarus pulex*
    (Amphipoda)' (2020) and 'Chronic effects of Imidacloprid and Flupyradifurone on growth
    and reproduction of *Gammarus pulex* under two different temperature regimes' (2021)
o   Course assistant in the MSc course 'Chemical Stress Ecology and Ecotoxicology' (2021)

Oral Presentations

o   *The influence of temperature on the lethal and sublethal effects of two insecticides ,
    midacloprid and flupyradifur one to Gammarus pulex.* SETAC Europe 31st annual
    meeting, 3-6 May 2021, Online

SENSE coordinator PhD education

Dr. ir. Peter Vermeulen